

TECHNISCHE UNIVERSITÄT MÜNCHEN

Lehrstuhl für Bodenkunde

Biogeochemical interfaces in natural and artificial soil systems: specific surface area,
phenanthrene sorptive properties and formation of organo-mineral associations

Geertje Johanna Pronk

Vollständiger Abdruck der von der Fakultät Wissenschaftszentrum Weihenstephan für
Ernährung, Landnutzung und Umwelt der Technischen Universität München zur Erlangung
des akademischen Grades eines

Doktor der Naturwissenschaften

genehmigten Dissertation.

Vorsitzender: Univ.-Prof. Dr. J. P. Geist

Prüfer der Dissertation: 1. Univ.-Prof. Dr. I. Kögel-Knabner
2. Univ.-Prof. Dr. K. U. Totsche
(Friedrich-Schiller-Universität, Jena)

Die Dissertation wurde am 27.07.2011 bei der Technischen Universität München eingereicht
und durch die Fakultät Wissenschaftszentrum Weihenstephan für Ernährung, Landnutzung
und Umwelt am 25.10.2011 angenommen.

I Summary

Soils are among the most complex materials on earth (Young and Crawford, 2004). They consist of heterogeneous mixtures of different mineral, organic and biological components that are usually not well defined, and are associated in a complex hierarchical structure that can be regarded as one large biogeochemical interface (Totsche et al., 2010; Young and Crawford, 2004). The characterization of biogeochemical interfaces in soils is essential to gain a mechanistic understanding of their role in the many processes occurring in soil. The physical, chemical, and biological heterogeneity of these interfaces produces a multitude of reactive sites that control the fate and effect of chemicals in soils (Totsche et al., 2010). In order to gain a mechanistic understanding of the interplay and interdependencies of physical, chemical and biological processes that occur at these biogeochemical interfaces in soil, the German Research Foundation (DFG) started the Priority Program “Biogeochemical interfaces in soil” in 2007.

The objective of this dissertation was to study the effect of different components on the development and properties of biogeochemical interfaces in soil. In order to achieve this, existing interfaces of natural soils were characterized and the development of new interfaces was studied in a new large-scale incubation experiment with so-called ‘artificial soils’. Biogeochemical interfaces in natural soils were characterized by (i) determining the contribution of iron oxides to specific surface area (SSA) of soil and its particle size fractions and its importance for stabilization of microaggregates and interactions with organic matter (OM), and (ii) characterization of the sorptive interface for hydrophobic molecules in relation to the SSA and OM content and properties, by phenanthrene sorption experiments to the bulk natural soil and selected particle size fractions. The formation of interfaces in the artificial soils was followed by studying (i) the development of macro- and microaggregation and formation of organo-mineral associations, and (ii) the changes in OM distribution and composition with time and its effect on phenanthrene sorption

The natural soil samples used were taken from arable topsoils at two well-characterized long-term field experiments in Ultuna, Sweden and Scheyern, Germany. Samples were taken from two different plots at the Ultuna site, one of which had been fertilized with $\text{Ca}(\text{NO}_3)_2$ and the other with manure. This provided two samples with the same texture and mineralogy, but different organic carbon (OC) content. The artificial soils were

produced in the laboratory from pure minerals, sterilized manure as an OC source and a microbial inoculum extracted from a natural soil. Artificial soils with eight different compositions were mixed from the model materials illite, montmorillonite, ferrihydrite, boehmite, and charcoal. The soils were incubated in the dark at constant water content and sampled after 3, 6, 12 and 18 months.

The contribution of weakly crystalline and crystalline oxides to the SSA of particle size fractions of the three natural soils was determined after particle size fractionation. The obtained silt and clay fractions were treated with hydrogen peroxide, extracted with oxalate and dithionite and the SSA of all fractions was determined using BET-N₂. Results show that stable microaggregates were present in the coarse and medium silt fractions of all soils that could not be dispersed physically even at the highest ultrasonic dispersion energy and were probably stabilized by organic matter and iron oxides. Iron oxides were a major contributor to the SSA of all particle size fractions and the losses of carbon after oxalate and dithionite extraction showed that a major part of the organic matter in all particle size fractions was stabilized by iron oxides, even in these clay rich soils. Weakly crystalline oxide surface area did not increase with decreasing particle size and calculated negative surface areas for some of the fine fractions indicated that weakly crystalline oxides were present as coatings on other minerals. The results demonstrate the importance of (iron) oxides for microaggregation and stabilization of organic matter in soil. However, the actual interface provided by these oxides varies with particle size and crystallinity depending on the occlusion of mineral surfaces by organic matter and weakly crystalline oxides.

Phenanthrene was used as a representative for hydrophobic organic chemicals to probe the sorptive capacity of the interface of the natural soils from Ultuna at different particle sizes. Batch sorption experiments with phenanthrene were carried out with the bulk soil as well as the fine (0.2-6.3 μm) and coarse (6.3-63 μm) particle size fractions of the soils. The SSA of the bulk soil and particle size fractions was determined by BET-N₂ and ethylene glycol monoethyl (EGME) retention. Organic matter was characterized by solid-state ¹³C NMR spectroscopy. The sorption capacity was higher after particle size fractionation, indicating that the aggregated structure of the bulk soil should be taken into account for the estimation of soil sorptive capacity. The surface area-normalized Freundlich isotherm coefficients of phenanthrene were linearly related to the organic carbon content per m². This

indicates that the capacity for phenanthrene sorption of this soil depends both by the size of the interface and by the amount of OM present at the surface of the available interface.

The development of the artificial soils with incubation time was monitored by a general characterization of the artificial soil material at each sampling time. The pH, OC and N content, extractable Fe, Al and Si was measured, and the amount of macroaggregates > 2 mm was determined by sieving. Density fractionation was performed at densities of 1.8 and 2.4 g cm⁻³ to separate particulate OM, microaggregates and the mineral fraction. The SSA of the microaggregate fraction and the amount of OC associated with microaggregates and minerals was determined. The SSA of the model materials and the artificial soils at the start of incubation was determined by BET-N₂. The artificial soils developed quickly and CO₂ respiration occurred during the entire 18-month incubation time. The actual SSA of the 'soils' was significantly lower than the sum of the SSA of the pure model materials indicating that occlusion of mineral surfaces by interaction between OM and minerals occurred almost immediately after incubation started. Macro- and microaggregates were formed within 3 months of incubation. The amount of mineral and microaggregate associated OC increased during the entire incubation time, until a maximum of 19% of the OC present was associated with microaggregates and minerals. Macroaggregation decreased after 12 months of incubation probably due to decreasing biological activity. The turnover of macroaggregates and continuing formation of microaggregates was consistent with the aggregate hierarchy model. Less macroaggregation was observed in the soil where no clay mineral was present, indicating that clay minerals were important for the formation of macroaggregates. Ferrihydrite and boehmite did not affect the macro- or microaggregation in this experiment. The results of density fractionation indicate that OM was mainly associated with the clay minerals, probably due to the neutral pH of the artificial soils, leading to a low or negative surface charge of the oxides. The artificial soil incubation experiment showed that interface development and the building of macro- and microaggregates took place within a relatively short time scale.

The OC distribution in the artificial soils with particle size, and in particular the coarse (> 63 µm) and fine (<20 µm) fractions was determined after particle size fractionation. This showed that the OC present was redistributed from the coarse to the fine fractions of the artificial soils during incubation. The C/N ratios and ¹³C NMR spectroscopy indicate that proteinacious material may have been selectively preserved in the fine fractions. This may

point to strong interaction between proteins and mineral surfaces. Phenanthrene sorption was performed to the <20 μm fraction of artificial soils containing illite, ferrihydrite and charcoal after 3 and 12 months of incubation. After 3 months, a difference in sorption isotherm shape could be seen between the soil containing illite and the soils containing ferrihydrite. After 12 months of incubation phenanthrene sorption to the samples slightly increased, and all differences in phenanthrene sorption between artificial soil compositions at this time-step could be explained by OC content. From this, it can be concluded that phenanthrene sorption to ferrihydrite may have occurred in the 3 months incubated samples, but that with incubation time the interfaces matured and OM content alone determined phenanthrene sorption.

The artificial soil incubation experiment showed that interface development in these artificial soils took place within a relatively short time scale. The artificial soils developed from mixtures of clean model materials to a complex, aggregated soil-like system. This experiment therefore offers a valuable model where the formation and interactions of soil properties and processes can be studied in a well-defined system. However, the artificial soils represent a simplified system in which the effect of changing environmental conditions and the external input of, for example, OM was excluded. These factors are important for biogeochemical interfaces in natural systems, and should be considered when extrapolating the results from the artificial soils. Overall, the results from this dissertation demonstrate that biogeochemical interfaces in soil are not only determined by the different components present, but foremost by the interaction between these components.

II Zusammenfassung

Böden gehören zu den komplexesten Materialien auf der Erde (Young und Crawford, 2004). Sie bestehen aus heterogenen Mischungen verschiedener mineralischer, organischer und biologischer Komponenten, die normalerweise nicht gut definiert werden können und in einer komplexen hierarchischen Struktur assoziiert sind, die als eine große biogeochemische Grenzfläche angesehen werden kann (Totsche et al, 2010; Young und Crawford, 2004). Die Charakterisierung biogeochemischer Grenzflächen in Böden ist wesentlich, um ein mechanistisches Verständnis über ihre Rolle als Transformatoren, Puffer, Akkumulatoren und Filter von Energie und von im Wasser gelösten sowie dispergierten Partikel zu gewinnen. Aus der physikalischen, chemischen und biologischen Heterogenität dieser Grenzflächen ergibt sich eine Vielzahl von reaktiven Stellen, die die Wirkung von Chemikalien in Böden kontrollieren (Totsche et al., 2010). Um ein mechanistisches Verständnis für das Zusammenspiel und die Abhängigkeiten von physikalischen, chemischen und biologischen Prozessen, die bei diesen biogeochemischen Grenzflächen im Boden ablaufen, zu gewinnen, startete die Deutsche Forschungsgemeinschaft (DFG) im Jahr 2007 das Schwerpunktprogramm "Biogeochemische Grenzflächen im Boden".

Ziel dieser Dissertation war es, die Wirkung verschiedener mineralische und organische Komponenten auf die Entwicklung und Eigenschaften biogeochemischer Grenzflächen im Boden zu studieren. Um dies zu erreichen, wurden die vorhandenen Grenzflächen von natürlichen Böden charakterisiert und die Entwicklung neuer Grenzflächen in einem neuartigen Inkubationsexperiment mit so genannten "künstlichen Böden" untersucht. Biogeochemische Grenzflächen in natürlichen Böden wurden untersucht durch (i) Bestimmung des Beitrags von Eisenoxiden an der spezifischen Oberfläche des Bodens und seiner Korngrößenfraktionen, und der Bedeutung von Eisenoxiden für die Stabilisierung von Mikroaggregaten und Interaktionen mit organischer Substanz. Sowie durch (ii) Charakterisierung der Sorptionseigenschaften der Grenzflächen für hydrophobe Moleküle in Bezug auf die spezifische Oberfläche und den Gehalt an organischer Substanz, indem das Verhalten von Phenanthren im Gesamtboden und ausgewählten Korngrößenfraktionen der natürlichen Böden bestimmt wurde. Die Bildung von Grenzflächen in künstlichen Böden wurde durch das Studium (i) der Entwicklung von Makro- und Mikroaggregaten und der Bildung von organo-mineralischen Komplexen, und (ii) der Änderungen der organischen

Kohlenstoffverteilung und -zusammensetzung mit der Zeit und ihrer Auswirkung auf das Sorptionsverhalten von Phenanthren bestimmt.

Die natürlichen Bodenproben wurden aus Ackerland-Oberböden von zwei gut charakterisierten Langzeit-Feldversuchen in Ultuna, Schweden und Scheyern, Deutschland genommen. Die Proben aus Ultuna wurden von zwei verschiedenen Standorten genommen, von denen einer mit $\text{Ca}(\text{NO}_3)_2$, und der andere mit Stallmist gedüngt war. Dies lieferte zwei Proben mit gleicher Textur und Mineralogie, aber unterschiedlichem organischen Kohlenstoffgehalt. Die künstlichen Böden wurden im Labor aus reinen Mineralen, sterilisiertem Stallmist als Kohlenstoffquelle und einem aus natürlichen Boden gewonnenen mikrobiellen Inokulum hergestellt. Künstliche Böden mit acht unterschiedlichen Zusammensetzungen wurden aus ein oder mehreren der Modellmaterialien Illit, Montmorillonit, Ferrihydrit, Böhmit und Holzkohle gemischt. Die Böden wurden im Dunkeln bei konstantem Wassergehalt inkubiert und nach 3, 6, 12 und 18 Monaten beprobt.

Der Beitrag der schwachkristallinen und kristallinen Oxide zur spezifischen Oberfläche der Korngrößenfraktionen der drei natürlichen Böden wurde nach Korngrößenfraktionierung bestimmt. Die erhaltenen Schluff- und Tonfraktionen wurden mit H_2O_2 , Oxalat und Dithionit extrahiert, und die spezifische Oberfläche aller Fraktionen wurde mittels BET- N_2 bestimmt. Die Ergebnisse zeigen, dass stabile Mikroaggregate in den groben und mittleren Schlufffraktionen aller Böden vorkommen. Diese Mikroaggregate wurden vermutlich vor allem durch organische Substanz und Eisenoxide stabilisiert. Die berechnete Oberfläche der Eisenoxide machte einen wesentlichen Teil der spezifischen Oberfläche aller Fraktionen aus. Die Kohlenstoffverluste nach Oxalat- und Dithionit-Extraktion wiesen darauf hin, dass ein großer Teil der organischen Substanz in allen Fraktionen durch Eisenoxide stabilisiert wurde, obwohl die verwendeten Böden tonreich waren. Die spezifische Oberfläche der schwachkristallinen Oxide nahm nicht mit abnehmender Korngrößen zu und die berechnete negative Oberfläche einiger feiner Fraktionen deutet darauf hin, dass andere Minerale mit schwachkristallinen Eisenoxide beschichtet waren. Diese Ergebnisse demonstrieren die Bedeutung der (Eisen-)Oxide für die Mikroaggregation und Stabilisierung von organischer Substanz in Böden. Allerdings unterscheidet sich die tatsächlich verfügbare Grenzfläche der Oxide in Böden mit unterschiedliche Korngröße und Kristallinität der Oxiden, abhängig von der Bedeckung der mineralischen Oberflächen durch organische Substanz und schwachkristalline Oxiden.

Phenanthren wurde als Modellsubstanz für hydrophobe organische Chemikalien benutzt, um die Sorptionskapazität der natürlichen Böden aus Ultuna in unterschiedlichen Körngrößenfraktionen zu bestimmen. Batch-Sorptionsversuche wurden am Gesamtboden und einer feinen (0.2-6.3 μm) sowie an einer groben (6.3-63 μm) Fraktion des Bodens durchgeführt. Die spezifische Oberfläche der Proben wurde mittels BET-N₂ und Ethylen Glykol Monoethyl (EGME) Retention bestimmt, und die organische Substanz wurde mit Festkörper ¹³C NMR Spektroskopie charakterisiert. Die Phenanthren-Adsorptionskapazität nahm nach der Körngrößenfraktionierung zu, was darauf hinweist, dass die Aggregatstruktur des Gesamtbodens bei der Bestimmung der Adsorptionskapazität des Bodens berücksichtigt werden sollte. Die Sorptionskoeffizienten der auf die spezifischen Oberfläche normalisierten Phenanthren Freundlich-Isotherme waren linear mit dem Gehalt an organische Kohlenstoff pro m² der Probe korreliert. Dies deutet darauf hin, dass die Phenanthren-Sorptionskapazität in diesen Böden sowohl von der Größe der Oberfläche als auch von der Menge der organischen Substanz auf der Oberfläche abhängt.

Die Entwicklung der künstlichen Böden mit der Dauer der Inkubation wurde durch Charakterisierung des Bodenmaterials nach jeder Probenahme verfolgt. Dafür wurden folgende Parameter gemessen: pH -Wert, organischer C- und N-Gehalt und die Menge an extrahierbarem Fe, Al und Si. Die Menge der Makroaggregate > 2 mm wurde durch Sieben bestimmt. Partikuläre organische Substanz, Mikroaggregate und die mineralische Fraktion wurden mittels sequenzieller Dichtefraktionierung bei Dichten von 1,8 und 2,4 g cm⁻³ getrennt. Die spezifische Oberfläche der Modellmaterialien und der künstlichen Böden zur Beginn der Inkubation wurde durch BET-N₂ bestimmt. Die künstlichen Böden zeigten eine schnelle Entwicklung, und während der gesamten Inkubationszeit fand CO₂ Freisetzung statt. Die tatsächliche spezifische Oberfläche der künstlichen Böden war deutlich geringer als die Summe der spezifischen Oberflächen der Modellmaterialien, was darauf hinweist, dass eine Makierung von mineralischen Oberflächen mit organischem Material durch Interaktionen zwischen organischer Substanz und Mineralen schon unmittelbar nach Inkubationsanfang stattfand. Makro- und Mikroaggregate wurden schon innerhalb der ersten 3 Monate der Inkubationszeit gebildet. Die Menge des in der mineralischen und in der Mikroaggregat-Fraktion gebundenen organischen Kohlenstoffs nahm bis zum Ende der Inkubationszeit zu. Wobei ein Maximum von 19% der Gesamtmenge des organischen Kohlenstoffs in den künstlichen Böden in der Mikroaggregat- und mineralischen Fraktion erreicht wurde.

Makroaggregation nahm nach 12 Monaten Inkubation wieder ab, was durch eine abnehmende biologische Aktivität erklärt werden kann. Die Dynamik der Makroaggregate und die gleichzeitig fortlaufende Neubildung von Mikroaggregaten in den künstlichen Böden passen zum Modell der Aggregathierarchie. Makroaggregation war geringer in demjenigen künstlichen Boden, der kein Tonmineral enthielt, was darauf hinweist, dass Tonminerale wichtig für die Bildung von Makroaggregaten sind. Ferrihydrit und Böhmit hatten keinen Einfluss auf Mikro- und Makroaggregation. Die Ergebnisse der Dichtefraktionierung zeigen, dass organische Substanz hauptsächlich mit Tonmineralen assoziiert war. Ursache hierfür ist wahrscheinlich, dass aufgrund der neutralen pH-Werte der künstlichen Böden, die Oxide eine nur geringe positive oder sogar eine negative Oberflächenladung hatten und dadurch eine geringe Affinität für organische Substanz aufwiesen. Das Inkubationsexperiment mit künstlichen Böden zeigte, dass die Entwicklung der biogeochemischen Grenzflächen sowie die Bildung von Mikro- und Makroaggregaten innerhalb einer relativ kurzen Zeitspanne stattfinden kann.

Die Verteilung des organischen Kohlenstoffs in den groben ($>63 \mu\text{m}$) und feinen ($<20 \mu\text{m}$) Fraktionen der künstlichen Böden wurde mittels Korngrößenfraktionierung bestimmt. Es zeigte, dass eine Verlagerung der organischen Substanz von der groben zur feinen Fraktion mit zunehmender Inkubationszeit stattfand. Das C/N-Verhältnis und die Ergebnisse der ^{13}C NMR Spektroskopie wiesen darauf hin, dass proteinartiges Material selektiv in den feinen Fraktionen angereichert wurde. Dies deutet auf eine präferentielle Interaktion zwischen Proteinen und mineralischer Oberfläche hin. Phenantren-Sorptionsexperimente wurden mit ausgewählten 3 und 12 Monate inkubierten Proben aus der Fraktion $<20 \mu\text{m}$ der künstlichen Böden durchgeführt, die Illit, Ferrihydrit und Holzkohle enthielten. In den 3 Monate inkubierten Proben wurde ein Unterschied in der Form der Phenanthren-Sorptionsisothermen zwischen dem künstlichen Boden, der nur Illit enthielt, und den Böden, die Ferrihydrit enthielten, beobachtet. Die Phenanthren-Sorption in den 12 Monate inkubierten Proben war etwas höher als diejenige der 3 Monate inkubierten Proben, und alle Unterschiede im Sorptionsverhalten der 12 Monate inkubierten Proben konnten durch Unterschiede im Kohlenstoffgehalt erklärt werden. Hieraus folgt, dass in den 3 Monate inkubierten Böden Phenanthren-Sorption an Ferrihydrit stattfinden konnte, dass sich aber mit der Zeit die Grenzflächen weiter entwickelten, und damit Phenanthren-Sorption nur noch durch den Gehalt an organischer Substanz bestimmt wurde.

Das Inkubationsexperiment mit den künstlichen Böden zeigte, dass die Entwicklung der biogeochemischen Grenzflächen in diesen künstlichen Böden innerhalb einer relativ kurzen Zeit stattfand. Die künstlichen Böden entwickelten sich von Mischungen aus sauberen Modellmaterialien zu komplexen, aggregierten Systemen. Dieses Experiment bietet damit ein wertvolles Modell, an dem Bildung und Wechselwirkungen von Bodeneigenschaften und Prozessen in einem genau definierten System untersucht werden konnten. Allerdings stellen die künstlichen Böden ein vereinfachtes System dar, in dem die Wirkung von sich ändernden Umweltbedingungen und der externe Eintrag von z. B. organischer Substanz ausgeschlossen wurde. Diese Faktoren sind für biogeochemische Schnittstellen in natürlichen Systemen wichtig und sollten bei der Extrapolation der Ergebnisse aus den künstlichen Böden berücksichtigt werden. Insgesamt zeigen die Ergebnisse dieser Dissertation, dass biogeochemische Grenzflächen im Boden nicht nur durch die verschiedenen Komponenten des Bodens, sondern vor allem auch durch die Interaktionen zwischen diesen Komponenten bestimmt werden.

III Index

I	SUMMARY	I
II	ZUSAMMENFASSUNG	V
III	INDEX	X
IV	LIST OF FIGURES	XII
V	LIST OF TABLES	XIV
VI	GLOSSARY	XV
1	INTRODUCTION AND STATE OF THE ART	1
1.1.1	<i>Iron oxides</i>	1
1.1.2	<i>Specific surface area as a measure of the biogeochemical interface</i>	2
1.1.3	<i>OM-mineral associations and aggregation</i>	3
1.1.4	<i>The sorptive interface for hydrophobic chemicals</i>	5
1.2	OBJECTIVES	6
1.2.1	<i>Aim: to characterize the properties of mature interfaces in natural arable soil and determine the contribution of iron oxides to the soil surface area</i>	7
1.2.2	<i>Aim: the characterization of the sorptive interface of natural soils and particle size fractions for hydrophobic organic chemicals by phenanthrene sorption</i>	7
1.2.3	<i>Aim: to study the development of biogeochemical interfaces and determine formation of aggregates and organo-mineral associations during artificial soil incubation</i>	8
1.2.4	<i>Aim: to study the development of organic matter properties and composition, and the effect of organic matter and mineral components on the phenanthrene sorptive interface during artificial soil incubation</i>	8
2	MATERIALS AND METHODS	10
2.1	NATURAL SOILS	10
2.2	ARTIFICIAL SOIL INCUBATION	11
2.2.1	<i>Experimental set-up</i>	11
2.2.2	<i>Model materials</i>	12
2.2.3	<i>Artificial soil incubation and sampling</i>	13
2.3	FRACTIONATION AND SAMPLE PREPARATION	14
2.3.1	<i>Particle size fractionation</i>	14
2.3.2	<i>Density fractionation</i>	14
2.3.3	<i>Organic matter oxidation</i>	15
2.4	ANALYTICAL METHODS	16
2.4.1	<i>Sample characterization, pH, C and N content and texture</i>	16
2.4.2	<i>Specific surface area (SSA)</i>	16
2.4.3	<i>Oxide extraction</i>	17
2.4.4	<i>Solid-state ¹³C NMR</i>	19
2.5	PHENANTHRENE SORPTION EXPERIMENTS	20
2.5.1	<i>Batch experiments</i>	20
2.5.2	<i>Phenanthrene extraction and quantification</i>	21
2.5.3	<i>Isotherm modelling</i>	22
3	IRON OXIDES AS MAJOR AVAILABLE INTERFACE COMPONENT IN LOAMY ARABLE TOPSOILS	23
3.1	RESULTS	23
3.1.1	<i>Texture and particle size fractionation</i>	23
3.1.2	<i>Characterization of the particle size fractions</i>	25
3.1.3	<i>Specific surface area of the iron oxides</i>	28
3.1.4	<i>Carbon loss due to oxide extraction</i>	29
3.2	DISCUSSION	31
3.2.1	<i>Stable microaggregates in the coarse and medium silt fraction</i>	31
3.2.2	<i>Oxide surface area and association with organic carbon</i>	32

4	COMBINING SPECIFIC SURFACE AREA AND ORGANIC MATTER CONTENT TO DETERMINE THE PHENANTHRENE SORPTIVE INTERFACE OF AN ARABLE TOPSOIL	38
4.1	RESULTS AND DISCUSSION	38
4.1.1	<i>Organic matter properties and SSA</i>	38
4.1.2	<i>Phenanthrene sorption: isotherm shape and model discrimination.....</i>	41
4.1.3	<i>Increase in phenanthrene sorption after particle size fractionation</i>	43
4.1.4	<i>Phenanthrene sorption related to carbon concentration and SSA</i>	45
5	DEVELOPMENT OF BIOGEOCHEMICAL INTERFACES IN AN ARTIFICIAL SOIL INCUBATION EXPERIMENT; AGGREGATION AND FORMATION OF ORGANO-MINERAL ASSOCIATIONS	48
5.1	RESULTS	48
5.1.1	<i>Model materials</i>	48
5.1.2	<i>Incubation and bulk properties of the artificial soils</i>	49
5.1.3	<i>Macroaggregation.....</i>	50
5.1.4	<i>Microaggregation</i>	51
5.2	ARTIFICIAL SOIL DEVELOPMENT; MICROBIAL ACTIVITY AND AGGREGATE FORMATION	52
5.2.1	<i>Incubation and microbial activity</i>	52
5.2.2	<i>Fast coverage of mineral surfaces by organic matter (OM).....</i>	53
5.2.3	<i>Formation of macroaggregates.....</i>	54
5.2.4	<i>Formation and SSA of microaggregates</i>	55
5.3	THE EFFECT OF MINERAL COMPOSITION AND CHARCOAL	57
5.3.1	<i>Importance of clay mineral presence for macroaggregation.....</i>	57
5.3.2	<i>Low effect of ferrihydrite and boehmite on aggregation.....</i>	57
5.3.3	<i>Effect of charcoal on aggregation.....</i>	59
6	ORGANIC MATTER DYNAMICS AND THE DEVELOPMENT OF THE PHENANTHRENE SORPTIVE INTERFACE IN AN ARTIFICIAL SOIL INCUBATION EXPERIMENT.....	61
6.1	RESULTS	61
6.1.1	<i>OM distribution and composition.....</i>	61
6.1.2	<i>Phenanthrene sorption</i>	67
6.2	DISCUSSION	71
6.2.1	<i>OM dynamics</i>	71
6.2.2	<i>Development of the phenanthrene sorptive interface.....</i>	73
6.3	THE ARTIFICIAL SOIL SYSTEM IN COMPARISON TO NATURAL SOILS.....	75
7	DEVELOPMENT OF THE ARTIFICIAL SOILS OVER TIME; PROCESSES AND OPEN QUESTIONS	77
8	CONCLUSIONS AND OUTLOOK.....	80
9	REFERENCES	83
10	ACKNOWLEDGEMENTS.....	94
	CURRICULUM VITAE.....	96
	PUBLICATIONS AND PRESENTATIONS.....	97

IV List of figures

Figure 1. Mixing of the model materials and initial wetting of the artificial soil batches.	11
Figure 2. Examples of the artificial soils during incubation	13
Figure 3. Overview of the density fractionation procedure.	15
Figure 4. Batch with soil sample used for the phenanthrene sorption experiments.....	21
Figure 5. Schematic overview of the phenanthrene extraction method.	22
Figure 6. % mass contribution to different particle size fractions from texture analysis.....	23
Figure 7. Particle size distribution after particle size fractionation. The mass % of aggregates indicated was calculated from the difference between particle size fractionation and texture analysis.....	24
Figure 8. Schematic overview of the effect of H ₂ O ₂ oxidation and oxalate and dithionite extraction on microaggregates and clay sized particles and their specific surface area...	36
Figure 9. BET-N ₂ versus EGME specific surface area (SSA) of bulk soil and particle size fractions in m ² g ⁻¹	39
Figure 10. Phenanthrene sorption isotherms of the coarse (6.3-63 μm) (squares) and fine (0.2-6.3 μm) (triangles) fraction and the bulk soil (diamonds) of UL-Ca and UL-m.....	42
Figure 11. Summed isotherms of the coarse and fine fraction compared to bulk soil isotherms for UL-Ca (a) and UL-m (b).	44
Figure 12. Freundlich isotherm coefficient (K _f) versus organic carbon content in mg C g ⁻¹ (a) and the Freundlich isotherm coefficient normalized to BET-N ₂ surface area (K _f m ⁻²) versus carbon content per square meter (mg C m ⁻²) (b).....	46
Figure 13. Mass % of aggregates > 2 mm determined by dry sieving of air-dried artificial soils after 3, 6, 12 and 18 months of incubation.....	51
Figure 14. Microaggregate and mineral-associated organic carbon defined as the carbon detected in the 1.8 – 2.4 g cm ³ plus the > 2.4 g cm ³ fraction after 3, 6, 12 and 18 months of incubation.....	52
Figure 15. Cumulative CO ₂ respiration of the artificial soils in mg CO ₂ -C g dry soil ⁻¹	61
Figure 16. Fungal hyphae observed in the artificial soil after 1 month of incubation.	62
Figure 17. Organic carbon stocks in mg C (g bulk soil) ⁻¹ of the particle size fractions with incubation time.....	63
Figure 18. Carbon and nitrogen content in mg g ⁻¹ of the <20 μm particle size fractions.	64
Figure 19. Solid-state ¹³ C NMR spectra of the charcoal and manure model materials used and <20 μm particle size fraction of the manure	65

Figure 20. Solid-state ^{13}C NMR spectra of the $<20\ \mu\text{m}$ fraction, and the bulk sample after 3 months of incubation, of the artificial soil containing illite (IL) with incubation time....	65
Figure 21. Solid-state ^{13}C NMR spectra of the $<20\ \mu\text{m}$ particle size fraction and the microaggregate ($1.8\text{-}2.4\ \text{g cm}^{-3}$) density fraction of artificial soil	66
Figure 22. Phenanthrene sorption isotherms of the $<20\ \mu\text{m}$ particle size fractions of the artificial soils after 3 (A) and 12 (B) months of incubation.	68
Figure 23. Phenanthrene sorption isotherms of the $<20\ \mu\text{m}$ fraction of the artificial soils after 12 months of incubation were phenanthrene concentration adsorbed to the sample is expressed in $\mu\text{g (g sample)}^{-1}$ (A) and in $\mu\text{g (mg OC)}^{-1}$ (B).....	70
Figure 24. The development of the artificial soils with incubation time.	77
Figure 25. Schematic overview of the studied processes occurring in the artificial soils with incubation time, and related open questions and hypotheses.....	78

V List of tables

Table 1. The composition of the artificial soils in % mass contribution of each model component	10
Table 2. Sample properties of bulk soil and particle size fractions.....	26
Table 3. Surface area stocks calculated for each fraction by multiplying the respective specific surface area by the mass contribution in % of the bulk soil.....	27
Table 4. BET-N ₂ specific surface area (SSA) and C constant of UL-Ca before and after organic matter removal by H ₂ O ₂ oxidation.	27
Table 5. Calculated surface areas (BET-N ₂) of the crystalline and weakly crystalline oxides and residue in m ² g ⁻¹ of the complete sample.....	29
Table 6. Carbon associated with weakly crystalline and crystalline oxides and the residue after dithionite extraction.....	30
Table 7. Texture, organic carbon content of the soils, and % mass contribution of carbon of the fractions to the total carbon content of the soil	38
Table 8. The organic carbon content (OC), C/N ratio, BET-N ₂ and EGME specific surface area (SSA) and sessile drop method contact angle of the samples used for phenanthrene sorption experiments	40
Table 9. Freundlich isotherm parameters	41
Table 10. Properties of the model materials.....	48
Table 11. Organic carbon (OC) content and C/N ratio of the bulk artificial soils, and the BET-N ₂ specific surface area (SSA) of the bulk soils and the range of SSA detected for the density fraction of 1.8-2.4 g cm ⁻³	49
Table 12. Oxalate, dithionite and Na-pyrophosphate extractable Fe, Al and Si of the bulk artificial soils in mg g ⁻¹	50
Table 13. Bulk organic carbon (OC) and N content and C/N ratio at t=1 (start of incubation) and t=4 (18 months of incubation), standard deviations were calculated from the three replicates for each artificial soil composition.	62
Table 14. Properties of the samples used for phenanthrene sorption experiments; organic carbon content (OC), C/N ratio and the BET-N ₂ specific surface area (SSA).....	67
Table 15. Sorption isotherm coefficients calculated using the Freundlich and Langmuir isotherm models.	69

VI Glossary

B	boehmite
BET	Brunauer-Emmett-Teller equation
CH	charcoal
EGME	ethylene glycol monoethyl ether
Fe _d	dithionite extractable iron
Fe _o	oxalate extractable iron
FH	ferrihydrite
IL	illite
K _f	Freundlich isotherm coefficient
K _{f_oc}	Freundlich isotherm coefficient normalized to organic carbon content
M	manure
MT	montmorillonite
NMR	nuclear magnetic resonance
OC	organic carbon
OM	organic matter
PAH	polyaromatic hydrocarbons
QC	clay-sized quartz
QS	quartz sand
QSi	silt-sized quartz
SCE	Scheyern soil
SSA	specific surface area
UL-Ca	Ultuna soil, fertilized with Ca(NO ₃) ₂
UL-m	Ultuna soil, fertilized with manure

1 Introduction and state of the art

Soils are among the most complex biological materials on earth (Young and Crawford, 2004). They consist of heterogeneous mixtures of different mineral, organic and biological components that are usually not well defined, and are associated in a complex hierarchical structure that can be regarded as one large biogeochemical interface (Totsche et al., 2010; Young and Crawford, 2004). The characterization of biogeochemical interfaces in soils is essential to gain a mechanistic understanding of their role as transformers, buffers, accumulators, and filters of energy, water, and dissolved as well as dispersed particles. The physical, chemical, and biological heterogeneity of these interfaces produces a multitude of reactive sites that control the fate chemicals in soils (Totsche et al., 2010).

1.1.1 Iron oxides

An important step towards the structural and functional characterization of the soil biogeochemical interface is the study of the type of particle surfaces present. Due to their large specific surface area (SSA) and high reactivity, pedogenic oxides, next to clay minerals, are among the most important mineral phases providing interfaces in soil. Although several types of oxides (Fe, Al, Mn and others) occur in soil, iron oxides are expected to play an important role in the stabilization of organic matter and formation of soil aggregates and have therefore received specific attention. Iron oxides are often present in soil as the weakly crystalline mineral ferrihydrite that consists of nanoparticles with ill-defined structure and composition (Qafoku 2010). Its high surface area and reactivity make it an important interface component in soils, even at low concentrations, but due to its low structural arrangement it remains difficult to identify. Ferrihydrite was successfully identified with X-ray diffraction (XRD) in soils only at concentrations greater than 5-10 % mass (Childs, 1992, Schwertmann et al. 1982). Some information on the crystallinity and the presence of ferrihydrite can be gained by chemical extraction methods. Iron oxides are usually differentiated in weakly crystalline (oxalate extractable) oxides and crystalline (dithionite extractable minus oxalate extractable) oxides (Cornell and Schwertmann, 1996). Previous studies have shown that iron oxides, and in particular oxalate extractable iron, are related to aggregate stability (Pinheiro-Dick and Schwertmann, 1996; Duiker et al., 2003). Furthermore, iron oxides strongly interact with organic matter in soil and play an important part in the stabilization of organic matter (Kaiser and Guggenberger, 2000; Eusterhues et al., 2005; Kleber et al., 2005). The

stabilization of organic matter by iron oxides is usually explained by the sorption of organic matter on the oxide surface (Tipping, 1981; Wagai and Mayer, 2007 and references therein), but iron oxides can also interact with organic matter by co-precipitation and by complexation with organic molecules (Wagai and Mayer, 2007; Eusterhues et al., 2008).

Iron oxide reactivity is often related to its large SSA, which is in the range of 200-1200 m² g oxide⁻¹ (Borggaard, 1982; Eusterhues et al., 2005; Hiemstra et al., 2010a). This can be related to the microporosity and the extent to which the surface is covered by organic matter. The standard method for detection of SSA in soil is BET-N₂ adsorption (Brunauer et al., 1938). An additional source of information from this method is the calculation of the so-called C constant, which is a measure of the enthalpy of nitrogen adsorption to the sample. Previous studies using BET-N₂ have shown that dithionite extractable oxides are a major contributor to SSA in subsoil horizons of an acid forest soil (Eusterhues et al., 2005) and in the particle size fractions < 6 µm of three sandy to loamy arable soils (Kiem and Kögel-Knabner, 2002). From these studies, it was concluded that iron oxides are mainly present in soil as small particles with high specific surface areas. However, surface area determination of the iron oxides in these studies was done after removal of organic matter. Hiemstra et al. (2010a, 2010b) showed that the reactive surface area of iron oxides in soil, detected by phosphate adsorption, is negatively related to its coverage by organic matter. To further assess the actual contribution of iron oxides to the available surface area in soil and the reactive interface, it is necessary to measure SSA changes after iron extraction without first removing organic matter. This would also avoid effects of the chemical treatment, necessary to remove organic matter, on the mineral surfaces present (Mikutta et al., 2005).

1.1.2 Specific surface area as a measure of the biogeochemical interface

Besides the physicochemical and chemical properties of the surfaces, the SSA is a major factor controlling the reactivity of biogeochemical interfaces in soil, as it determines the size of the total interface present. Two techniques are widely used to determine the SSA of soils. The most common is BET-N₂ adsorption (Brunauer et al., 1938). This method can detect the external SSA and, to some extent, the microporosity of the sample. However, the method has a low sensitivity for organic matter (OM), because of the kinetically limited diffusion of nitrogen into the small micropores of organic matter at the low temperatures at which nitrogen adsorption is performed (De Jonge & Mittelmeijer-Hazeleger, 1996; Echeverria et al., 1999). This may result in a severe underestimation of the size of the organic

surface area present in the sample (Chiou et al., 1990). An alternative method for SSA determination in soil is ethylene glycol monoethyl ether (EGME) retention (van Reeuwijk, 2002). EGME is a polar organic molecule with a high affinity for soil organic matter (SOM). Furthermore, it also quantifies the SSA of clay interlayers. Therefore, EGME retention probes different regions of the sample surface and, used in combination with the BET-N₂ method of SSA detection, offers information on the potential interfaces present on OM. However, this method should be used with caution on samples with high OM content, as the addition of EGME can change the solid phase density of OM, leading to an overestimation of the OM SSA (De Jonge & Mittelmeijer-Hazeleger, 1996). The relation between the SSA detected with the two methods in soils was found to be mainly related to the clay mineralogy of the soil (Yukselen & Kaya, 2006). However, when the mineralogy is the same, it would be expected that the EGME SSA of a soil will increase disproportionately relative to its BET-N₂ SSA with increasing OM content. Only few studies have investigated both BET-N₂ and EGME SSA of soils. Nonetheless, the use of EGME and BET-N₂ in combination may provide a useful tool to determine the relative importance of OM surfaces for the soil interface.

1.1.3 OM-mineral associations and aggregation

A major process with respect to the composition and properties of the soil interface is the association between OM and minerals and the formation of micro- and macroaggregates (Kögel-Knabner et al., 2008). The large SSA of clay minerals and pedogenic oxides provides living space for microorganisms and potential sites for adsorption of organic chemicals (Huang et al., 2005; Totsche et al., 2010). Sorption of OM to mineral surfaces also leads to a decrease in the mineral surface area available for colonization by microorganisms and sorption of organic chemicals in soil due to their occlusion with OM (Kaiser and Guggenberger, 2003; Wagai et al., 2009). It has often been observed that OC content increases with decreasing particle size (Christensen 2002). Incubation experiments by for example Leinweber and Reuter (1992) and Grosbellet et al. (2011) have shown that coarse particulate OM will be broken down and accumulated in the finer fractions of the soil. Over the last years it has become commonly accepted that an important factor for stabilization of OM in soil is its association with minerals in the small particle size fractions (Lützwow et al. 2006, Sollins et al. 2007 and references therein). Furthermore, the C/N ratio of soil OM usually decreases with decreasing particle size, and several studies have shown that proteinacious material is common in organo-mineral associations (Kleber et al. 2007 and references therein). This has led to a proposed conceptual model by Kleber et al. (2007) that

states that formation of organo-mineral associations starts with the development of a film of organic molecules on the mineral surface that then provide a so-called 'hydrophobic zone' where other organic molecules can be bound.

Aggregate formation is controlled by soil flora and fauna, environmental variables like drying/wetting and freezing/thawing cycles, and physical interactions between soil particles. Much importance is attributed to the effect of environmental variables like drying/wetting and freezing/thawing cycles on aggregation (Bravo-Garza et al., 2009; Bullock et al., 1988; Denef et al., 2001a; Smucker et al., 2007; Watts et al., 2005). However, it may be that biological activity is just as important for initial aggregate formation as abiotic factors. In particular, biological activity affects aggregate formation due to the growth of plant roots and fungal hyphae and the production of extra cellular polysaccharides (EPS) and root exudates that entangle mineral particles and glue them together Angers and Caron, 1998; Oades, 1993; Omoike and Chorover, 2006; Six et al., 2004; Tisdall et al., 1997). Abiotic processes that lead to the formation and stabilization of aggregates include static interactions between minerals and cation bridging. Furthermore, mineral interactions may be relevant for aggregation processes. Pedogenic oxides have a high capacity to form associations with OM and interact with other mineral particles (Barral et al., 1998; Duiker et al., 2003) and also clay minerals have been shown to be important for aggregate formation and stability (Denef and Six, 2005; Ruiz-Vera and Wu, 2006). However, more information on the effect of the presence of different minerals like pedogenic oxides and clay minerals on aggregate formation is still needed (Abiven et al., 2009).

The formation and turnover of macro- and microaggregates is usually described by the aggregate hierarchy model (Oades, 1984; Tisdall and Oades, 1982). This model assumes that the formation of macroaggregates is mainly controlled by OM availability, and that macroaggregates will be disrupted once the OM that binds them is decomposed. Microaggregates on the other hand, are gradually formed within macroaggregates, and are generally more stable and have longer OM turnover times compared to macroaggregates (Abiven et al., 2009; Oades, 1984; Six et al., 2000; Tisdall and Oades, 1982). Experiments on aggregate formation are usually carried out with dispersed natural soil (Denef et al., 2002; Falsone et al., 2007; Materechera et al., 1992). In natural soils organo-mineral associations and microorganisms are already present that may promote fast formation of new aggregates (Six et al., 2000). Aggregate formation from clean mineral particles and particulate OM on

material not yet colonised by microorganisms may proceed at a different time scale and be affected by different factors and processes. The initial interactions between OM and minerals and the formation of organo-mineral complexes and aggregates can be studied in soil chronosequences (Dümig et al., 2011; Egli et al., 2010; Leinweber and Reuter, 1992). However, the conditions at time zero in these studies usually have to be extrapolated from later stages in soil development (Schaaf et al., 2011).

1.1.4 The sorptive interface for hydrophobic chemicals

A substance moving through the soil may be exposed to surfaces with different characteristics, depending on its chemical properties. At high OM contents, hydrophobic organic molecules in particular adsorb preferentially to hydrophobic surfaces (Xing & Pignatello, 2005) that may not be detected by BET-N₂ and EGME due to the reasons discussed above. Moreover, both BET-N₂ and EGME detect mineral surfaces that are of minor relevance for the sorption of hydrophobic organic chemicals in soils at high SOM contents (Delle Site, 2001). Hydrophobic molecules are expected to interact preferentially with hydrophobic sites on the interface. The measurement of the soil contact angle may give some additional information on the presence of these hydrophobic sites and may be related to the sorption of hydrophobic chemicals. A surface is considered hydrophobic when the contact angle is above 90°, while a contact angle between 0° and 90° indicates a nonhydrophobic (subcritical) range for water repellency (Siebold et al., 1997). A relation between soil hydrophobicity as determined from the contact angle and sorption of the hydrophobic molecule diuron has previously been found by (Chaplain et al., 2008). The sorptive interface present in a soil is expected to change with particle size and aggregation due to the changes in the availability of surface sites. While the clay fraction of soil is often considered most important for due to its large SSA, the silt fraction, which may be partially composed of microaggregates (Virto et al., 2008) may also provide an important sorptive interface.

Polycyclic aromatic hydrocarbons (PAH) are one of the main groups of organic contaminants that commonly occur in soils. The elucidation of the behaviour of PAH in soil gives us a tool to characterize the sorptive interfaces present there with respect to the specific properties of these substances. Phenanthrene is used as a model substance to represent PAH as it is intermediate in molecular size and behaviour. Sorption of phenanthrene to soil is mainly related to the organic carbon content of the soil (Fall et al, 2003, Celis et al., 2006). The capacity of a soil to retain phenanthrene can be linearly related to the carbon content, which

has lead to the use of the K_{oc} (distribution coefficient between the solid and the water phase divided by carbon concentration) to explain phenanthrene sorption. However, a wide range of K_{oc} values have been measured for soils, which shows that the carbon concentration alone cannot completely explain phenanthrene sorption. Several studies have shown that the type of organic matter present in the soil has an effect on phenanthrene sorption (e.g. Chefetz and Xing, 2009 and references therein), sorption rates and isotherm shape (Huang et al., 2003). Furthermore, several studies have shown that mineral surfaces can be important for phenanthrene sorption (Mader et al., 1997, Thompson et al., 2001, Müller et al., 2007). And recent research has indicated that the interaction between minerals and OM and the resulting change in OM structure and availability of sorption sites is important for phenanthrene sorption (Celis et al., 2006, Bonin and Simpson, 2007, Pan et al., 2007, Ahangar 2008). How the sorption behaviour of phenanthrene is affected by the presence of different mineral components can therefore provide much information about the properties of the sorptive interface present in the soil.

1.2 Objectives

In 2007, the German Research Foundation (DFG) granted the Priority Program “Biogeochemical interfaces in soil” in order to gain a mechanistic understanding of the interplay and interdependencies of physical, chemical and biological processes that occur at biogeochemical interfaces in soil, and their effect on the fate and behaviour of organic chemicals. The priority program consists of a large interdisciplinary research program within Germany and Austria. The objective of this work was to study the effect of different components on the development and properties of biogeochemical interfaces in soil. In order to achieve this goal, existing interfaces of natural soils were characterized and the development of new interfaces was studied in a new large-scale incubation experiment with so-called ‘artificial soils’. These artificial soils were produced in the laboratory from pure minerals, OM and a microbial inoculum extracted from a natural soil. The artificial soils were composed in 8 different compositions of model components thought to be important materials providing interfaces in natural soils due to their large SSA and reactivity. The components considered were the clay minerals illite and montmorillonite, ferrihydrite and boehmite as representation of pedogenic iron and aluminium oxides, and charcoal. The formation of artificial soils was initiated by incubating these materials with sterilized manure as OC source and a microbial starting community extracted from a natural arable soil, and incubated up to

18 months. The interfaces formed in the artificial soils were then compared to the natural soils studied. Based on the overall objective of the study the following four aims were defined:

1.2.1 Aim: to characterize the properties of mature interfaces in natural arable soil and determine the contribution of iron oxides to the soil surface area

It was aimed to determine the actual contribution of (iron) oxides, in association with organic matter, to the interface area of particle size fractions of agricultural topsoil, as depending on the contribution of oxides of different crystallinity. Oxalate and dithionite extractions were carried out without removal of soil OM so that the actually available iron oxide interface, in interaction with OM, could be determined. Three typical European arable soils were chosen from well-characterized sites. Two of these samples came from the same location, but have received different fertilizer treatment leading to different OC contents. As the mineralogy and texture of these samples was the same, comparison of these two samples allowed for a study of the effect of changing OM content on the oxide surface area. Particle size fractionation was used to separate the soils into fractions with different SSA, organic matter content and degree of microaggregation and to study how oxide surface properties depend on particle size. Microaggregate content was investigated by comparing the results from particle size fractionation after physical dispersion with texture analysis after H₂O₂ oxidation of organic matter. SSA (BET-N₂) measured before and after oxalate and dithionite extraction was used to gain information on the nature of the weakly crystalline and crystalline oxides present in the soils and their relative contribution to soil surface area at different particle sizes.

1.2.2 Aim: the characterization of the sorptive interface of natural soils and particle size fractions for hydrophobic organic chemicals by phenanthrene sorption

To determine the relationship between total SSA and the available surface area for hydrophobic chemicals, sorption experiments with the hydrophobic molecule phenanthrene were performed with two samples from a well-characterized clayey loamy arable topsoil from Ultuna, Sweden. Phenanthrene was used as a model substance to represent PAH because of its intermediate molecular size. Sorption experiments were performed with the bulk soil and two particle size fractions to provide a range of samples with different SSA from the same

material, and also to compare the characteristics of the sorptive interface of a fine (0.2 -2 μm) versus a coarse (6.3-63 μm) fraction of the soil. These fractions contain the main part of the OC present in the soils and are therefore expected to represent the most relevant fractions for phenanthrene sorption. The SSA of the particle size fractions was determined by BET-N₂ and EGME and the relation between the SSA detected by these two methods and the OM content of the samples was examined. This may provide more information on the importance of OM surface as an interface in soil. Two soil samples from the same location at two sites with a different fertilizer treatment history, and therefore different OM contents, were used to elucidate the effect of OM content on the sorptive interface.

1.2.3 Aim: to study the development of biogeochemical interfaces and determine formation of aggregates and organo-mineral associations during artificial soil incubation

The development of micro- and macroaggregates and the initial formation of organo-mineral associations was studied. The experimental design used excluded the influences of environmental conditions on aggregate formation, and therefore represents a simplified model system that can be used to study the formation of micro- and macroaggregates from clean well-defined materials. Aggregation of soils is a very complex process that is affected by many interacting processes. The reduced and simplified model system was used specifically study the effects of microbial activity and mineral interactions on the aggregation occurring during incubation.

1.2.4 Aim: to study the development of organic matter properties and composition, and the effect of organic matter and mineral components on the phenanthrene sorptive interface during artificial soil incubation

The distribution of OM over particle size fractions with time and development of the OM composition of the fine fraction was studied in order to determine the turnover of OM by microorganisms and development of OM properties during artificial soil incubation. In order to gain more insight into the contribution of specific minerals to sorption of phenanthrene to soil and to study the development of the sorptive interface over time, phenanthrene sorption experiments were carried out to artificial soils with different mineral compositions. Due to the

clearly defined composition and texture of the artificial soils, the specific effect of mineral composition on phenanthrene sorption, and its development during formation and maturation of the biogeochemical interfaces present in the artificial soils could be studied.

2.2 Artificial soil incubation

2.2.1 Experimental set-up

The artificial soil incubation experiment was carried out to facilitate the study of the initial formation of biogeochemical interfaces depending on mineral composition in well-defined soil-like systems with a known initial composition. Table 1 gives the composition of the different artificial soil mixtures composed of illite, montmorillonite, ferrihydrite, boehmite, and/or charcoal. All model materials were well-characterized before the start of the incubation. Quartz was assumed to be inert and quartz material of sand, silt and clay size was used to provide texture for the artificial soils. All artificial soil compositions were prepared with the same texture. The amount of sand and clay mineral or clay-sized quartz added for each composition (table 1) was varied slightly to account for differences in the particle size distribution of the clay minerals and the clay-sized quartz. These materials were added in such amounts that the mass of the fraction $< 6.3 \mu\text{m}$ always represented 6.4 % of the total soil mass. The added ferrihydrite, boehmite and charcoal were accounted as part of the mass of the $< 6.3 \mu\text{m}$ fraction because of their high reactivity and SSA. Dried and sterilized manure was used as an organic carbon (OC) source, as this material is a major source of OM in arable soils and is already partly decomposed, which makes it more akin to soil OM than fresh plant material. A microbial community was extracted from a well-characterized arable soil to ensure that a microbial community was present that could be related to that found in natural soils of interest. The mixing and wetting of the artificial soils is shown in figure 1.



Figure 1. Mixing of the model materials (A, B) and initial wetting of the artificial soil batches.

Artificial soil batches were prepared for 4 sampling times (3, 6, 12 and 18 months of incubation) and three replicates were prepared for each composition and time step, resulting in a total number of 96 batches consisting of 1 kg artificial soil each. The artificial soils were

incubated in the dark in an incubation chamber. These incubation conditions were chosen to avoid complications due to variable environmental influences so that the interpretation of the experimental results could be focused on the effect of artificial soil composition and incubation time alone.

2.2.2 Model materials

Quartz (Quarzwerte GmbH, Frechen, Germany) was used in three different grain sizes, sand-sized (Quartz Sand Haltern, H33), silt-sized (Millisil W11 H) and clay-sized (Silmicron VP 795-10/1) and used to simulate soil texture. The montmorillonite (Ceratosil WG, Süd-Chemie AG, Moosburg, Germany) was used without further preparation. The illite (Inter-ILI Mernöki Iroda, Hungary) was ground and dry sieved to a grain size $< 63 \mu\text{m}$. A 6-line ferrihydrite was synthesized in the laboratory according to the method of Schwertmann and Cornell (1991). Boehmite (Capatal A Alumina, Sasol North America, Westlake, Louisiana) was selected for its similar SSA as ferrihydrite and used as received. Charcoal was produced from commercial barbecue charcoal that was ground and dry sieved to a grain size of 60-200 μm . Manure from a long-term fertilization experiment in Bad Lauchstädt was used as an OM source for the artificial soils. It was air dried, sieved $< 2 \text{ mm}$ and autoclaved 4 times. The mineralogy of the illite, montmorillonite and ferrihydrite was checked using X-ray diffraction (XRD) (PW 1830 generator, Philips, Eindhoven, the Netherlands). An extensive characterization of the clay minerals and their surface properties can be found in Macht et al. (in press). The sand ($> 63 \mu\text{m}$) content of the model materials was determined by sieving and the grain size distribution of the $< 63 \mu\text{m}$ fraction of the illite, montmorillonite and clay-sized quartz was determined by X-ray attenuation (SediGraph 5100/Master Tech 051, Micromeritics GmbH, Mönchengladbach, Germany).

The water extractable community from a Eutric Cambisol from Ultuna, Sweden was used as microbial inoculum for the artificial soils. The extract was prepared by shaking a suspension of the soil for 2 hours with gravel and subsequently centrifugate it at 1000 g for 12 minutes. The supernatant was then transferred to a new vial and centrifuged at 4000 g for 30 minutes and the precipitate was suspended in 10 ml of water per vial and used as the stock inoculum. The ratio of g soil to ml inoculant produced was 1:15, and 60 ml of inoculant was added for each kg of artificial soil. The batches were mixed thoroughly after inoculation to ensure homogeneous distribution of the microbial communities.

2.2.3 Artificial soil incubation and sampling

The artificial soils were incubated in the dark at an average temperature of 20°C (figure 2). The batches were kept at a constant water content of 60% of the maximum water holding capacity and were gently mixed weekly to ensure homogeneous conditions. The initial wetting of the artificial soils was done with a 0.01 M CaCl₂ solution to provide a simple background soil solution matrix with an ionic strength typical for soils. The soils were inoculated 3 days after the matrix solution was added to the artificial soil mixtures. There were therefore 3 days at the start of the experiment during which abiotic interactions could occur. The day of inoculation was taken as t=0 for the incubation experiment. The microbial activity of the soils was tested regularly by measuring the CO₂ respiration of the artificial soils. For this purpose, an aliquot of 20 g of the artificial soils was incubated for 5 days in a separate airtight glass bottle. CO₂ was adsorbed in 0.01 N NaOH and the amount of CO₂ adsorbed was determined by titration of the remaining base according to the method of Isermeyer (1951). Respiration measurements were performed using three replicate batches for each artificial soil composition. The cumulative CO₂ respiration rates were calculated, and confidence intervals indicated based on maximum and minimum respiration rates for each point, as determined from the standard deviation of the three replicates for each composition. At the respective sampling times (3, 6, 12 and 18 months of incubation), three batches of each artificial soil composition were terminated and sampled. The soil material was air-dried and the mass contribution of aggregates > 2 mm was determined by dry sieving.

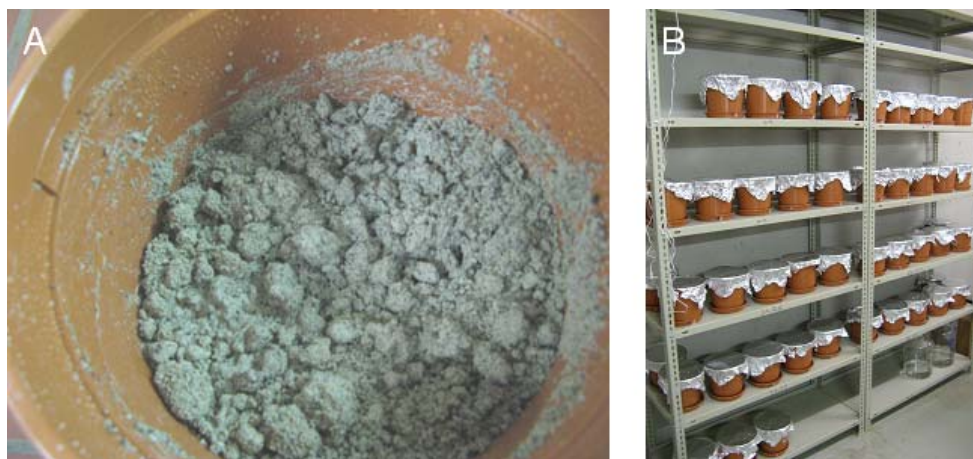


Figure 2. Examples of the artificial soils during incubation

2.3 Fractionation and sample preparation

2.3.1 Particle size fractionation

The soil samples were air-dried and the fraction of the soil > 2 mm removed by sieving. This fraction consisted of 1.8% mass of SCE, was negligible in UL-Ca and UL-m, and not present in the artificial soils. The natural soils were separated into seven size fractions: coarse and medium sand (200 - 2000 μm), fine sand (63 - 200 μm), coarse silt (20 - 63 μm), medium silt (6.3 - 20 μm), fine silt (2 - 6.3 μm), coarse clay (0.2 - 2 μm) and fine clay (< 0.2 μm). The method for aggregate disruption was adapted from Schmidt et al. (1999) and Amelung and Zech (1999). For ultrasonic dispersion, 150 ml of water was added to 30 g sample and treated with an energy of 60 J ml⁻¹ (dispersion tip Bandelin electronics, Sonoplus UW 2200, Berlin, Germany) to disrupt macro-aggregates (250-2000 μm), after which the coarse and medium sand fractions were separated by wet sieving to avoid the disruption of particulate organic matter. The remaining sample was treated with ultrasonic dispersion at different energies ranging from 100 to 800 J ml⁻¹. The results of the fractionation procedure at different energies were compared to texture analysis (see below) to determine the appropriate energy necessary to disrupt all microaggregates (< 250 μm). An energy of 200 J ml⁻¹ was chosen for the further fractionation of all soils. The fine sand and coarse silt fractions were separated by wet sieving. The clay, fine and medium silt fractions were separated by sedimentation. Coarse and fine clay were separated by centrifugation (Jouan KR4i, Jouan GmbH, Unterhaching, Germany). All fractions were freeze-dried before storage. The artificial soils were separated into a coarse and medium sand (200-2000 μm), fine sand (63-200) coarse silt (20-63) and medium + fine silt and clay fraction ($< 20\mu\text{m}$) by wet sieving. Ultrasonic dispersion with a total energy of 60 J ml⁻¹ was used to break up macroaggregates.

2.3.2 Density fractionation

Density fractionation was used to separate the artificial soil in four fractions; particulate organic matter > 20 μm (POM > 20 μm), particulate organic matter < 20 μm (POM < 20 μm), microaggregates and minerals (figure 3). For the fractionation procedure, 25 g of soil was suspended with 150 ml Na polytungstate with a density of 1.8 g cm⁻³ and subjected to ultrasonic dispersion at 60 J ml⁻¹ to disperse macroaggregates (dispersion tip Bandelin electronics, Sonoplus UW 2200, Berlin, Germany). Only low ultrasonic dispersion energy was used to preserve the newly formed microaggregates. The suspension was then centrifuged at 3074 g for 20 min (Jouan KR4i, Jouan GmbH, Unterhaching, Germany) and the

supernatant removed. 100 ml Na polytungstate was added to the sediment and centrifuged again. The supernatant of these two extractions was combined, washed and sieved $< 20 \mu\text{m}$ to produce the fractions of $\text{POM} > 20 \mu\text{m}$ and $\text{POM} < 20 \mu\text{m}$. Na polytungstate with a density of 2.4 g cm^{-3} was added to the sediment and this was shaken and centrifuged at 3074 g for 20 min to separate the organo-mineral and mineral fractions. This procedure was repeated twice. All samples were washed free of salt by pressure filtration until the electric conductivity was below $5 \mu\text{S cm}^{-1}$.

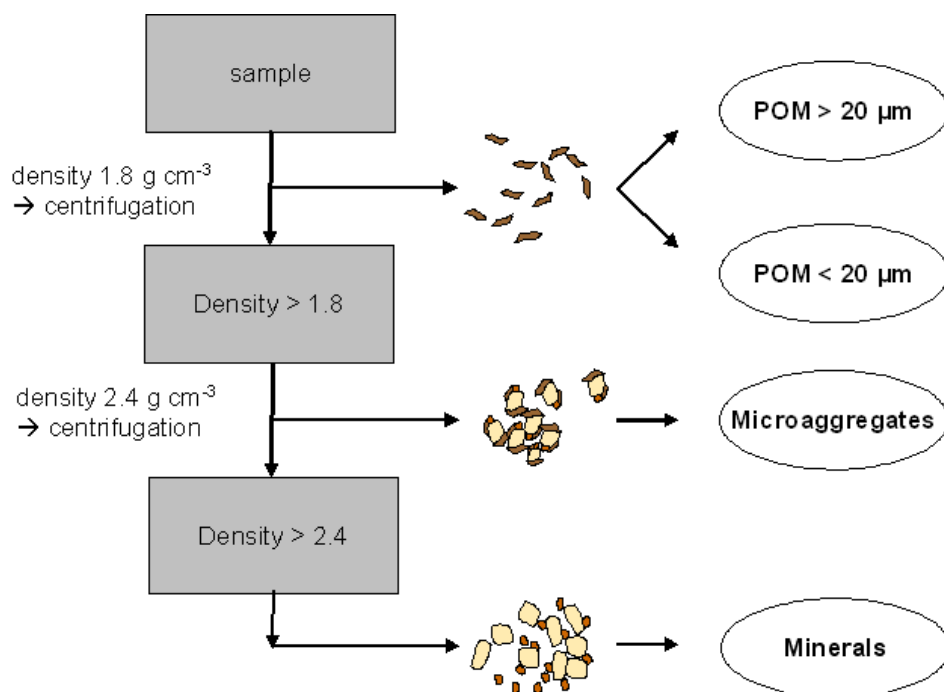


Figure 3. Overview of the density fractionation procedure, separating the sample into a particulate organic matter (POM), a microaggregates and a mineral fraction.

2.3.3 Organic matter oxidation

Organic matter oxidation was performed on the bulk soil and particle size fractions of UL-Ca. The H_2O_2 oxidation method was chosen for organic matter oxidation because it was also used in the texture analysis. Five gram of each sample was weighed into a glass beaker and an excess of H_2O_2 (30%) was added and allowed to react with the sample until no more bubbles could be seen. Then, 500 ml of distilled water was added to the samples and they were put into an oven at 60°C for 12 hours to remove excess H_2O_2 . The samples were then freeze-dried and kept for further analysis.

2.4 Analytical methods

2.4.1 Sample characterization, pH, C and N content and texture

The pH was determined in duplicate in 0.01 M CaCl₂ at a soil: solution ratio of 1:2.5. Carbon and nitrogen content were determined in duplicate by combustion and chromatographic separation with an elemental analyzer (Hekatech, Euro EA 3000, Wegberg, Germany). For the texture analysis, organic matter was removed from the bulk soils by oxidation with 30% H₂O₂. The sand fractions (> 63 μm) were separated by wet sieving and the remaining sample was dispersed with 0.4 N Na₄P₂O₇ and measured by X-ray attenuation (SediGraph 5100/Master Tech 051, Micromeritics GmbH, Mönchengladbach, Germany) to determine particle size distribution (adapted from Leifeld and Kögel-Knabner (2003)).

The contact angle (CA) of the natural soil samples used for phenanthrene sorption experiments (UL-m, UL-Ca and SCE) was determined with the Sessile Drop Method (SDM) (Bachmann *et al.*, 2003) using a contact angle microscope with video camera (OCA 20, DataPhysics, Filderstadt, Germany). A one-grain-layer of the homogenized sample was fixed on a glass slide with double sided adhesive tape and a drop of deionised water (V=3μL) placed on the surface. The placing of the drop and its subsequent behaviour was recorded and then the CA determined by drop shape analysis using the software SCA20 (DataPhysics, Filderstadt, Germany). CA was measured after 30 ms (initial CA) and after 1000 and 5000 ms.

2.4.2 Specific surface area (SSA)

The SSA was determined by two different methods, BET-N₂ and EGME retention. The EGME method of measuring surface area consists of drying the samples under vacuum and then applying EGME to it. The weight change of the sample was measured until it was less than 1 mg for 3 days. The surface area was then calculated assuming that EGME covered the sample in a monolayer. SSA can then be calculated from the size of the EGME molecule and the total weight of EGME adsorbed on the sample. The analysis was performed following the method of van Reeuwijk (2002).

BET-N₂ is a standard method for measuring surface area in soils based on physisorption of N₂ gas on a sample at 77 K (Brunauer *et al.*, 1938). SSA was calculated using the BET equation:

$$\frac{1}{W((P_0/P)-1)} = \frac{1}{W_m C} + \frac{C-1}{W_m C} \left(\frac{P}{P_0} \right) \quad (1)$$

where W is the weight of gas adsorbed at relative pressure P/P_0 and W_m is the weight of the adsorbate at monolayer coverage of the sample surface. C is a constant related to the enthalpy of nitrogen adsorption on the sample and depends on sample properties. Nitrogen adsorption was measured at 11 points in the partial pressure range of 0.05 to 0.3 with an Autosorb-1 analyzer (Quantachrome, Syosset, NY, USA). Before measurement, water was removed from the sample surface by outgassing for 14-20 hours in vacuum under helium flow at 40 °C.

C constant

The C constant is related to the enthalpy of nitrogen gas on the sample surface. It can be calculated by rewriting the BET equation. In a BET plot with P/P_0 on the x-axis and $1/(W((P_0/P)-1))$ on the y-axis, the C constant is calculated as:

$$C = \frac{s}{i} + 1 \quad (2)$$

where s is the slope and i is the intersect with the y-axis of the BET plot.

The use of the entire BET isotherm can lead to large errors in the calculation of the C constant (Mayer, 1999). Therefore, the residual between the measured partial pressure points and the BET isotherm was calculated and from this, the 3 to 5 points where the isotherm is steepest were selected manually and used for the calculation of the C constant. A detailed discussion of the calculation procedure can be found in Mayer (1999). C constants were only calculated for samples for which total adsorbent surface area detected exceeded 4 m². The C constant of soil material is affected by the organic matter content of the sample and the microporosity (Mayer, 1999; Wagai et al., 2009). High organic matter coverage of the surface will lead to a low C constant, as the affinity of N₂ to the organic matter surface is low. A microporous surface on the other hand will lead to a high C constant.

2.4.3 Oxide extraction

Soluble Fe, Al und Si contents of the artificial soils containing ferrihydrite, boehmite and clay-sized quartz were determined after CuCl₂ (Juo and Kamprath, 1979), dithionite (Mehra

and Jackson, 1960), oxalate (Schwertmann, 1964) and Na-pyrophosphate extraction (van Reeuwijk, 2002). Extractable Fe, Al and Si content were determined by ICP-OES (Vista-Pro, Varian). For the natural soils, oxides were extracted using dithionite-citrate-bicarbonate (DCB) (Mehra and Jackson, 1960) and oxalate (Schwertmann, 1964) extraction on separate samples. Iron and aluminum and silicon release was measured with inductively coupled plasma optical emission spectroscopy (ICP-OES) (Vista-Pro, CCD simultaneous, Varian, Darmstadt, Germany). The oxalate extraction method is commonly used to extract only the poorly crystalline fraction of the iron oxides, whereas with the DCB extraction method, all iron oxides are extracted (Cornell and Schwertmann, 1996). Aluminum was present in the extracts of the natural soil samples at a concentration of approximately 10% of the iron concentration. As iron oxides were the dominant phase, the study of the natural soils was limited to these oxides. All analyses were performed on two replicates of each sample.

2.4.3.1 Sample properties after oxide extraction

The samples from the natural soils and their particle size fractions were saved after oxide extraction, centrifuged and washed with distilled water until the conductivity was less than 50 $\mu\text{S cm}^{-1}$. The samples were then freeze-dried and their carbon content and BET-N₂ SSA was determined. Care was taken to recover the complete sample and minimize any loss of material. The loss of SSA and carbon associated with the extraction of oxides by oxalate and dithionite was then calculated.

Surface area of the weakly-crystalline and crystalline oxides

The BET-N₂ SSA was determined before and after dithionite and oxalate extraction. Based on the applied methods, three fractions were defined that contributed to the total surface area of the sample: the weakly crystalline oxides, the crystalline oxides and the residue. The contribution of each fraction to the total surface area of the sample was calculated, and a correction was made to account for the loss of mass after extraction (Kiem and Kögel-Knabner, 2002). The SSA of the respective fractions was calculated as follows:

$$SSA_{residue} = SSA_{dit} \times f_{dit} \quad (3)$$

$$SSA_{weakly-crystalline-oxides} = SSA_{untreated} - (SSA_{ox} \times f_{ox}) \quad (4)$$

$$SSA_{crystalline-oxides} = SSA_{untreated} - SSA_{residue} - SSA_{weakly-crystalline-oxides} \quad (5)$$

where $SSA_{\text{untreated}}$, SSA_{dit} and SSA_{ox} are the BET- N_2 SSA in $\text{m}^2 \text{g}^{-1}$ of the untreated, the dithionite, and the oxalate extracted samples, respectively, and f_{dit} and f_{ox} are the weight fractions of sample left over after dithionite and oxalate extraction.

Carbon loss after oxide extraction

Carbon concentrations were determined before and after extraction with dithionite and oxalate. Carbon associated with the extracted oxides is dissolved by this treatment and the loss of carbon after extraction gives information about the amount of carbon associated with these oxides. Carbon associated with weakly crystalline and crystalline oxides in $\text{mg C (g soil)}^{-1}$ was calculated according to the following equations:

$$C_{\text{residue}} = C_{\text{dit}} \times f_{\text{dit}} \quad (6)$$

$$C_{\text{weakly-crystalline-oxides}} = C_{\text{untreated}} - (C_{\text{ox}} \times f_{\text{ox}}) \quad (7)$$

$$C_{\text{crystalline-oxides}} = C_{\text{untreated}} - C_{\text{residue}} - C_{\text{weakly-crystalline-oxides}} \quad (8)$$

where $C_{\text{untreated}}$, C_{dit} and C_{ox} are the concentration in mg C g^{-1} of the untreated, the dithionite and the oxalate extracted samples, respectively, and f_{dit} and f_{ox} are the weight fractions of sample left over after dithionite and oxalate extraction.

2.4.4 Solid-state ^{13}C NMR

The composition of the OM of selected samples was determined with solid-state ^{13}C nuclear magnetic resonance (NMR) spectroscopy. Prior to solid-state ^{13}C NMR measurement of the natural soil samples and selected particle size fractions, the mineral phase was removed with 10% HF according to the method described by (Gonçalves *et al.*, 2003) to avoid the interference of iron. The extraction procedure was repeated 5 times. Carbon content before and after extraction was measured and the recovery of OC after HF extraction was calculated. Extraction of the mineral phase by HF was not required for the artificial soils due to their low iron contents.

Samples were analyzed with a DSX 200 spectrometer (Bruker Biospin, Rheinstetten, Germany) operating with a cross-polarization magic angle spinning (CP MAS) technique at the resonance frequency of ^{13}C . The acquisition parameters included a spinning rate of 6.8 kHz, a contact time of 0.2 ms and a pulse delay between 0.2 and 0.6 s. Chemical shifts were

calibrated relative to tetramethylsilane (0 ppm). Depending on the carbon concentration, a minimum of 11 000 scans were accumulated for each sample. A line broadening of 75 Hz was applied. The contributions to the various C groups were determined by integration of their signal intensity in their respective chemical shift regions by means of the instrument software. Chemical shift regions were used as follows, alkyl C 0-45 ppm, O/N-alkyl C 45-110 ppm, aryl-C 110-160 ppm and carbonyl/carboxyl/amide C 160-220 ppm (Knicker & Lüdemann, 1995).

2.5 Phenanthrene sorption experiments

Sorption experiments were carried out on the bulk soil and particle size fractions of the natural soils from Ultuna (UL-Ca and UL-m) and on selected < 20 μm fractions of the artificial soils that were incubated 3 and 12 months. The particle size fractions of UL-Ca and UL-m considered were the recombined fractions of coarse + medium silt (6.3-63 μm), hereafter referred to as the ‘coarse fraction’, and fine silt + coarse clay (0.2-6.3 μm), hereafter referred to as the ‘fine fraction’, and on the bulk soil (< 2000 μm). The coarse fraction represented 29% of the mass of the bulk soil consisting in itself of 37% coarse and 63% medium silt, whereas the fine fraction represented 44% mass of the bulk soil and consisted of 34% fine silt and 66% coarse clay. These two fractions were chosen for the sorption experiments because they represent the main part of the OC present in the soil with 20% of the total soil carbon content for the coarse + medium silt and 62 % for the fine silt + coarse clay fraction, respectively.

2.5.1 Batch experiments

Phenanthrene sorption experiments were carried out in batch experiments (figure 4) in a concentration range of approximately 10 to 50% of the water solubility of phenanthrene (OECD, 2000). The water solubility of phenanthrene was taken as 1.1 mg l^{-1} (Vowles & Mantoura, 1987). A preliminary kinetic experiment from 3 to 72 hours showed that 24 hours of reaction time was sufficient to reach apparent equilibrium (data not shown).

One gram of sample was added to 75 ml of 0.01 M CaCl_2 solution, containing $2 \cdot 10^{-6}$ M AgNO_3 to prevent microbial activity. The batches were equilibrated for 24 hours, before phenanthrene dissolved in 50 μl methanol was added to the batches. The same volume of methanol was added to all samples to eliminate matrix effects. Each batch experiment

included one control with only soil material and control batches with only phenanthrene for each concentration and a blank. The batches were equilibrated for 24 hours and continuously shaken horizontally at 125 rpm to ensure sample homogeneity and to avoid sedimentation. After equilibration, the batches were centrifuged; the supernatant was decanted and used for further extraction.



Figure 4. Batch with soil sample used for the phenanthrene sorption experiments.

2.5.2 Phenanthrene extraction and quantification

Phenanthrene-D10 was added to the samples as an internal standard and used for the quantification. The phenanthrene was extracted using a solid phase extraction (SPE) method adjusted from (Müller et al., 2007) (figure 5). Finally, phenanthrene was eluted from the columns using 8 ml of a hexane: dichloromethane 4:1 mixture. Fluorene-D10 was added as a recovery standard and the phenanthrene concentrations were determined using gas chromatography mass spectroscopy (GC-MS) (GC 8000 Top, MS Voyager, Fisons Instruments) with an OPTIMA-5-Accent Fused Silica capillary column (length 30 m x inner diameter 25 mm x film thickness 0.25 μm). 1.0 μl of sample was injected splitless at an injector temperature of 280°C. Helium was used as carrier gas with a constant flow rate of 1 ml min^{-1} . The oven program started with 4 min at 85°C, then increased with 15°C min^{-1} to 160°C and stayed at this temperature for 2 min. The temperature was then increased to 230°C at a rate of 5°C min^{-1} and kept there for another 2 min.

Phenanthrene and phenanthrene-D10 were produced by Ultra Scientific (North Kingstown, RI, USA). Phenanthrene had a matrix of methanol and a concentration of $5011 \pm 25 \mu\text{g mL}^{-1}$ and phenanthrene-D10 a matrix of dichloromethane and a concentration of $1002 \pm 5 \mu\text{g mL}^{-1}$. The fluorene-D10 (Cambridge Isotope Laboratories Inc, Andover, MA, USA) had

a matrix of isooctane and a concentration of $200 \mu\text{g mL}^{-1}$ with a purity of 98%. All solvents used were of Pestinorm purity grade.

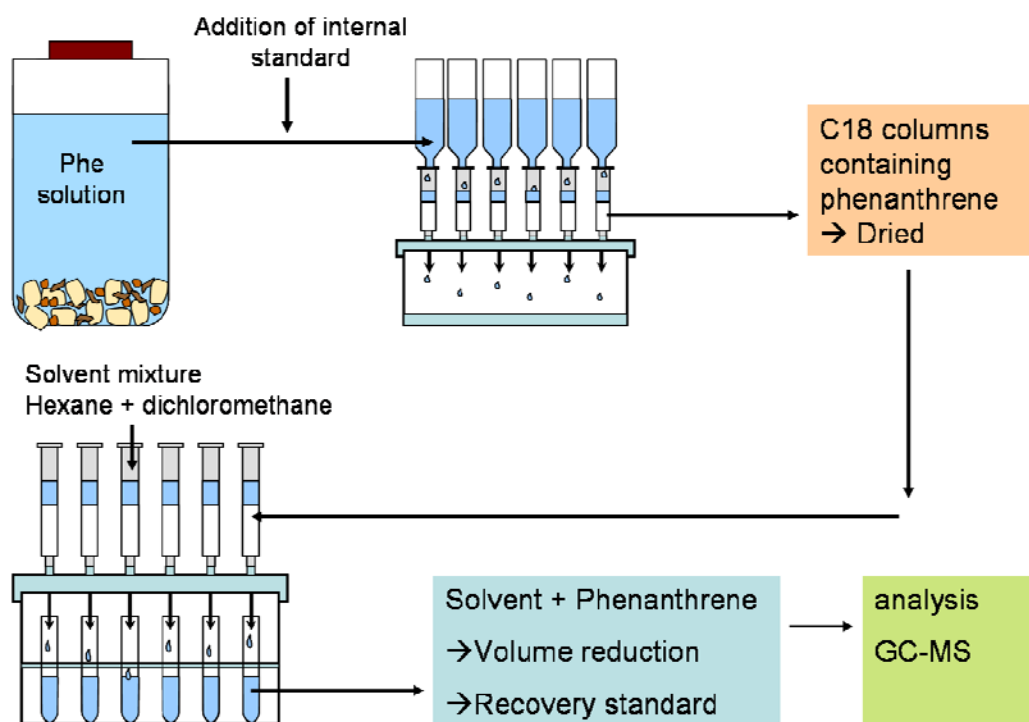


Figure 5. Schematic overview of the phenanthrene extraction method.

2.5.3 Isotherm modelling

The experimental isotherms were mathematically analyzed using a model discrimination approach similar to (Müller *et al.*, 2007), to identify the best fit sorption isotherm model. Among others, the linear-, the Langmuir, the multi-site Langmuir-, the BET and the Freundlich-sorption models were used within a constrained non-linear least squares algorithm. The goodness of fit criteria used to identify the best-fit-model were the root mean square error, the adjusted coefficient of determination and reference criteria that directly compared the competing models. In almost all cases, best performance was found for the Freundlich isotherm model (equation 1)

$$C_{(s)s} = K_f C_{(s)aq}^{1/n} \quad (1)$$

where $C_{(s)s}$ is the concentration of phenanthrene adsorbed to the solid phase at equilibrium in $\mu\text{g g}^{-1}$, $C_{(s)aq}$ is the equilibrium concentration of phenanthrene in the liquid phase in $\mu\text{g mL}^{-1}$, K_f is the Freundlich adsorption coefficient in mL g^{-1} . The value $1/n$ is a measure which relates to the distribution of the heat of adsorption and thus to the heterogeneity of the sorbent.

3 Iron oxides as major available interface component in loamy arable topsoils

3.1 Results

3.1.1 Texture and particle size fractionation

Particle size fractionation after dispersion of the soils at different ultrasonic energy levels from 100 to 800 J ml⁻¹ did not result in significant changes in particle size distribution (figure 6). For UL-Ca, a slight increase in the mass contribution of fine silt (6.3-63 μm) could be seen at the highest energy level (800 J ml⁻¹), but no differences were detected at any energy level for the other fractions. For the Luvisol (SCE), a slightly decreasing trend with dispersion energy was seen for the coarse silt (20-63 μm) content, but no clear change in particle size distribution with dispersion energy occurred in the other fractions.

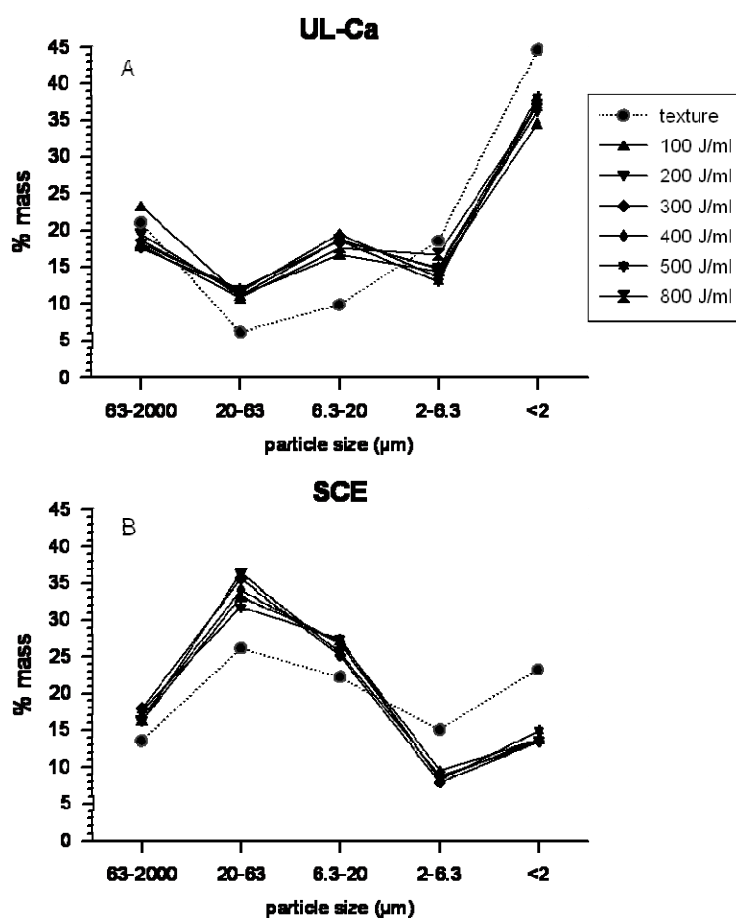


Figure 6. % mass contribution to different particle size fractions from texture analysis (dotted line) and particle size fractionation (black lines) of Ultuna (A, UL-Ca) and Scheyern (B, SCE) soils at ultrasonic dispersion energies between 100 and 800 J ml⁻¹.

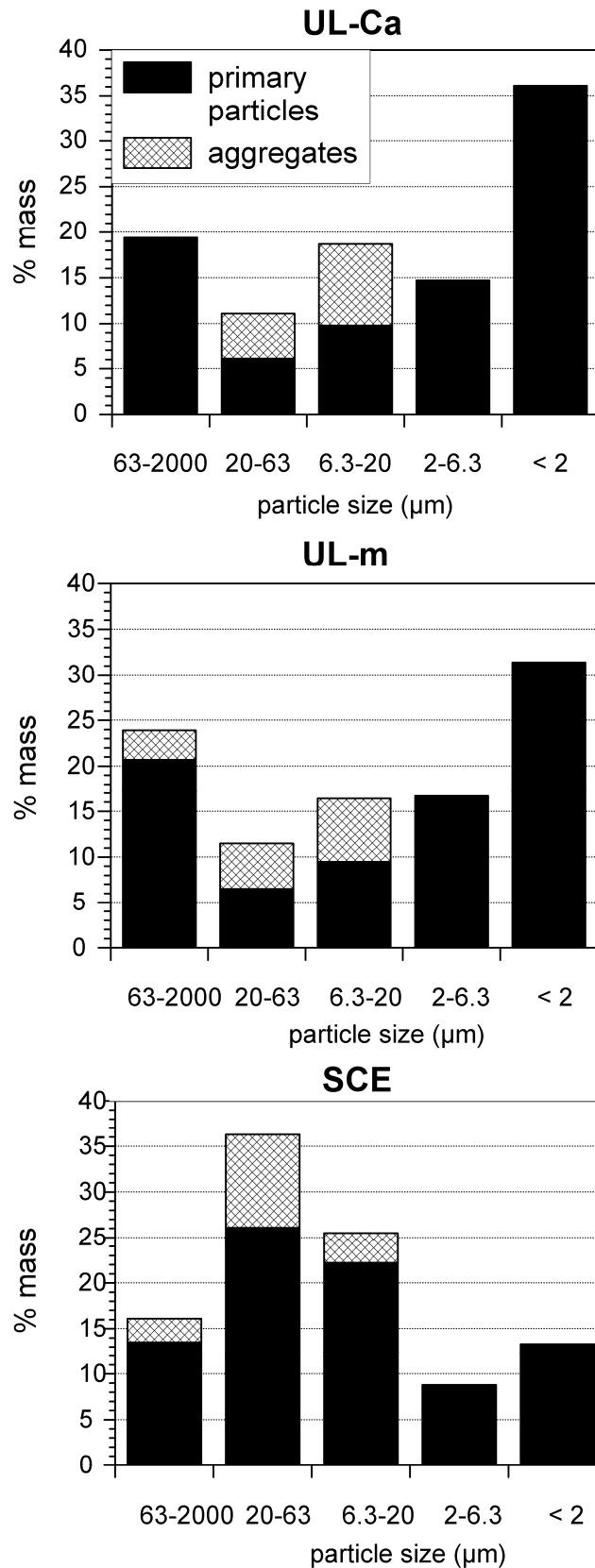


Figure 7. Particle size distribution after particle size fractionation. The mass % of aggregates indicated was calculated from the difference between particle size fractionation and texture analysis. The data of particle size fractionation with a dispersion energy of 200 J ml^{-1} were used.

However, there was a discrepancy with texture analysis. Fractionation resulted in a significantly larger content of coarse and medium silt particles and a lower fine silt and clay content compared to textural analysis in all three soils. This indicates that the silt fractions gained by particle size fractionation were in fact composed of both primary particles and microaggregates that were not broken up by the dispersion method (figure 7). When regarded as mass contribution to the bulk soil, 12 to 14% of the total soil mass was redistributed from the coarse + medium silt fraction to the fine fractions by the chemical treatments performed before texture analysis, compared to particle size fractionation. This gives a decrease of 42 to 48% of the amount of coarse and medium silt present from particle size fractionation to texture analysis for UL-Ca and the manure fertilized Cambisol (UL-m). In SCE, the decrease was not as large, with a decrease of 28 and 13% for coarse and medium silt, respectively, but this still represents 14% of the total soil mass. Based on the calculated presence of microaggregates after particle size fractionation the fractions were grouped as 'coarse fraction' (medium and coarse silt, sand) and 'fine fraction' (fine silt and clay).

3.1.2 Characterization of the particle size fractions

The carbon content (table 2) of all soils was relatively low with carbon concentrations between 14.7 and 21.1 mg C g⁻¹. As expected, carbon concentration increased and the C/N ratio decreased with decreasing particle size (Christensen, 1992). The additional organic carbon in UL-m, when compared to UL-Ca, was mainly present in the sand and coarse silt fractions and in the fine silt fraction. The carbon concentrations in the clay fractions were only slightly higher in UL-m with respect to UL-Ca.

The iron content of UL and SCE (table 2) was similar with 3.88 to 4.50 mg g⁻¹ oxalate extractable iron (Fe_o) and 7.32 to 8.14 mg g⁻¹ dithionite extractable iron (Fe_d) for the bulk soils. Both Fe_o and Fe_d content increased with decreasing particle size to a maximum of 12.12 mg g⁻¹ Fe_o in the fine clay fraction of SCE and 27.43 mg g⁻¹ Fe_d for the fine clay fraction of UL-Ca. The Fe_o/Fe_d ratio (table 2), which indicates the relative mass contribution of weakly crystalline and crystalline oxides, was similar for all soils. Although slightly higher values were observed for UL-m compared to UL-Ca and SCE, no clear trend in Fe_o/Fe_d ratio with particle size could be seen.

Table 2. Sample properties of bulk soil and particle size fractions. SSA is specific surface area, Fe_o represents oxalate extractable iron and Fe_d represents dithionite extractable iron.

Soil	Fraction (μm)	% mass of bulk	C (mg g^{-1})	N (mg g^{-1})	C/N	Fe _o (mg g^{-1})	Fe _d (mg g^{-1})	Fe _o /Fe _d	BET-N ₂ SSA (m^2g^{-1})
UL-Ca	bulk soil		14.7	1.50	9.8	4.50	7.35	0.61	19.7
	2000-200	3.3	6.4	0.20	31.8	3.73	n.d. [†]	n.d. [†]	3.6
	63-200	16.0	1.8	0.10	18.4	1.46	3.82	0.38	1.6
	20-63	11.0	8.3	0.49	16.9	1.84	3.47	0.53	2.6
	6.3-20	18.5	10.9	0.79	13.9	1.71	3.61	0.47	5.6
	2-6.3	14.5	18.7	1.57	11.9	3.33	5.81	0.57	10.6
	0.2-2	29.3	21.6	2.58	8.4	6.75	14.94	0.45	32.5
	< 0.2	7.4	30.0	3.82	7.9	8.50	27.43	0.31	78.1
UL-m	bulk soil		21.1	2.19	9.6	3.88	7.32	0.53	13.1
	2000-200	4.2	32.0	1.84	17.4	n.d. [†]	n.d. [†]	n.d. [†]	4.4
	63-200	19.9	7.7	0.50	15.5	1.39	2.47	0.56	0.9
	20-63	11.5	18.6	1.26	14.8	2.01	3.07	0.65	2.2
	6.3-20	16.4	10.4	0.83	12.5	1.81	2.98	0.61	6.2
	2-6.3	16.7	27.6	2.63	10.5	3.43	6.17	0.56	16.1
	0.2-2	29.0	26.0	3.13	8.3	6.59	13.05	0.51	29.0
	< 0.2	2.4	31.3	3.24	9.7	11.54	21.44	0.54	49.7
SCE	bulk soil		15.1	1.68	9.0	4.13	8.14	0.51	6.9
	2000-200	7.4	26.6	1.14	23.3	n.d. [†]	n.d. [†]	n.d. [†]	n.d. [†]
	63-200	8.5	5.7	0.37	15.3	3.21	4.32	0.74	2.6
	20-63	35.8	5.3	0.40	13.3	1.07	2.15	0.50	1.6
	6.3-20	25.1	7.3	0.76	9.7	1.94	4.58	0.42	4.4
	2-6.3	8.7	34.9	3.68	9.5	7.48	15.82	0.47	13.3
	0.2-2	13.1	37.8	4.88	7.7	12.12	25.39	0.48	31.1
	< 0.2	1.4	62.3	14.8	4.2	n. d. [†]	n. d. [†]	n. d. [†]	21.3

[†] n. d.: not determined

The BET-N₂ SSA of the bulk soils ranged between 6.9 and 19.7 m² g⁻¹ for the three bulk soils. SSA increased with decreasing particle size (table 2). The SSA of the particle size fractions of UL-Ca and UL-m are relatively similar except for the fine clay where UL-m has a lower SSA. The relative contribution of each particle size fraction to the bulk soil SSA was calculated by multiplying its SSA by the mass contribution in % of the bulk soil. This showed that particle size fractionation did not increase the SSA of UL-Ca and UL-m, as the bulk SSA was the same as the sum of all particle size fractions (table 3), and only a slight increase was seen in SCE.

Table 3. Surface area stocks calculated for each fraction by multiplying the respective specific surface area by the mass contribution in % of the bulk soil.

Fraction (μm)	UL-Ca (m^2g^{-1})	UL-m (m^2g^{-1})	SCE (m^2g^{-1})
bulk soil	19.7	13.1	6.9
2000-200	0.1	0.2	n.d. †
63-200	0.3	0.2	0.2
20-63	0.3	0.3	0.6
6.3-20	1.0	1.0	1.1
2-6.3	1.5	2.7	1.2
0.2-2	9.5	8.4	4.1
< 0.2	5.8	1.2	0.3
sum	18.5	13.9	7.4

† n.d.: not determined

For UL-Ca, SSA of the particle size fractions was also measured after H_2O_2 oxidation in order to investigate the effect of this treatment on the SSA (table 4). The efficiency of carbon oxidation by H_2O_2 was determined by measuring OC of the samples before and after H_2O_2 oxidation. The so determined amount of carbon oxidized was > 90% of the total OC content in all samples tested (data not shown). Removal of the organic matter caused an increase in the SSA in the bulk soil and clay fractions, but no increase was seen in the fine silt and coarse fractions and SSA decreased in the medium silt fraction. A decrease in C constant also occurred in the silt fractions (2-63 μm), while there was a clear increase of the C constants in the clay fractions (< 2 μm).

Table 4. BET- N_2 specific surface area (SSA) and C constant of UL-Ca before and after organic matter removal by H_2O_2 oxidation.

Fraction (μm)	SSA (m^2g^{-1})		C constant	
	untreated	H_2O_2	untreated	H_2O_2
bulk soil	19.7	26.9	139	109
63-200	1.6	1.6	b. d. l. †	b. d. l. †
20-63	2.6	2.1	85	b. d. l. †
6.3-20	5.6	3.0	67	51
2-6.3	10.6	10.9	79	43
0.2-2	32.5	39.2	101	123
<0.2	78.1	97.2	77	155

† b. d. l.: below detection limit; a minimum total adsorbent surface present of 4 m^2 is required for the calculation

3.1.3 Specific surface area of the iron oxides

Mass recoveries of the samples after iron extraction were between 92 and 97% for oxalate and 72 to 97% for dithionite extraction for all fractions except the fine clay. Recovery decreased with decreasing particle size. The recovery of the fine clay fractions was much lower than that of the other fractions, probably due to the loss of colloids in the washing procedure. In UL-Ca and the oxalate extracted fraction of UL-m, reasonable amounts of fine clay were recovered (between 61 and 89%), but recoveries for the other samples were so low that the data were excluded from the calculation.

The calculated distribution of surface area between crystalline ($SSA_{\text{crystalline oxides}}$) and weakly crystalline oxides ($SSA_{\text{weakly crystalline oxides}}$) and residue material (SSA_{residue}), which represents all non extractable minerals and the remaining organic matter in the sample, showed that oxides contribute significantly to SSA of the bulk soil and all particle size fractions (table 5). Based on the difference between the calculated SSA_{residue} and the original SSA, the SSA_{residue} represented only ~ 20 to 50% (except for UL-m fine sand) of the original SSA of the sample, whereas the mass recoveries after dithionite extraction showed that the residue consisted of more than 72% of the mass for all samples.

The $SSA_{\text{crystalline oxides}}$ and SSA_{residue} increased with decreasing particle size (table 5). However, $SSA_{\text{weakly crystalline oxides}}$ did not show this trend. For the bulk sample of all three soils, the fine clay fraction (<0.2 μm) of UL-Ca and the clay fractions (0.2-2 and <0.2 μm) of UL-m, the calculated $SSA_{\text{weakly crystalline oxides}}$ even was negative due to a detected increase in SSA after oxalate extraction.

In the Ultuna soils, the dominant oxide type contributing to the surface area changed from the coarse (>6.3 μm) to the fine (< 6.3 μm) fractions. In the coarse fractions, the $SSA_{\text{weakly crystalline oxides}}$ was larger than or similar to the $SSA_{\text{crystalline oxides}}$ whereas in the fine fractions, the $SSA_{\text{weakly crystalline oxides}}$ was small or negative and the $SSA_{\text{crystalline oxides}}$ increased. For SCE, the relative contribution of weakly crystalline and crystalline oxides stayed the same for all particle size fractions except the sand, and $SSA_{\text{weakly crystalline oxides}}$ was low compared to $SSA_{\text{crystalline oxides}}$ and SSA_{residue} .

Table 5. Calculated surface areas (BET-N₂) of the crystalline and weakly crystalline oxides and residue in m²g⁻¹ of the complete sample.

Soil	Fraction (μm)	Weakly crystalline oxides (m ² g ⁻¹)	Crystalline Oxides (m ² g ⁻¹)	Residue (m ² g ⁻¹)	Total (m ² g ⁻¹)
UL-Ca	bulk soil	-1.8	15.3	6.1	19.7
	63-200	0.9	-0.2	0.9	1.6
	20-63	1.2	0.4	1.0	2.6
	6.3-20	2.0	2.2	1.4	5.6
	2-6.3	1.6	4.5	4.5	10.6
	0.2-2	1.8	14.7	16.0	32.5
	< 0.2	-10.6	33.8	54.9	78.1
UL-m	bulk soil	-2.5	9.0	6.6	13.1
	63-200	0.2	0.0	0.7	0.9
	20-63	1.2	0.2	0.8	2.2
	6.3-20	3.5	1.7	1.0	6.2
	2-6.3	3.2	8.2	4.8	16.1
	0.2-2	-5.3	17.5	16.8	29.0
	< 0.2	-24.4	n. d. †	n. d. †	49.7
SCE	bulk soil	-0.8	3.5	4.2	6.9
	63-200	1.8	0.4	0.05	2.6
	20-63	0.2	0.6	0.9	1.6
	6.3-20	0.7	1.9	1.8	4.4
	2-6.3	0.7	6.1	6.6	13.3
	0.2-2	1.7	14.8	14.6	31.1
	< 0.2	n. d. †	n. d. †	n. d. †	21.3

† n.d.: not determined

3.1.4 Carbon loss due to oxide extraction

For both dithionite and oxalate extraction, organic substances were added in the form of citrate and oxalate, respectively. These substances may have adsorbed to the sample, which would have increased the carbon content of the residue sample after extraction. This may have caused a slight underestimation in the amounts of oxide-associated carbon calculated. These values should therefore be seen as the lower estimate of the amounts of oxide associated carbon. The fine clay samples were excluded from the calculation because of their low mass recoveries.

Carbon contents of the samples decreased significantly after oxide extraction, which indicates that in all samples, significant amounts of carbon were associated with oxides (table 6). When calculated as a percentage of the total amount of OC present in the samples, the total oxide associated carbon (weakly crystalline + crystalline oxides) accounted for 35 to 70% of the total OC content. However, the residue (non-oxide-associated carbon) was the largest fraction in all but the coarse silt and fine sand fractions. The ratio of total oxide associated carbon to total extracted iron ($C_{\text{all oxides}}/Fe_d$) decreased with particle size (sand fractions excluded) in the Ultuna soils but increased from medium silt (6.3-20 μm) to the finer fractions in SCE.

Table 6. Carbon associated with weakly crystalline and crystalline oxides and the residue after dithionite extraction in mg C g^{-1} sample, the total original carbon content mg C g^{-1} , and the ratio of total dithionite extracted carbon ($C_{\text{all oxides}}$) to total dithionite extracted iron (Fe_d) where † indicates not determined.

Soil	Fraction (μm)	Weakly crystalline oxides (mg C g^{-1})	Crystalline oxides (mg C g^{-1})	Residue (mg C g^{-1})	Total (mg C g^{-1})	$C_{\text{all oxides}}/Fe_d$ (mg C g^{-1})
UL-Ca	bulk soil	0.8	4.7	9.2	14.7	0.7
	63-200	1.0	0.4	0.4	1.8	0.4
	20-63	4.8	0.4	3.1	8.3	1.5
	6.3-20	2.9	4.9	3.1	10.9	2.2
	2-6.3	0.1	5.6	13.1	18.7	1.0
	0.2-2	1.2	8.3	12.1	21.6	0.6
	< 0.2	n. d. †	n. d. †	n. d. †	n. d. †	n. d. †
UL-m	bulk soil	2.5	2.3	16.3	21.1	0.6
	63-200	6.1	1.0	0.6	7.7	2.9
	20-63	13.2	0.5	4.9	18.6	4.5
	6.3-20	1.1	5.3	4.0	10.4	2.1
	2-6.3	0.2	7.5	20.9	28.6	1.2
	0.2-2	3.8	7.4	14.9	26.0	0.9
	< 0.2	n. d. †	n. d. †	n. d. †	n. d. †	n. d. †
SCE	bulk soil	0.9	3.9	10.2	15.1	0.6
	63-200	1.9	0	3.9	5.7	0.4
	20-63	2.5	0.4	2.4	5.3	1.4
	6.3-20	1.1	0	6.4	7.3	0.2
	2-6.3	5.8	1.8	27.3	34.9	0.5
	0.2-2	9.3	10.2	18.3	37.8	0.8
	< 0.2	n. d. †	n. d. †	n. d. †	n. d. †	n. d. †

3.2 Discussion

3.2.1 Stable microaggregates in the coarse and medium silt fraction

The differences between texture analysis and particle size fractionation seen here indicate that a large amount of stable aggregates was present in the coarse and medium silt fractions of both UL and SCE (figure 7), that could be dispersed chemically, but not physically by ultrasonic treatment. The lack of an increase in SSA after particle size fractionation (table 3) was unexpected and further showed that ultrasonic dispersion and the particle size fractionation procedure did not make new surfaces available that could be measured with BET-N₂. This result may indicate that physical dispersion did not disrupt microaggregates in these soils and created no new surfaces. By comparison, between particle size fractionation and texture analysis, Leifeld and Kögel-Knabner (2003) showed that significant amounts of microaggregates were present in the samples from Scheyern. In addition, using a similar comparison between ultrasonic dispersion and chemical disruption, Gerzabek et al. (2006) showed that microaggregates were present in the silt fractions of the Ultuna soil. However, they used low ultrasonic dispersion energy of 53 J ml⁻¹ (SCE) and 0.2 kJ g⁻¹ (UL) specifically to avoid disruption of microaggregates. Our results show that these microaggregates are in fact very stable and could not be disrupted by physical dispersion even at high energies up to 800 J ml⁻¹.

To elucidate the main agents responsible for the stabilization of these microaggregates, SSA and the BET-N₂ C constant of the particle size fractions of UL-Ca were determined before and after H₂O₂ oxidation of organic matter (table 4). H₂O₂ oxidation was also used as chemical dispersant for texture analysis, and the comparison of surface properties before and after oxidation may give an indication of the main compounds stabilizing these microaggregates. It is expected that organic matter was the main stabilizer of the microaggregates. However, H₂O₂ treatment can also cause the dissolution of weakly crystalline iron oxides (Mikutta et al., 2005) which may also stabilize microaggregates. It may be possible to distinguish between these two possible stabilizing agents by the calculated BET-N₂ C constants before and after H₂O₂ oxidation. It is expected that the C constant increases after organic matter oxidation, as organic matter-free surface has a higher enthalpy of N₂ adsorption. This was observed in the clay fractions where the SSA and C constant clearly increased after H₂O₂ oxidation. This increase is consistent with the increasing affinity of N₂ adsorption on the surface after removal of organic matter and an increase in the

availability of micropores that were previously clogged by organic matter as has been reported before (Eusterhues et al., 2003; Kaiser and Guggenberger, 2003). However, the decrease in SSA and C constant in the silt fraction is unexpected and can only be explained by a loss of microporosity as well as organic matter. Weakly crystalline oxides provide a major part of the available surface area in the silt fractions (table 5), and a loss of these species could have led to the observed decrease in surface area and C constant. This indicates that these (microporous) iron oxides were dissolved in these fractions by the H₂O₂ oxidation, which would have led to the observed disruption of microaggregates. These results indicate that iron oxides, next to organic matter, are a stabilizing agent for the microaggregates.

The dispersion techniques used in particle size fractionation are usually aimed at dividing the soil into primary organo-mineral complexes (Christensen, 1992). However, Chenu and Plante (2006) and Virto et al. (2008) have shown by transmission electron microscopy (TEM) that microaggregates were still present in clay and silt fractions after 'complete dispersion' and concluded that these aggregates are present as tightly bound complexes functioning as separate entities. The energies required for a full dispersion of such aggregates are likely to produce results not applicable to nature because they would also result in the breakdown of organic and mineral particles (von Lützow et al., 2007). The highly stable microaggregates found in these soils support this concept and indicate that these microaggregates can represent a complex interface where organic matter and (iron) oxides are closely associated. For the characterization of available interfaces in soil, they should be viewed as separate entities, as the surfaces occluded within these stable microaggregates are probably not available for further interactions.

3.2.2 Oxide surface area and association with organic carbon

The Fe_o and Fe_d contents determined for the bulk soils and particle size fractions were of the same order of magnitude as values reported for the A horizon of a Dystric Cambisol and the EA horizon of a Haplic Podzol by (Eusterhues, 2005) and agricultural topsoils (Kiem, 2002). Overall, the extracted oxides contribute only a small portion to the total mass of the bulk soil and all particle size fractions. Iron concentrations increase with decreasing particle size and are highest in the < 2 μm fractions of all soils. This corresponds with the current knowledge that ferrihydrite is predominantly present in the form of nanoparticles, and is an important source of naturally occurring nanoparticles (Qafoku, 2010). It may be that the ferrihydrite is only present in the coarser fractions because it is attached to larger particles. An estimation of

the average size of the iron oxide particles was made from the Fe_d content and total oxide SSA and assuming an iron mass content of the oxides of 66%, a density of $3.8 \text{ cm}^3 \text{ g}^{-1}$ and round particles, as was described by Eusterhues (2005). This resulted in an estimated particle diameter of 20 to 100 nm for the bulk soils and all particle size fractions $< 63 \mu\text{m}$. This is in agreement with the results reported by Eusterhues (2005) who reported an average particle size of 2 to 7.5 nm for ferrihydrite and goethite, and confirms that the iron oxides were probably mainly present as nanoparticles.

As discussed above, the SSA of UL-Ca and UL-m did not increase, and the SSA of SCE only slightly increased, after aggregate disruption and particle size fractionation (table 3). This indicates that the calculated oxide surfaces of the particle size fractions may be taken as representative for the biogeochemical interfaces available in soil. The calculation of weakly crystalline and crystalline oxide surface area (table 5) shows that iron oxides were significant contributors to SSA in all particle size fractions, even in these soils with high clay mineral content and without the removal of organic matter. Eusterhues et al. (2005) and Kiem and Kögel-Knabner (2002) showed that the dithionite extractable fraction of the soil dominated SSA in the bulk soil and particle size fractions of a sandy forest soil and sandy to loamy agricultural soils after organic matter oxidation with $Na_2S_2O_8$. The soils examined here had much higher clay mineral content. Therefore, it was expected that iron oxides would be less important for the SSA in these soils. The contribution of iron oxides to the SSA was significant, with 40 to 70 % for the bulk soils and approximately 50% for the coarse clay fraction of all soils. However, the mass contribution of iron oxides, as calculated from the mass recoveries of the samples after dithionite extraction (data not shown), was below 14 % and 28% of the bulk soil and coarse clay fraction, respectively.

The crystalline oxide surface areas found for the bulk soil samples were in the range reported by Hiemstra et al. (2010a) of $3\text{-}30 \text{ m}^2 \text{ g}^{-1}$ reactive oxide surface area for agricultural top soils, determined by phosphate adsorption and surface complexation modeling. This indicates that the method of oxide surface detection by BET- N_2 after dithionite extraction gives a reasonable indication of the amount of available oxide surface in the soil. The significant loss of carbon from all soils after oxide extraction (table 6) indicates that iron oxides may stabilize a major part of the organic matter in these soils.

The $C_{\text{all oxides}}/Fe_d$ ratio (table 6) is much higher than would be expected from simple sorption of organic matter to oxides. The maximum sorption capacity of organic carbon to iron oxides observed is $0.22 \text{ g OC g-Fe}^{-1}$ (Wagai and Mayer, 2007 and references therein). Part of this carbon may be associated with other oxides like e.g. aluminum oxides. However, as these species are present at much lower concentrations in these soils, this would not change the ratio noticeably. Wagai and Mayer (2007) found that the amounts of carbon associated with iron oxides could not be explained by sorption alone and concluded that carbon must also be associated with iron oxides in other forms like co-precipitates or occlusion in iron-stabilized aggregates. The high $C_{\text{all oxides}}/Fe_d$ ratio found here supports this theory.

Weakly crystalline oxide surface area in general was low and even increases in SSA were observed after oxalate extraction, resulting in negative calculated weakly crystalline surface areas for UL-Ca fine clay, UL-m coarse and fine clay and the bulk soil samples. These negative values can only be explained by the release of new surfaces that were covered by these oxides before. This could be due to the presence of weakly crystalline oxides as coatings on other minerals. The new surfaces created had a higher SSA as the oxide coating that was removed. As weakly crystalline oxides typically have a very high SSA, this implies that the SSA of the weakly crystalline oxides has been reduced by other factors. The increase in SSA after oxide extraction of UL-m coarse clay is marked by a larger loss of carbon compared to the respective coarse clay fraction of UL-Ca (3.8 versus 1.2 mg C g^{-1}). This difference may indicate that the increase in SSA observed was largely due to a loss of organic matter that, in association with weakly crystalline oxides, covered mineral surface. A coating of OM on the weakly crystalline oxides, or the presence of co-precipitates of OM and weakly crystalline oxides would also explain their unexpectedly low SSA relative to the new surfaces created. Another possibility is that the oxides bound together microaggregates, and that surfaces occluded within these aggregates were released by the extraction. The relatively low surface areas of the weakly crystalline oxides in the other fine fractions of all three soils and the lack of increase of weakly crystalline surface area with particle size, may indicate that new surfaces were uncovered in these fractions as well.

Increases in SSA after oxalate extraction have been observed before for pure clay minerals (kaolinite, illite and smectites/illite); although it was not confirmed whether this increase in SSA was due to removal of oxide coatings on the minerals or due to mineralogical changes (Helios Rybicka and Calmano, 1988). Borggaard (1982) also discussed the possible

presence of weakly crystalline oxides as coatings on other minerals and observed that the release of 'occluded' surface area after oxide extraction may lead to an underestimation of the calculated oxide SSA. The SSA for clean ferrihydrite reported in literature is generally very high with values reported between 200-1200 m² g oxide⁻¹ (Borggaard, 1982; Eusterhues et al., 2005; Hiemstra et al., 2010a). The low surface area contribution of the weakly crystalline oxides detected here suggests that the weakly crystalline oxides especially were intimately associated with, or coated by, organic matter resulting in low SSA complexes.

The calculated weakly crystalline and crystalline oxide surface area of UL-Ca and UL-m (table 5) showed similar relations between particle size and oxide surface area. This probably reflects their similar mineralogy, soil type and location. Both showed a change in dominant oxide contribution to surface area from weakly crystalline in the coarse fractions to crystalline oxides in the fine fractions. The effect of fertilizer treatment and different organic matter content between the soils was small, although the much lower (negative) weakly crystalline surface area of UL-m in the coarse clay fraction can be explained by the higher organic matter content of UL-m in this fraction. Carbon losses in the sand (63-200 µm) and coarse silt (20-63 µm) fraction of UL-m were also much higher than in UL-Ca, but this is probably due to the loss of particulate organic matter during extraction. The oxide surface areas and amounts of oxide-associated carbon calculated for SCE are in the same order of magnitude as UL. However, a slight increase in weakly crystalline oxide surface area from fine silt to coarse clay was seen, and weakly crystalline oxide surface area contributed less to SSA than crystalline oxides in all particle size fractions of this soil.

The change in main oxide contributor to SSA from weakly crystalline in the coarse fractions to crystalline in the fine fractions of UL was not reflected by a similar change in Fe_o/Fe_d ratio (table 1). This indicates that a relative increase in mass contribution of weakly crystalline oxides compared to crystalline oxides does not lead to a corresponding increase in its contribution to the available surface area. This may be explained by the different functioning of the two oxide forms whereby some surfaces may, for example be preferentially covered by organic matter. Furthermore, the lack of correlation may be due to the different forms in which weakly crystalline and crystalline oxides are present. The mass versus surface area ratio would change depending on whether the oxide is present as a particle or as a coating on another mineral.

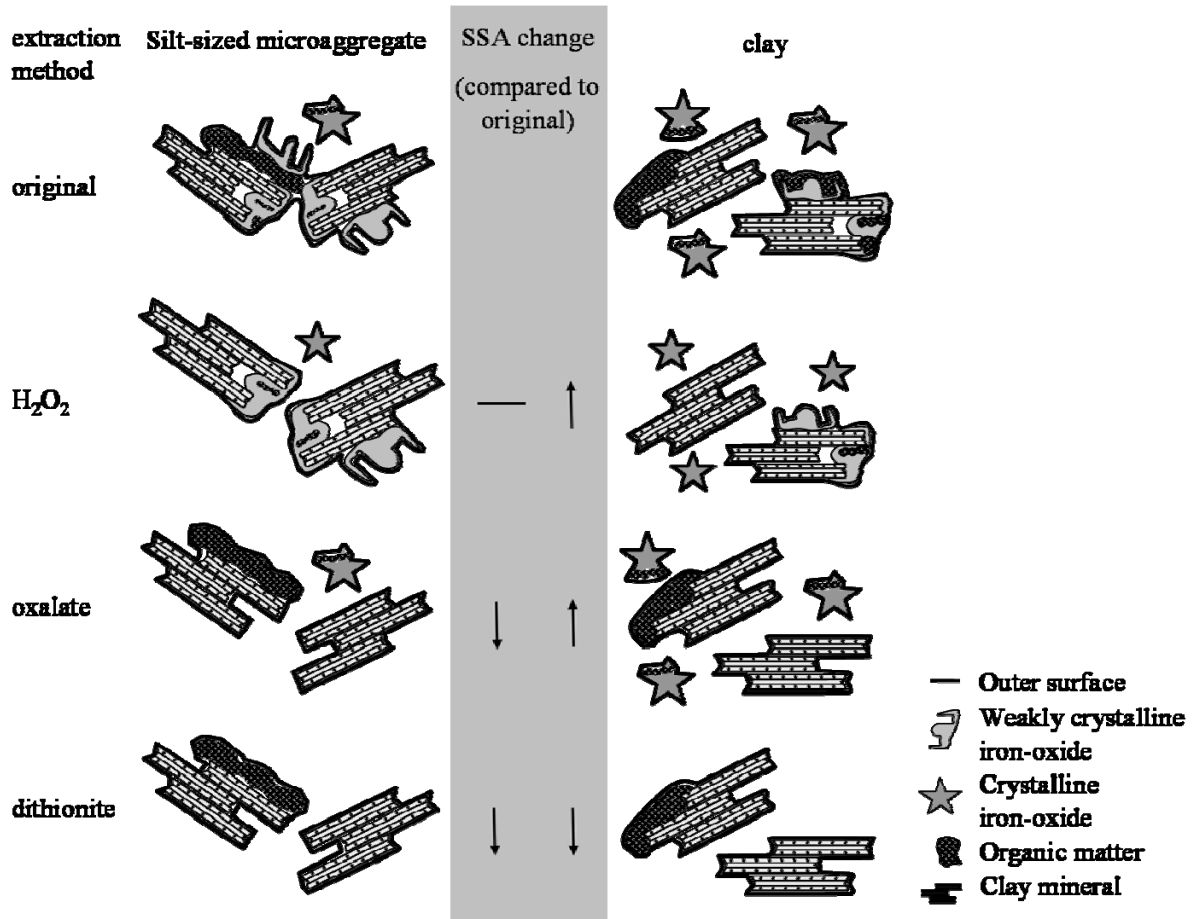


Figure 8. Schematic overview of the effect of H₂O₂ oxidation and oxalate and dithionite extraction on microaggregates and clay sized particles and their specific surface area (SSA). SSA increases are indicated by (↑), decreases by (↓) and no change by (-).

A schematic overview of the proposed effects of H₂O₂ oxidation and oxide extraction on the silt-sized microaggregates and clay particles is presented in figure 8. The change in dominant oxide contribution to SSA from weakly crystalline in the coarse fractions to crystalline in the fine fractions of the UL soils suggests a change in dominant phase in which iron oxides were present with particle size. Possibly, the observed pattern is related to the aggregation of the Ultuna soils, where the weakly crystalline oxides in the coarse + medium silt fractions are present as co-precipitates or complexes with organic matter, forming the microaggregates. These microaggregates were also observed by the comparison of texture analysis and particle size fractionation, and the effects of the H₂O₂ oxidation on the silt fractions further support these findings. In the fine fractions, weakly crystalline oxides may be more present as coatings on other minerals, therefore releasing surface area after their removal, whereas crystalline iron oxides, present as primary particles, could be major contributors to SSA in these fractions.

The shift in carbon association from the weakly crystalline oxides in the coarse fractions to the crystalline oxides in the fine fractions in the Ultuna soils supports the theory that weakly crystalline oxides play an important role in the silt fractions of these soils as co-precipitates or aggregate forming agents. Crystalline oxides, on the other hand, are more important in the fine fractions, possibly providing a large surface area where organic matter can be adsorbed. This shift is soil specific, as the association with weakly crystalline and crystalline oxides did not change with particle size in SCE.

Overall, these data demonstrate the importance of iron oxides for microaggregation and the stabilization of organic matter. The large contribution of oxides to the SSA shows that they contribute significantly to the available interfaces in arable topsoils. Removal of iron oxides can lead to a significant loss of surface area, but also to the release of mineral surfaces that were occluded before, in particular by weakly crystalline oxides. This indicates that these interfaces are probably present as a close and complex association between organic matter, iron oxides and other minerals, whose function and properties depend on particle size, crystallinity and soil type. Even if the SSA of the iron oxides is reduced by its interaction with organic matter, the oxide-OM complex still contributes to the soil structure, stabilizing micro-aggregates and providing sorption sites for organic chemicals.

4 Combining Specific Surface Area and Organic Matter Content to Determine the Phenanthrene Sorptive Interface of an Arable Topsoil

4.1 Results and discussion

4.1.1 Organic matter properties and SSA

Carbon concentration increased with decreasing particle size, and C/N ratio decreased from the coarse (6.3-63 μm) to the fine (0.2-6.3 μm) fraction (table 7, table 8). This relation is typical for soils and has been observed before (Christensen, 1992), which indicates that this soil and its particle size fractions may be taken as a typical representation of interfaces in soil. Solid-state ^{13}C NMR spectroscopy was performed on the samples used in the phenanthrene sorption experiment and showed only slight differences in organic matter (OM) composition between the two particle size fractions and the bulk soil (supplementary material 1). The O/N alkyl and alkyl C groups related peaks were the main contributors to the spectra. Aromatic carbon was present in relatively low amounts. The carbon recovery of the HF extraction was between 78 and 88%. We therefore assume that the extract gave a reasonable representation of the OM in the samples. It appears that the alkyl to O/N-alkyl ratio was slightly higher in UL-Ca compared to UL-m (0.66 versus 0.71) and increased with decreasing particle size, from 0.57 to 0.76 for UL-Ca, and from 0.68 to 0.82 for UL-m respectively.

Table 7. Texture, organic carbon content of the soils, and % mass contribution of carbon of the fractions to the total carbon content of the soil. The combined fractions used for the sorption experiments are marked in light (fine fraction) and dark grey (coarse fraction). Error margins are indicated as the deviation between duplicates.

Fraction (μm)	texture / % mass	UL-Ca		UL-m	
		/ mg C g ⁻¹ of fraction	/ % of bulk soil	/ mg C g ⁻¹ of fraction	/ % of bulk soil
bulk soil		14.7 ± 0.1		21.1 ± 0.02	
63-200	16.1	1.8 ± 0.4	1.9	7.7 ± 0.04	5.9
20-63	11.1	8.3 ± 0.7	6.3	18.6 ± 1.2	9.8
6.3-20	18.7	10.9 ± 0.8	13.9	10.4 ± 0.02	9.2
2-6.3	14.7	18.7 ± 0.3	18.8	27.6 ± 1.6	19.2
0.2-2	29.0	21.6 ± 2.0	42.8	26.0 ± 0.6	35.9
< 0.2	7.1	30.0 ± 1.8	14.6	31.3 ± 0.2	10.6

This indicates that the OM was slightly more decomposed in UL-m than in UL-Ca, and with decreasing particle size (Baldock et al., 1997; Quideau et al., 2000). These small differences observed with ^{13}C NMR spectroscopy were not expected to influence the sorption behaviour of the samples. The effect of OM on phenanthrene sorption for these samples is therefore most probably represented by the OC content.

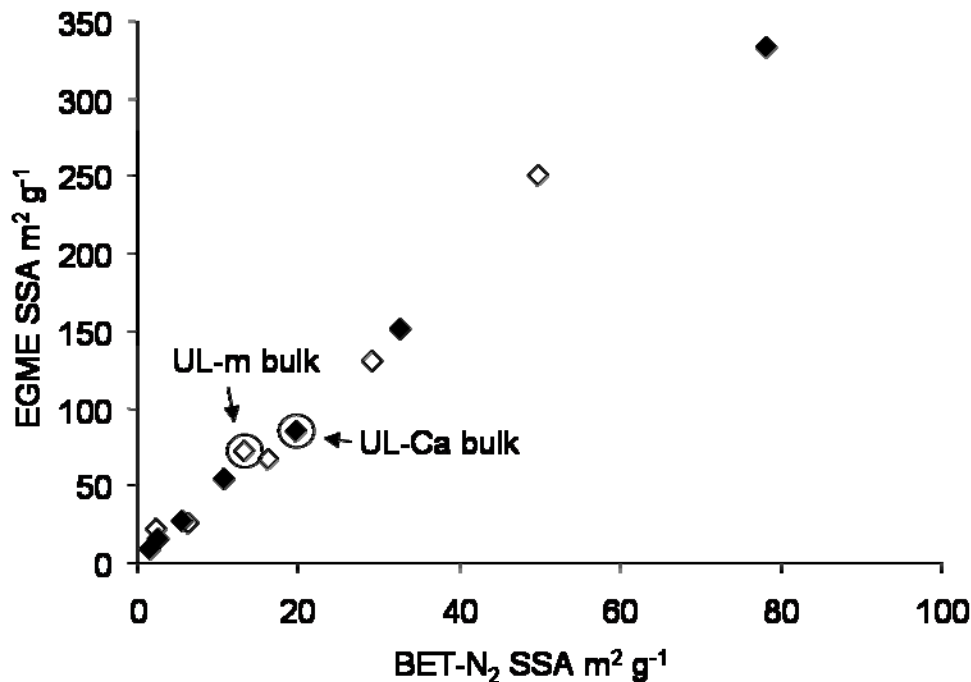


Figure 9. BET-N₂ versus EGME specific surface area (SSA) of bulk soil and particle size fractions of UL-Ca (black diamonds) and UL-m (open diamonds) in m²g⁻¹.

The SSA of the particle size fractions was similar for both soils (table 7) with an EGME SSA of all samples of approximately 4 to 5 times higher than the BET-N₂ SSA. This can be explained by the potential of EGME to also probe the micropores of OM and inner surfaces of clay minerals in addition to the outer surface area detected with nitrogen at 77K. Both BET-N₂ and EGME SSA detected for the bulk soil of UL-Ca were higher than for UL-m with 19.7 m² g⁻¹ and 13.1 m² g⁻¹ for BET-N₂ and 86 m² g⁻¹ and 53 m² g⁻¹ for EGME, respectively. A possible explanation for the decrease in SSA of the bulk soil of UL-m with respect to UL-Ca may be an increase in (micro)-aggregation as a consequence of the different fertilizer treatment (Gerzabek et al., 2006). The BET-N₂ and EGME SSA of both UL-Ca and UL-m were within the range of values reported for bulk soils and particle size fractions in literature (Kiem & Kögel-Knabner, 2002; Eusterhues et al., 2005; Yukselen & Kaya, 2006) and the ratio of EGME to BET-N₂ SSA found was the same as that reported for an illite dominated soil (Yukselen & Kaya, 2006). The SSA determined by BET-N₂ and EGME for

Table 8. The organic carbon content (OC), C/N ratio, BET-N₂ and EGME specific surface area (SSA) and sessile drop method contact angle (CA-SDM) after 30 ms (initial CA) and 5000 ms of the samples used for phenanthrene sorption experiments. Errors indicate deviation between duplicates for the OC, C/N and SSA and standard deviation of six replicates for the CA-SDM.

Sample		OC	C/N	BET-N ₂ SSA	EGME SSA	CA-SDM	CA-SDM
		/ mg g ⁻¹		/ m ² g ⁻¹	/ m ² g ⁻¹	30 ms / °	5000 ms / °
UL-Ca	bulk	14.6 ± 0.1	9.9 ± 0.1	19.7 ± 0.4	86 ± 1.0	16.0 ± 2.5	0
	coarse	9.7 ± 0.7	14.7 ± 0.1	4.4 ± 0.4	22 ± 1.6	12.8 ± 3.0	0
	fine	19.4 ± 1.9	10.4 ± 1.2	18.5 ± 0.4	89 ± 0.4	17.6 ± 0.6	3.4 ± 0.5
UL-m	bulk	21.1 ± 0.02	9.6 ± 1.0	13.1 ± 0.4	53 ± 0.7	11.4 ± 4.1	0
	coarse	13.2 ± 0.5	13.1 ± 0.3	4.6 ± 0.4	23 ± 1.3	14.2 ± 2.4	0
	fine	26.5 ± 1.2	9.5 ± 0.4	20.6 ± 0.4	89 ± 0.4	20.8 ± 2.0	3.5 ± 1.1

both soils and all particle size fractions shows a linear correlation through the origin (figure 9), where both BET-N₂ and EGME SSA increase with decreasing particle size. The OC content also increased with decreasing particle size (table 7); however, this did not change the linear relationship between the BET-N₂ and EGME SSA. This indicates that the availability of organic matter micropores, detectable by EGME but not by BET-N₂, did not increase much with organic matter content. Otherwise, a disproportionate increase in the EGME SSA with increasing OM content would have been observed, resulting in a nonlinear relationship between BET-N₂ and EGME SSA. Thus, the linear relationship observed here shows that the relative contribution of mineral, organic and clay interlayer surfaces to the BET-N₂ and EGME SSA did not change notably with particle size. This result is unexpected, as the organic matter content increased with decreasing particle size. Taken together our results may indicate that the interface properties also remained similar with decreasing particle size and between the two soil treatments.

The determined contact angles (table 8) show that all samples had a small initial contact angle. The contact angle was most stable in the fine fractions where a measurable contact angle could still be detected after 5000 ms. No difference in contact angle was seen between UL-Ca and UL-m. The small but non-zero contact angle showed that the sample surfaces were mainly hydrophilic, but that a certain amount of hydrophobic compounds was present in the soil. The slight increase in contact angle from the coarse to the fine fraction together with a slight increase in stability points to a higher abundance of hydrophobic

compounds in this particle size fraction (Ellerbrock et al., 2005). This is in accordance with the slightly higher abundance of alkyl groups detected for these fractions by solid-state ^{13}C NMR spectroscopy. Our results indicate that the fine fraction had a slightly higher capacity for phenanthrene sorption compared to the coarse fraction and the bulk soil.

Overall, the characterization of the SOM showed only small differences in OM properties between the samples. The linear relationship between BET- N_2 and EGME further suggests that the surface properties of the sample did not change with particle size. We conclude that it may be possible for these samples to relate sorption only to the OM content and SSA of the sample. The slight variations in sample properties as examined above are considered to be of minor importance.

4.1.2 Phenanthrene sorption: isotherm shape and model discrimination

The Freundlich isotherm, which was found to be the best fitting model for all samples, is observed for sorption where either the sorptive energy decreases with increasing adsorbate concentration or where sorption takes place to heterogeneous sites with different sorptive energies (Delle Site, 2001; Limousin et al., 2007). It may be interpreted as the superposition of multiple Langmuir-type processes with separate affinities and saturation coefficients for each particular type of site present that is relevant for the sorptive interface (Limousin et al., 2007).

Table 9. Freundlich isotherm parameters, where K_f is the Freundlich isotherm coefficient, $1/n$ is a measure of sorption linearity and R^2_{adj} is the isotherm correlation coefficient adjusted for the number of isotherm parameters.

		K_f ml g $^{-1}$	$1/n$	R^2_{adj}
UL-Ca	bulk	96 ± 16.4	0.73 ± 0.07	0.997
	coarse	84 ± 6.9	0.76 ± 0.03	0.996
	fine	178 ± 24.5	0.80 ± 0.07	0.993
UL-m	bulk	192 ± 13.7	0.92 ± 0.04	0.995
	coarse	128 ± 13.1	0.77 ± 0.05	0.993
	fine	402 ± 31.3	0.97 ± 0.03	0.994

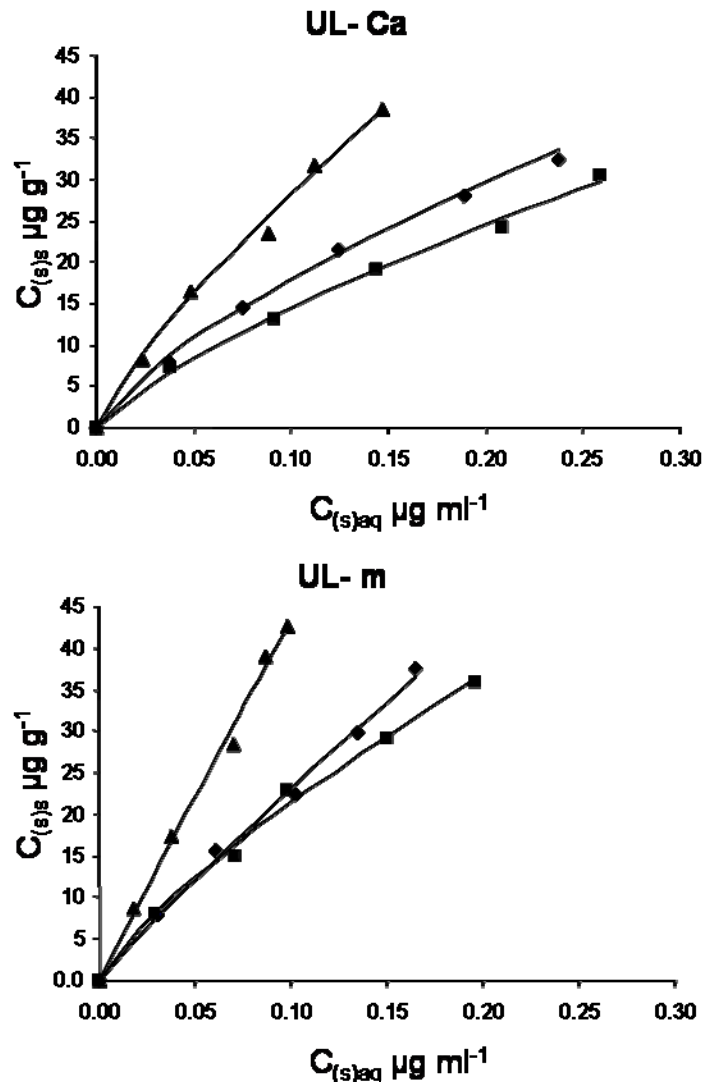


Figure 10. Phenanthrene sorption isotherms of the coarse (6.3-63 μm) (squares) and fine (0.2-6.3 μm) (triangles) fraction and the bulk soil (diamonds) of UL-Ca and UL-m. $C_{(s)aq}$ represents the concentration of phenanthrene in solution after incubation in μg phenanthrene g^{-1} .

The complex interaction of mineral, organic and biological compounds of the soil biogeochemical interface leads to a heterogeneous substrate with a great variety of organic and mineral surfaces present. Furthermore, in recent years, it has been shown that the properties and composition of soil OM itself is heterogeneous at the micrometer scale (Lehmann et al., 2008), leading to the presence of many different sites with different sorption energies. Based on the considered models, it is expected that this complex and heterogeneous system is best described by the Freundlich isotherm, which takes into account this wide variety of sorption sites at the interface.

The sorption isotherm of the coarse fraction lies slightly below the isotherm for the bulk soil, whereas the isotherm for the fine fraction lies distinctly above the isotherm of the bulk soil (figure 10). Sorption for the bulk soil and each fraction is higher in UL-m compared to UL-Ca. The calculated Freundlich coefficients (table 9) show higher sorption capacities for UL-m compared to UL-Ca and higher sorption capacities for the fine fraction compared to the coarse fraction and the bulk soil. The sorption isotherms all show convex curvature resulting in values of $1/n$ smaller than 1 (table 9). Sorption linearity increased from the coarse to the fine fraction and from UL-Ca to UL-m and in general with increasing OM content. This may be because the phenanthrene concentrations used in the sorption experiments were further from the maximum sorptive capacity of these samples, or because the sorption process was more of the partitioning type for these samples. The calculated Freundlich coefficients are of the same order of magnitude as values reported in literature for agricultural soils (Carmo et al., 2000; Amellal et al., 2006; Celis et al., 2006) and may therefore be taken as a typical representation for this type of soil.

4.1.3 Increase in phenanthrene sorption after particle size fractionation

The contribution of sorption in the fine and coarse fraction to the bulk soil was calculated and compared to the measured isotherm for the bulk soil to test whether the fractionation procedure resulted in an increase of available sorption sites. This was done by multiplying the respective adsorption in $\mu\text{g phenanthrene g sample}^{-1}$ for each isotherm point by the fractional mass contribution of that fraction to the bulk soil (0.29 and 0.44 for the coarse and fine fraction, respectively) and calculating the summed isotherms. The summed isotherm of the fine + coarse fraction corresponds to 91 to 101 % of bulk soil sorption for UL-Ca and 102 to 112 % of bulk soil sorption of UL-m (figure 11a and b). These results show that the coarse and fine fraction combined represent 73 % of the bulk soil mass, but their combined phenanthrene sorption capacity is equal to or greater than that of the bulk soil. The sand and fine clay fraction that were not included in the sorption experiments are expected also to contribute to phenanthrene sorption due to the presence of particulate OM in the sand fraction and the high carbon concentration and SSA of the fine clay fraction. From these results, we conclude that phenanthrene sorption capacity increased considerably after particle size fractionation. A similar increase in phenanthrene sorption capacity after ultrasonic treatment and disruption of micro-aggregation was found by (Hundal & Thompson, 2006) for a clay-rich soil.

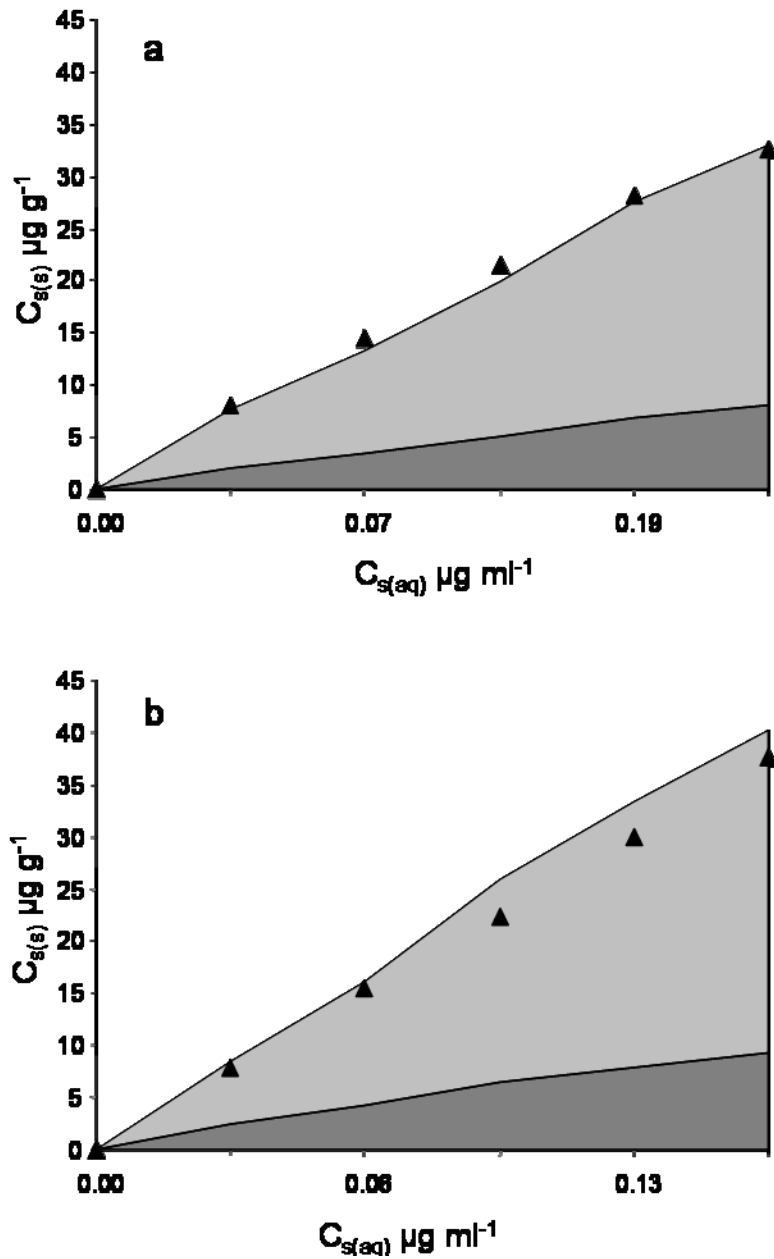


Figure 11. Summed isotherms of the coarse and fine fraction compared to bulk soil isotherms for UL-Ca (a) and UL-m (b) with the calculated contribution of the coarse fraction (dark grey) and the fine fraction (light grey) and the isotherm of the bulk soil (triangles). $C_{s(aq)}$ represents the concentration of phenanthrene in solution after incubation in $\mu\text{g phenanthrene ml}^{-1}$ and $C_{s(s)}$ represents the concentration of phenanthrene adsorbed on the sample after incubation in $\mu\text{g phenanthrene g}^{-1}$.

The increase in sorption capacity was unexpected, as the summed surface area of all particle size fractions determined by BET- N_2 was close to the SSA determined for the bulk soils (data not shown). This shows that no new surfaces were created that could be detected by BET- N_2 . The EGME SSA also did not reflect the increase in phenanthrene sorption capacity, as BET- N_2 and EGME were linearly related. The observed increase in sorptive capacity for phenanthrene after particle size fractionation must therefore be due to other

factors. One possible explanation is that fractionation procedure created new hydrophobic organic surfaces that were not detected by BET-N₂ or EGME retention. Furthermore, it is possible that the extensive treatments (ultrasonic dispersion, washing with distilled water, freeze-drying) caused a change in the structure of the OM present, increasing its sorptive capacity. The increase in sorption capacity after particle size fractionation indicates that the structure of the soil interface is important for its sorptive capacity and must be taken into account, when comparing data from extensively treated and fractionated samples to the actual sorptive behaviour of the interface as it is present in soil.

4.1.4 Phenanthrene sorption related to carbon concentration and SSA

The K_f values increased with increasing OC content (figure 12a). However, no clear correlation was found between the K_f and the carbon concentration. Some of the K_f values observed clearly deviate from the general trend. The relation between OC content and phenanthrene sorption is well-established in literature (Karickhoff et al., 1979; Delle Site, 2001). The remaining differences in sorption are usually explained by differences in the composition of the OM and especially the presence of aromatic and aliphatic organic molecules has been shown to affect phenanthrene sorption (Chefetz & Xing, 2009). However, ¹³C NMR spectroscopy showed only small differences between the samples examined here. This may be because ¹³C NMR spectroscopy gives the bulk composition of the OM present, which may not be representative for the type of OM at the surface. Furthermore, phenanthrene sorption to mineral surfaces may also take place (Müller et al., 2007) although this is expected to be of minor importance for these soils due to their high OC content.

An additional factor that affects sorption is the SSA of the samples. To estimate the effect of size of the interface area, for which SSA is a proxy, on phenanthrene sorption, the K_f per unit surface area ($K_f \text{ m}^{-2}$) was plotted against the carbon concentration per unit surface area (mg C m^{-2}) (figure 12b). A clear linear relationship was observed for five of the six samples examined. This indicates that, although phenanthrene sorption is mainly related to the OM content, the concentration of OM per unit surface area is the main parameter determining the sorptive interface for phenanthrene. The fine fraction of UL-m did not fit well into this relation with a higher sorption than would be expected from the relation between the other samples. This could be due to a slightly different composition of the OM in this fraction, or possibly due to differences in the structure and interactions between minerals and OM. This

has also been shown by e.g. studies by (Bonin & Simpson, 2007; Ahangar et al., 2008) who found that interaction of organic matter with minerals may change its structure and reduce the amount of available sorption sites on the organic matter, thereby reducing its sorptive capacity.

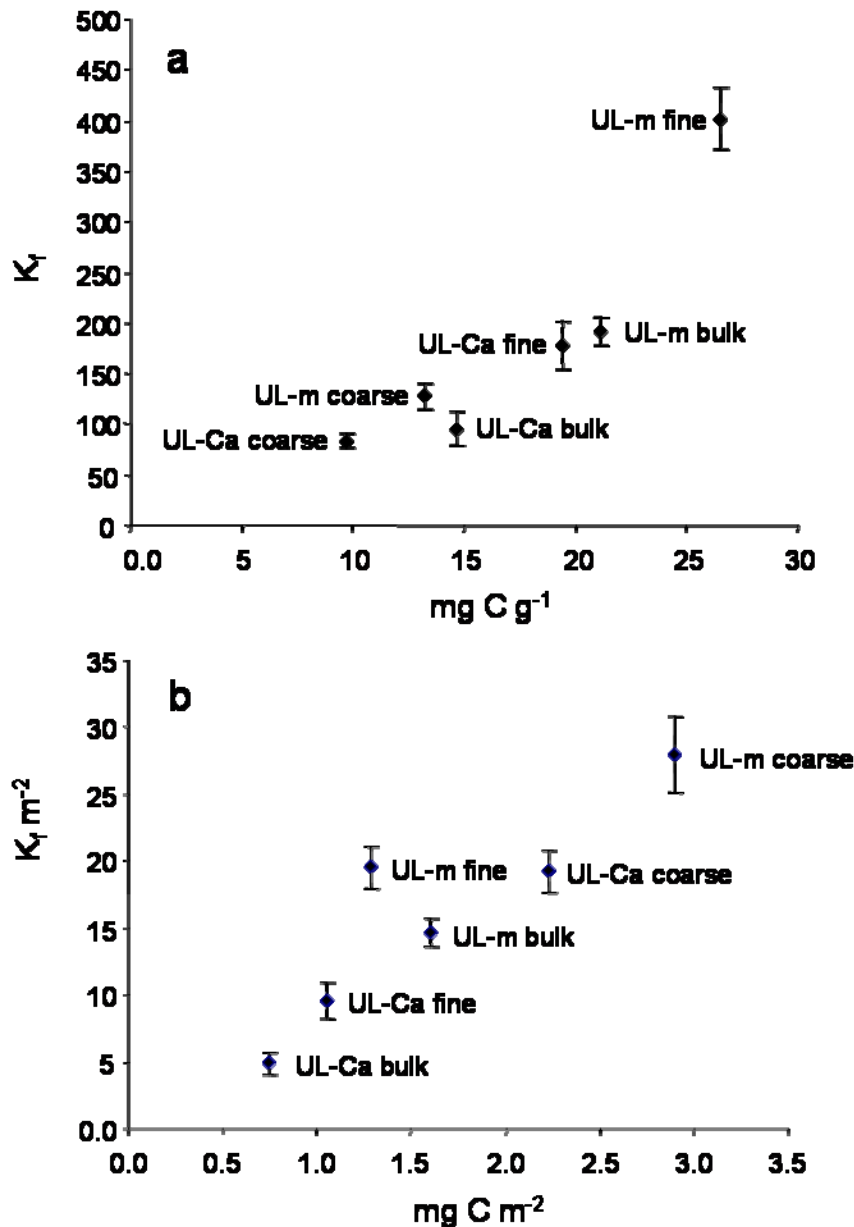


Figure 12. Freundlich isotherm coefficient (K_f) versus organic carbon content in mg C g^{-1} (a) and the Freundlich isotherm coefficient normalized to BET- N_2 surface area ($K_f \text{ m}^{-2}$) versus carbon content per square meter (mg C m^{-2}) (b).

Previous studies have attempted to relate the sorption of hydrophobic molecules to the SSA determined by either BET- N_2 or EGME (Mader et al., 1997; Carmo et al., 2000; Hundal et al., 2001; Kang & Xing, 2005; Müller et al., 2007; Luo et al., 2008; Mittal & Rockne, 2008). (Hundal et al., 2001) tried to relate phenanthrene sorption by reference smectites to the BET- N_2 and EGME surface area and found no correlation for either method. (Müller et al.,

2007) also found no relation between BET-N₂ SSA and mineral surfaces of quartz, goethite and montmorillonite. (Carmo et al., 2000) measured BET-N₂ SSA in relation to phenanthrene sorption to bulk soil and particle size fractions and also found no direct relation. It was observed that the K_f normalized to the SSA was smaller for the clay fractions as for the other samples, which is consistent with the findings presented here. They concluded that the BET-N₂ SSA is not a good measure for the sorption of hydrophobic molecules because it may detect mineral surfaces that usually are of less relevance for sorption of hydrophobic molecules. (Luo et al., 2008) tested BET-N₂ and EGME SSA and phenanthrene sorption before and after removal of OM. They found that both EGME SSA and phenanthrene sorption decreased after OM removal, whereas BET-N₂ SSA increased which perhaps may be explained by the high affinity of EGME and phenanthrene for OM compared to N₂. They concluded that BET-N₂ SSA was not a suitable measure for sorption capacity because this method fails to account for inner microporosity of the soil. These studies show that phenanthrene sorption cannot be directly correlated to either BET-N₂ or EGME SSA because these methods also detect surfaces that are of less relevance for sorption of hydrophobic molecules or fail to detect micropores that are relevant for sorption. However, SSA may be related to sorption because it provides a measure of the size of the interface where sorption can take place. By normalizing the carbon content to the SSA, we could explain most differences in phenanthrene sorption capacity for the soil studied here.

Overall, the sorptive capacity for a hydrophobic molecule like phenanthrene is not directly related to the SSA as determined by traditional methods. However, the carbon concentration per unit area is a good measure for the sorptive capacity for this particular soil. Note that only short-term sorption was examined here. Over longer time scales of months, diffusion of phenanthrene into micropores of OM may take place, resulting in a larger sorption capacity and different isotherm. These long-term effects may change the relationship between SSA, OM content and phenanthrene sorption at larger time scales of months to years and should be a focus of future research.

5 Development of biogeochemical interfaces in an artificial soil incubation experiment; aggregation and formation of organo-mineral associations

5.1 Results

5.1.1 Model materials

An overview of the properties of the model materials can be found in table 10. Some carbon was present in the pure montmorillonite, ferrihydrite and boehmite, but overall, the model materials were relatively clean. All inorganic materials were subjected to DNA extraction to check whether microbes were found and little to no DNA was found in all materials, indicating that the model materials were no source of microbes in the artificial soils (Ding and Smalla, personal communication). The BET-N₂ and EGME SSA (table 10) show that ferrihydrite and boehmite had the largest SSA, although their contribution to the bulk soil SSA is low due to their low mass content.

Table 10. Properties of the model materials, where texture is divided in sand (> 63 µm), silt (2-63 µm) and clay (< 2 µm), cation exchange capacity (CEC) of the clay minerals, carbon and nitrogen content and specific surface area (SSA) determined by BET-N₂ and EGME retention. Standard error was within 5% for all data, determined for duplicates of each sample.

name	model component	_ texture _			CEC cmol kg ⁻¹	C mg g ⁻¹	N mg g ⁻¹	SSA m ² g ⁻¹	
		sand %	silt %	clay %				BET-N ₂	EGME
QS	quartz sand	100				0.05	0.01	0.1	b. d. l. ^a
QSi	silt-sized quart	6	94			0.05	0.01	1	b. d. l.
MT	montmorillonite	8	25	67	85.97	2.38	0.01	71	436
IL	illite		50	50	16.65	0.18	0.16	40	108
QC	clay-sized quartz		26	74		0.16	0.11	15	21
FH	ferrihydrite		–	100	–	3.5	3.4	247	217
B	boehmite	–	100	–		4.6	0.1	298	383
CH	charcoal	100				750	3.8	45	333
M	manure	86	–	14	–	330	30	5	95

Table 11. Organic carbon (OC) content and C/N ratio of the bulk artificial soils at the start (t=0) and after 18 months (t=4) of incubation, and the BET-N₂ specific surface area (SSA) of the bulk soils and the range of SSA detected for the density fraction of 1.8-2.4 g cm⁻³ (microaggregates). SSA of the bulk artificial soils was calculated from the SSA and mass contribution of each model material (calc) and determined at t=0 after 3 days of incubation (actual). Standard errors of OC content were calculated from the deviation between duplicates, the BET-N₂ standard deviation was below 0.4 m²g⁻¹ for all samples.

soil composition	pH		OC mg g ⁻¹		C/N		SSA m ² g ⁻¹		
	t=0	t=4	t=0	t=4	t=0	t=4	bulk soil (t=0)		micro- aggregates m ² g ⁻¹
							calc	actual	
MT	7.7	7.7	16 ± 0.6	14 ± 0.9	11.5	10.2	5.0	3.1	- ^a
IL	7.6	7.4	16 ± 3.3	12 ± 0.2	11.3	9.9	3.8	2.9	28 - 52
FH	7.6	7.6	14 ± 1.2	13 ± 1.0	11.4	9.7	3.9	2.7	15 - 18
MT + IL	7.7	7.5	16 ± 0.9	13 ± 1.0	12.0	10.2	4.4	3.1	-
MT + CH	7.6	7.6	31 ± 2.4	26 ± 2.0	21.2	19.3	4.5	2.5	-
IL + FH	7.6	7.6	17 ± 2.5	12 ± 0.5	11.6	9.5	5.8	3.6	26 - 45
IL + B	7.6	7.5	14 ± 1.0	12 ± 1.0	11.4	9.8	6.3	3.7	28 - 82
IL + FH + CH	7.6	7.6	30 ± 1.4	28 ± 2.6	21.3	17.8	6.0	3.4	29 - 30

5.1.2 Incubation and bulk properties of the artificial soils

The mixtures quickly developed into aggregated structures and formation of macroaggregates was observed within days after the start of the incubation experiment. Fungal hyphae were observed in some of the artificial soils after several weeks of incubation, indicating that the soil microbial community was active. The visual evidence for the presence of these fungi disappeared after 2 to 3 months of incubation. CO₂ respiration was measured 1 to 2 times per month to check the microbial activity of the artificial soils. After an initial active stage of several weeks, CO₂ respiration reached a relatively constant level between 0.01 and 0.04 mg CO₂-C (g dry soil)⁻¹d⁻¹. The cumulative loss of carbon due to CO₂ respiration was estimated between 2.5 and 3.5 mg CO₂-C (g dry soil)⁻¹, which represents 17 to 23% of the total added carbon from the manure. No difference in CO₂ respiration occurred between artificial soils of different composition. The carbon concentration of the soils (table 11) decreased slowly over time. The difference in concentration between the start and finish of the incubation corresponds reasonably well with the estimated loss of carbon from the CO₂ respiration measurements. Subsequently, the C/N ratio of the soils decreased slightly with incubation time due to the loss of carbon as CO₂.

The SSA of the artificial soils (table 11) was between 2.5 and 3.7 m²g⁻¹ and varied slightly depending on soil composition. The bulk BET-N₂ SSA of the artificial soils was calculated from the contribution of each model component to the total SSA as determined by its SSA and mass contribution to the bulk soil (table 11). The actual SSA of the air-dried samples determined at t=0 (3 days after CaCl₂ was added, but before inoculation of the artificial soils) were 30 to 46% lower than these calculated values. The pH of all artificial soils remained constant during incubation at a pH of 7 to 7.6. The amounts of extractable Fe, Al and Si did not change with time. Therefore, concentrations were presented here as the average of all time steps (table 12). The amounts of Fe, Al and Si extracted with CuCl₂ and of Fe and Al extracted by Na-pyrophosphate were below 0.1 mg g⁻¹ for all samples. The dithionite extractable iron (Fe_d) content of the samples containing ferrihydrite corresponds well to the amount of iron that was added in the form of ferrihydrite. The amount of oxalate extractable iron (Fe_o) is low, with an Fe_d/Fe_o ratio for the ferrihydrite containing artificial soils between 0.13 and 0.19. Oxalate and Na-pyrophosphate extractable Si was found in all samples and was clearly higher in the soil containing clay-sized quartz (FH).

Table 12. Oxalate, dithionite and Na-pyrophosphate extractable Fe, Al and Si of the bulk artificial soils in mg g⁻¹. The average concentration from all time steps was used and the standard error indicated was calculated from these four replicates. Artificial soil composition is indicated by IL (illite), FH (ferrihydrite), B (boehmite) and CH (charcoal).

soil composition	extractable Fe		extractable Al		extractable Si	
	mg g ⁻¹		mg g ⁻¹		mg g ⁻¹	
	oxalate	dithionite	oxalate	dithionite	oxalate	Na-pyrophosphate
FH	0.80 ± 0.09	5.49 ± 0.27	0.03 ± 0.01	0.03 ± 0.01	0.91 ± 0.16	1.21 ± 0.10
IL + FH	0.95 ± 0.09	5.83 ± 0.23	0.04 ± 0.01	0.04 ± 0.01	0.29 ± 0.03	0.48 ± 0.03
IL + B	0.06 ± 0.01	0.41 ± 0.20	0.06 ± 0.04	0.19 ± 0.02	0.21 ± 0.03	0.34 ± 0.04
IL + FH + CH	0.89 ± 0.08	6.03 ± 0.14	0.04 ± 0.01	0.03 ± 0.01	0.36 ± 0.03	0.56 ± 0.04

5.1.3 Macroaggregation

The air-dried and sieved aggregates > 2 mm comprised a major part of all artificial soils at all sampling times (figure 13). The percentage of material present as macroaggregates increased until 12 months of incubation, after which a decrease in aggregation was observed in some of the artificial soils. The artificial soil that did not have a clay mineral present (FH) developed less aggregates > 2 mm than the artificial soils that did contain a clay mineral. No difference in aggregation was seen between the presence of the expandable clay mineral montmorillonite

and the non-expandable illite and for the soils with and without ferrihydrite and boehmite. The presence of charcoal had no effect on the initial amount of macroaggregates formed. However, a larger decrease in aggregation in the artificial soils containing charcoal (MT + CH and IL + FH + CH) was observed compared to respective soils without charcoal present (MT and IL + FH), starting after 1 year of incubation.

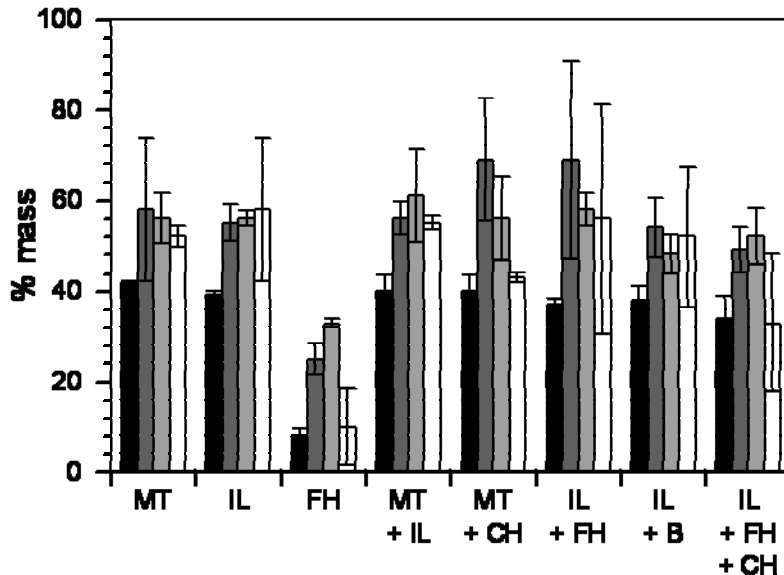


Figure 13. Mass % of aggregates > 2 mm determined by dry sieving of air-dried artificial soils after 3 months (■), 6 months (■), 12 months (■), and 18 months of incubation (□) for each artificial soil composition. Soil composition is indicated by MT (montmorillonite), IL (illite), FH (ferrihydrite), CH (charcoal) and B (boehmite). Error bars represent standard error of three replicates determined for each composition and sampling time.

5.1.4 Microaggregation

Density fractionation was performed on the illite containing artificial soil compositions. The montmorillonite containing mixtures were excluded because, due to the low specific density of the montmorillonite, the microaggregated fraction and the mineral fraction could not be separated successfully. The results of the density fractionation (figure 14) show the total amount of OC associated within the density fraction 1.8-2.4 g cm⁻³ (microaggregates) and the density fraction >2.4 g cm⁻³ (minerals). Together, these fractions represent the OM within microaggregates and OM associated with the mineral fraction. The amount of carbon bound in these fractions increased with time until the end of the incubation after 1.5 years. The amount of microaggregate and mineral-associated carbon represented 3 to 8% of the total OC present after 3 months of incubation, and this increased to 9 to 19% of the total OC present after 1.5 years of incubation. No effect of mineral composition and the presence of charcoal

on the amounts of microaggregate and mineral-associated carbon could be seen. The SSA of the microaggregates in the density fraction $1.8\text{--}2.4\text{ g cm}^{-3}$ was around $30\text{ m}^2\text{g}^{-1}$ for most of the artificial soils containing illite. The SSA of the density fraction $1.8\text{--}2.4\text{ g cm}^{-3}$ of the artificial soil containing clay-sized quartz instead of illite was lower with values between 15 and $18\text{ m}^2\text{g}^{-1}$, whereas some outliers with SSA up to $82\text{ m}^2\text{g}^{-1}$ were found for the mixtures containing boehmite (table 11).

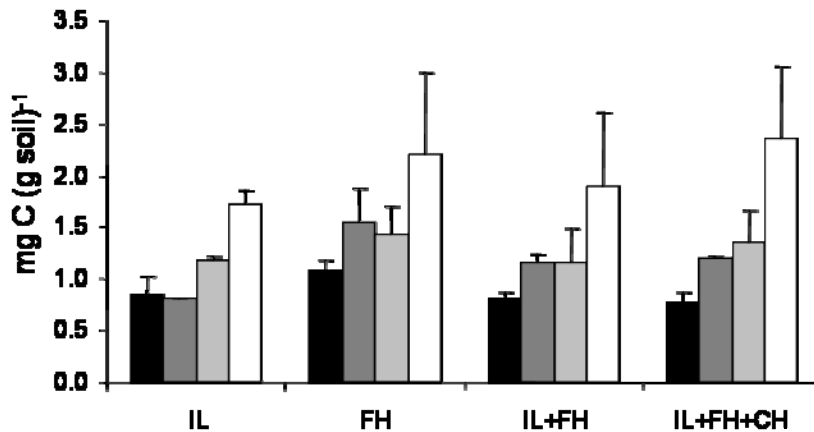


Figure 14. Microaggregate and mineral-associated organic carbon defined as the carbon detected in the $1.8\text{--}2.4\text{ g cm}^3$ plus the $> 2.4\text{ g cm}^3$ fraction after 3 (■), 6 (▣), 12 (□), and 18 (□) months of incubation. The error bars represent the difference between 2 duplicates determined for each composition and sampling time. Artificial soil composition is indicated by IL (illite), FH (ferrihydrite) and CH (charcoal).

5.2 Artificial soil development; microbial activity and aggregate formation

5.2.1 Incubation and microbial activity

The bulk artificial soil development at the start of incubation proceeded similarly for all compositions. The relatively constant neutral pH of all artificial soils may be due to buffering effects of the CaCl_2 solution added or to a high pH of the manure added as organic matter source. The similar pH for all soil compositions and replicates shows that chemical conditions in all artificial soils were similar. The CO_2 respiration measurements indicate that microbes were active during the entire time of incubation. DNA extraction showed that a microbial community was established within 90 days of incubation that varied depending on soil composition (Ding and Smalla, personal communication). Overall, the similar CO_2 respiration determined in all samples tested shows that the artificial soils behaved in a reproducible way and indicates that the development of the artificial soils was probably controlled by substrate availability. The total OC content (table 11) of the soils decreased with incubation time. The

total carbon loss from the soils, estimated from the differences in carbon content at the start of incubation ($t=0$) and after 18 months ($t=4$), was generally between 15 to 20% with a maximum of 33% and a minimum of 6%. Variability in carbon content between replicates was large, and therefore no significant difference in carbon loss between soil compositions could be seen.

5.2.2 Fast coverage of mineral surfaces by organic matter (OM)

The SSA of the artificial soils (table 11) was at the low end of the range of values found for natural soils (Eusterhues et al., 2005; Kiem and Kögel-Knabner, 2002; Wagai et al., 2009; Yukselen and Kaya, 2006) due to the large sand content of the soils and the low SSA of the sand and silt-sized quartz that provides the main matrix of the artificial soils (table 1 and 10). The difference between the calculated SSA and the actual SSA at the start of incubation indicates that association of OM to mineral surfaces took place within these 3 days, reducing the availability of the mineral surfaces. The decrease in SSA relative to that predicted from the model materials was between 23 and 46%. The difference between the calculated and actual SSA was most pronounced in the artificial soils containing charcoal. This may be due to the additional carbon added as charcoal to these soils. The BET- N_2 method has low affinity to OM and charcoal surfaces due to the kinetic restriction of nitrogen molecules into the small pores of these materials at the low temperature at which the measurement takes place (De Jonge and Mittelmeijer-Hazeleger, 1996). A larger carbon content of the soils may therefore lead to less available surfaces that can be successfully detected by BET- N_2 , and could indicate that interactions between charcoal and mineral surfaces took place. Additionally, it might be that the SSA of the charcoal itself (table 10) was reduced by preferential interactions with the manure and microbial inoculant added to the artificial soils. The large difference between predicted and actual SSA at $t=0$ shows that interactions between OM and minerals and the occlusion of mineral surfaces took place in a time frame in the order of days. During these 3 days of incubation, the soil solution had been added to the model materials, but they were not yet inoculated with the microbial community. This suggests that the reactions were predominantly abiotic. The occlusion of surfaces can therefore probably be explained by the sorption of OM on mineral surfaces and the aggregation of minerals due to physical interactions like van der Waals forces and electrostatic attraction. Sorption of OM on minerals and the consequent occlusion of surfaces has been observed before (Kaiser and Guggenberger, 2003; Kaiser and Guggenberger, 2007; Wagai et al., 2009) and is considered a

major process by which OM is stabilized in soil (von Lützow et al., 2008). Aggregation and subsequent occlusion of surfaces due to physical interactions may also have occurred at this short time scale due to static interactions between differently charged surfaces and the formation of calcium bridges with the calcium ions added as matrix solution. The large difference between the actual and calculated SSA of the artificial soils as found in this experiment shows that aggregation and sorption of OM took place almost immediately in the soils and lead to a significant reduction in the amount of mineral surfaces available.

5.2.3 Formation of macroaggregates

Macroaggregation was very fast and an aggregated structure was developed in all artificial soils within 3 months of incubation. Several studies have shown that formation of aggregates from dispersed soil can be established on a time-scale of several weeks (Bravo-Garza et al., 2009; Denef et al., 2001a; Denef et al., 2001b; Falsone et al., 2007; Materechera et al., 1992). However, these experiments were carried out with dispersed natural soil where organo-mineral formations and microaggregates are already present. In this experiment, clean materials were used, and it was not expected that macroaggregation would take place so quickly. The main processes of aggregate formation in these artificial systems were probably the attachment of particles by substances produced by microbial activity like EPS and fungal hyphae, static interactions between minerals and the mechanical stirring action that was required for homogenization of the batches. Stirring was done very carefully to avoid compressing the artificial soils and disturbing the aggregates. However, these mechanical actions probably had some effect on aggregation. Aggregation processes were restricted compared to those occurring in nature, and several factors that are important for soil aggregation like wetting/drying and freezing/thawing cycles and the effect of plants and soil animals on aggregation (Angers and Caron, 1998; Denef et al., 2002; Six et al., 2004) were excluded from this experiment. This gave the opportunity to focus on the effect of mineral composition alone in a system unaffected by changing environmental conditions that are usually considered important for aggregate formation. Our results indicate a major contribution of microbial exudates and residues on the formation of macroaggregates in this system. This effect may have been underestimated in favor of the effects of freezing/thawing and wetting/drying, which are often considered most relevant for macroaggregate formation (Bravo-Garza et al., 2009; Denef et al., 2001a; Smucker et al., 2007; Watts et al., 2005).

The decrease in macroaggregation in the artificial soils with time (figure 13) was most probably caused by the decrease of available OM in the system with incubation time. It is usually assumed that OM is of major importance for the stabilization of aggregates (Abiven et al., 2009; Six et al., 2004), and several studies have shown that macroaggregates generally have a relatively short lifetime because the OM that binds them is degraded as was represented in the conceptual models of Tisdall and Oades (1982) and Oades (1984). Further studies indicate that limitation in available OM has also affected microbial activity in the artificial soils (Schulz et al., Ding et al. and Kandeler et al., personal communication).

5.2.4 Formation and SSA of microaggregates

The similar amount of microaggregation and OC associated with microaggregates and minerals in all soils indicates that the production of microaggregates was controlled by OM availability and microbial activity. No effect of mineral composition on microaggregation was observed for the illite, quartz and ferrihydrite containing soils (figure 14). Formation of EPS is an important factor controlling the formation of microaggregates (Oades, 1993; Six et al., 2004). The type of mineral surfaces available may become more important at higher OM content and microbial activities, when the production of EPS is no longer limiting. Only few studies are available on the formation of microaggregates in initial soils. Leinweber and Reuter (1992) observed redistribution of carbon and nitrogen during a soil-formation pot experiment that lasted 34 years, and Egli et al. (2010) studied microaggregation and mineral associated OC by density fractionation in a proglacial area. They separated the < 1 , 1-1.6, 1.6-2 and > 2 g cm⁻³ fractions of initial soils from a chronosequence with a maximum age of 140 years. They observed increasing carbon content in the heaviest fraction with time, indicating increasing interaction between OM and minerals and found a maximum of 15% of soil OM associated with the heavy fraction after 140 years. This amount was already reached here after 18 months of incubation.

The SSA of the microaggregate fractions (table 11) is high when compared to the SSA of the bulk artificial soil. This shows that microaggregates were preferably formed from fine materials with a large surface area. The SSA of the microaggregates of around 30 m²g⁻¹ for the illite containing artificial soil is close to the SSA of the pure illite clay used. This indicates that the aggregates found here were preferably formed with illite. Some higher values were detected for the boehmite containing artificial soils, which may be explained by the

contribution of these high surface area oxides. The low SSA for the soil containing only quartz and ferrihydrite may be due to the formation of aggregates with the clay-sized quartz, which has a lower SSA than illite (table 10). The microaggregate SSA of the artificial soil containing illite and ferrihydrite was not larger than that of the soils containing only illite. This could indicate that the main part of the microaggregates present was formed with illite. Ferrihydrite microaggregates would be expected to have a higher SSA due to the higher SSA of ferrihydrite compared to illite (table 10). However, microaggregates composed of OM and ferrihydrite may have been too heavy to be separated from the mineral fraction, as ferrihydrite has a density of approximately 3.8 g cm^{-3} , whereas quartz, illite and boehmite have densities around 2.6 g cm^{-3} (Webmineral.com, 2010). Aggregates containing ferrihydrite would therefore be more likely to be present in the mineral fraction ($> 2.4 \text{ g cm}^{-3}$). However, the mass contribution of ferrihydrite in this fraction was so low that a difference between soils with and without ferrihydrite was not detectable. It is also possible that fewer microaggregates were formed with ferrihydrite. The OM content of the $1.8\text{-}2.4 \text{ g cm}^{-3}$ fraction is not higher for the soils containing ferrihydrite compared with the soil containing only illite (data not shown). This indicates that no or very little ferrihydrite aggregates were present in the microaggregate fraction, as their abundance was too low to change the OM content significantly. The total amount of microaggregated and mineral associated OC was similar for the artificial soil containing only illite and that containing both illite and ferrihydrite (figure 14).

Overall, only small changes were observed in the properties of the bulk artificial soil materials with increasing incubation time. To investigate the active fractions of the artificial soil, where development of interfaces took place, these regions need to be concentrated by particle size or density fractionation. The observed fast formation of macroaggregates and the subsequent decline of macroaggregation after 1 year of incubation together with the gradual increase in microaggregation over time fits well with the aggregate hierarchy model (Oades, 1984; Six et al., 2004; Tisdall and Oades, 1982). This model also states that microaggregates are gradually formed within macroaggregates and are more stable, whereas macroaggregates are less stable and will decline with increasing decomposition of the OM present in the system. With this experiment, we could show this process of formation of macro- and microaggregates from simple, pure and clean model materials to a soil-like system that took place within 18 months of incubation.

5.3 The effect of mineral composition and charcoal

5.3.1 Importance of clay mineral presence for macroaggregation

The lower amount of aggregates > 2 mm present in the artificial soil containing clay-sized quartz instead of a clay mineral (FH) indicates that the presence of clay minerals was important for the formation of macroaggregates in the artificial soils. As the soils all had the same texture, it has to be the specific physiochemical properties of the clay minerals that affect macro-aggregation. This may be due to static interactions and cation bridging of Ca^{2+} ions with the permanent negative charge of the clay minerals. An additional factor could be a difference in flocculation and aggregation behavior due to differences in particle shape. The clay minerals are present as platy particles whereas scanning electron microscopy (SEM) showed that the clay-sized quartz consisted of spherical particles (data not shown).

No difference in aggregation was seen between the expandable clay mineral montmorillonite and the non-expandable illite. It might be expected that the expandable interlayers of the montmorillonite would have some effect on aggregation. However, these properties are probably most relevant when the soil material is exposed to wetting and drying cycles, whereas the artificial soils in this incubation experiment were kept at a constant moisture level. Denef and co-authors (Denef and Six, 2005; Denef et al., 2002) examined aggregate formation and stability in soil containing 1:1 clay minerals (kaolinite) versus soil containing 2:1 clay minerals (illite). They found that more stable aggregates were formed in the soil containing 2:1 clay minerals, especially under the influence of biological activity. They further concluded that aggregate formation in the 1:1 soil was probably due to electrostatic interactions between 1:1 clay minerals and oxides. The illite and montmorillonite considered in this study are both 2:1 clay minerals. It is possible that aggregation would have been different if a 1:1 mineral like kaolinite had been used in this study. Overall, these results show that the presence of clay minerals is important for macro-aggregation due to their shape and specific surface properties.

5.3.2 Low effect of ferrihydrite and boehmite on aggregation

The constant extractable amounts of Fe, Al and Si present in the artificial soils over time indicate that the oxides were relatively stable during the entire incubation time. The low amounts of oxalate and dithionite extractable Al found indicate that the boehmite used for

artificial soils was not well soluble with these methods. Furthermore, it shows that no free Al was available in the artificial soils, as expected at the high pH of the artificial soils. The extractable Si found in all soils shows that the silt- and clay-sized quartz material used was probably not completely inert as it was previously assumed. The quartz may have been involved in the formation of organo-mineral complexes and microaggregates, especially in the artificial soil containing clay-sized quartz minerals. This may be contrary to processes occurring in nature, where quartz is considered to be of little relevance for the formation of aggregates and organo-mineral associations. The clay-sized quartz used here would probably not be stable in nature due to its high reactivity. As quartz is not thermodynamically stable at the earth surface, it would soon be dissolved. These results show that quartz is not a good model material for clay-sized material, and should not be used in future incubation experiments.

The low oxalate-extractable Fe content determined for the ferrihydrite containing soils was unexpected. Oxalate extractable Fe is generally considered an indicator of the amount of weakly crystalline iron oxides present, whereas dithionite-extractable Fe represents all Fe oxides (Cornell and Schwertmann, 1996). It was expected that ferrihydrite would behave like a weakly crystalline oxide and would be extractable by oxalate. However, the 6-line ferrihydrite that was synthesized represents a relatively well-crystallized form of ferrihydrite (Schwertmann and Cornell, 1991) and is therefore apparently not well extractable by oxalate. Furthermore, ferrihydrite in the artificial soils was present as distinct particles, whereas ferrihydrite in nature usually occurs as nano-particles and coatings on other minerals (Hochella et al., 2008; Qafoku, 2010; Wagai and Mayer, 2007) which may be better extractable than the synthetic ferrihydrite used here.

The low concentrations detected for CuCl_2 and Na-pyrophosphate extractable Fe and Al indicate that little of the ferrihydrite and boehmite associated with OM (Juo and Kamprath, 1979; Kaiser and Zech, 1996). This is further confirmed by the similar amounts of microaggregated carbon found independent of mineral composition (figure 14), and the microaggregate SSA close to $30 \text{ m}^2 \text{ g}^{-1}$, which indicates that most microaggregates were formed with illite instead of ferrihydrite or boehmite (see section 5.2.4). This apparent lack of effect of ferrihydrite on aggregation is unexpected, as ferrihydrite was found to be important for the formation of microaggregates in natural soils (Barral et al., 1998; Deneff and Six, 2005; Six et al., 2004; Wagai and Mayer, 2007). It may be that the relatively high crystallinity of the

ferrihydrate and boehmite chosen made them less reactive than the respective minerals occurring in natural soils. However, the model ferrihydrate and boehmite used did have a high SSA (table 10) which would make them important potential sorption sites in the artificial soil. One possible explanation for the apparently low reactivity of the ferrihydrate and boehmite is the high pH (7-7.6, table 11) of the artificial soils. This pH is close to the point of zero charge of synthetic ferrihydrate (Schwertmann and Fechter, 1982; Schwertmann and Taylor, 1989) which indicates that the ferrihydrate in the soils was close to neutral or negatively charged. Ferrihydrate in natural soils with a lower pH is usually positively charged, which is one of the reasons for its strong interactions with usually negatively charged organic substances and clay minerals (Denef et al., 2002). The close to neutral or negative surface charge that may occur in the artificial soils would decrease the affinity of ferrihydrate for OM. This may explain why the effect of ferrihydrate on macro- and microaggregation in our experiment was low, and why the presence of clay minerals with permanent charge was so important for aggregate formation. In this environment, the permanently charged clay mineral particles provide a preferable interface for interaction with microbes and OM. The microaggregates were further studied by nano-scale secondary ion mass spectrometry (NanoSIMS), which also indicated that OM was indeed predominantly associated with the clay minerals (Heister et al. 2011). Our results also suggest that other sorptive interactions between organic matter and iron oxide surfaces, such as the interactions between aromatic pi systems and iron oxide surfaces (Keiluweit and Kleber, 2009), which occur independent of pH, may not play a major role for the formation of organo-mineral associations in these soils, and that pH-dependent ligand-exchange is the relevant process (Chorover and Amistadi, 2001).

5.3.3 Effect of charcoal on aggregation

The presence of charcoal had no effect on microaggregation and a negative effect on macroaggregation. This negative effect on macroaggregate stability was unexpected. Previous studies have indicated that black carbon was preferentially included in microaggregates and it was speculated that black carbon might have a positive effect on aggregation (Brodowski et al., 2005; Brodowski et al., 2006). The interaction of black carbon with the mineral phase is explained by the formation of functional groups during transformation by biological activity that then lead to the formation of organo-mineral associations (Hilscher and Knicker, 2011a; Hilscher and Knicker, 2011b). However, black carbon can have a very different structure and chemical properties depending on its origin and conditions during charring. For example,

Kuzyakov et al. (2009) found very low biological activity and transformation rates for a more strongly charred black carbon material. It may be that the charcoal used in this study also was relatively strongly charred and that its reactivity and transformation rate were therefore low, leading to little formation of functional groups during the incubation time, and therefore less potential for interactions with minerals. The high degree of charring of the model material charcoal used in this study was confirmed by solid-state ^{13}C nuclear magnetic resonance (NMR) spectroscopy, which gave a spectrum with only an aromatic peak (see chapter 6, figure 19). The negative effect of charcoal on soil structure observed in this study may have important implications for the current discussion on biochar addition to soil. As it is discussed in the extensive review on biochar and its function in soil by Sohi et al. (2010) very little information is available on the effect of charcoal addition on soil micro- and macroaggregation, and this should be a focus for future research.

6 Organic matter dynamics and the development of the phenanthrene sorptive interface in an artificial soil incubation experiment

6.1 Results

6.1.1 OM distribution and composition

A small decrease in organic carbon (OC) content with time took place during artificial soil incubation due to respiration and loss of CO₂ (table 13). The nitrogen contents did not change with incubation time, leading to a gradual decrease in bulk C/N ratio of the artificial soils with time.

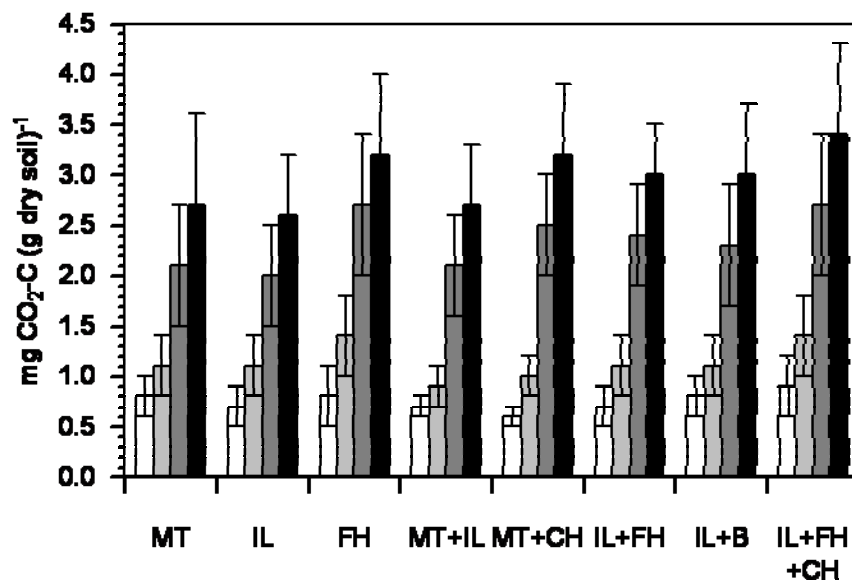


Figure 15. Cumulative CO₂ respiration of the artificial soils in mg CO₂-C g dry soil⁻¹ after 3 months (□), 6 months (▒), 12 months (▓), and 18 months of incubation (■). Soil composition is indicated by MT (montmorillonite), IL (illite), FH (ferrihydrite), CH (charcoal) and B (boehmite).

Cumulative CO₂ respiration (figure 15) was not significantly different between soil compositions, based on the calculated confidence intervals. The cumulative CO₂ release from the soils only containing quartz and a clay mineral (MT, IL and MT+IL) seems to be slightly lower than that of the other compositions. However, variability between replicates for the soil compositions was large, and no significant difference in CO₂ respiration between compositions was found. The CO₂ respiration rates were high (0.1-0.2 mg CO₂-C (g dry soil)⁻¹ d⁻¹) during the first few weeks of incubation, and after that decreased to a relatively constant

level of $0.01 - 0.04 \text{ mg CO}_2\text{-C (g dry soil)}^{-1} \text{ d}^{-1}$ for the rest of the incubation time. Fungal hyphae were observed in the soil after approximately 1 month of incubation (figure 16).



Figure 16. Fungal hyphae observed in some of the artificial soils after 1 month of incubation.

The OC stocks of the different particle size fractions were redistributed with time (figure 17.). Overall, the OC stock of the 200-2000 μm fraction decreased whereas the OC stock of the $<20 \mu\text{m}$ fraction increased. After 18 months of incubation, approximately 50 % of the OC of the 200-2000 μm fraction was either respired or transported to the finer fractions. For all of the artificial soil mixtures not containing charcoal, OC stocks in $\text{mg C (g bulk soil)}^{-1}$ were largest in the 200-2000 μm fraction during the entire incubation time. The 63-200 and 20-63 μm fractions did not really change with incubation time, and can probably be considered of less importance for those artificial soil compositions that did not contain charcoal. The charcoal material added had a particle size between 63 and 200 μm . The higher carbon contents, compared with the soils not containing charcoal, and the high C/N ratios of the smaller particle size fractions show that charcoal particles in the artificial soils were broken up and transported to the fine fraction.

Table 13. Bulk organic carbon (OC) and N content and C/N ratio at $t=1$ (start of incubation) and $t=4$ (18 months of incubation), standard deviations were calculated from the three replicates for each artificial soil composition.

Composition	OC mg g^{-1}		N mg g^{-1}		C/N	
	$t=0$	$t=4$	$t=0$	$t=4$	$t=0$	$t=4$
MT	16 ± 0.6	14 ± 0.9	1.4 ± 0.1	1.3 ± 0.1	11.5	10.2
IL	16 ± 3.3	12 ± 0.2	1.4 ± 0.3	1.2 ± 0.02	11.3	9.9
FH	14 ± 1.2	13 ± 1.0	1.3 ± 0.1	1.3 ± 0.1	11.4	9.7
MT+IL	16 ± 0.9	13 ± 1.0	1.3 ± 0.1	1.2 ± 0.1	12.0	10.2
MT+CH	31 ± 2.4	26 ± 2.0	1.5 ± 0.3	1.3 ± 0.2	21.2	19.3
IL+FH	17 ± 2.5	12 ± 0.5	1.5 ± 0.2	1.2 ± 0.02	11.6	9.5
IL+B	14 ± 1.0	12 ± 1.0	1.2 ± 0.1	1.2 ± 0.1	11.4	9.8
IL+FH+CH	30 ± 1.4	28 ± 2.6	1.4 ± 0.1	1.6 ± 0.2	21.3	17.8

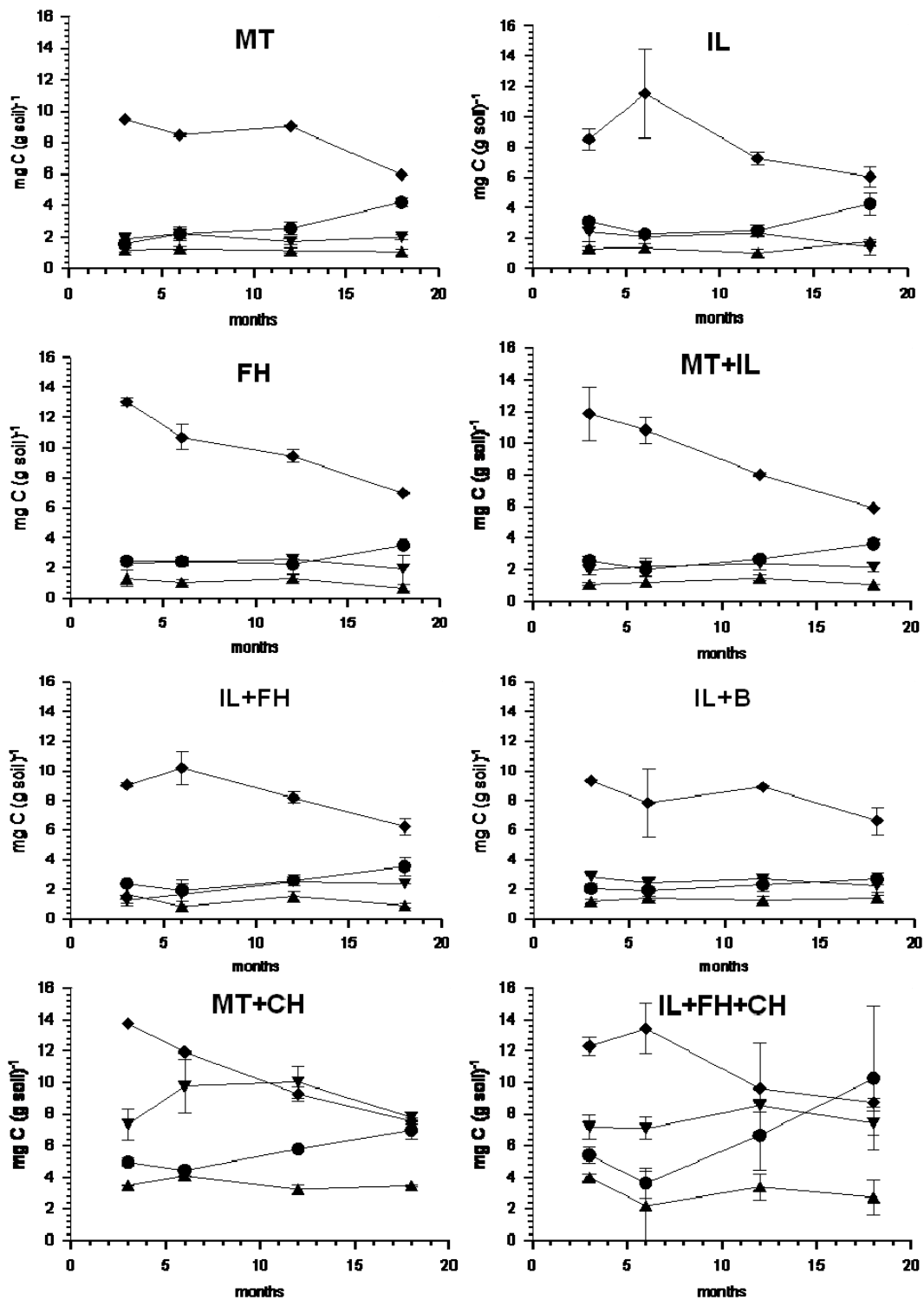


Figure 17. Organic carbon stocks in mg C (g bulk soil)⁻¹ of the particle size fractions with incubation time. The particle size fractions indicated are 200-2000 μm (◆), 63-200 μm (▼), 20-63 μm (▲) and <20 μm (●). Soil composition is indicated by MT (montmorillonite), IL (illite), FH (ferrihydrite), CH (charcoal) and B (boehmite). Error margins are based on the difference between 2 replicates per soil composition.

It may be that the sieving and fractionation procedure also had an effect on the charcoal particle size distribution (Schmidt, Rumpel et al. 1999), although only a low ultrasonic dispersion energy of 60 J ml^{-1} was used in the physical fractionation procedure. Overall, the variability in charcoal distribution over the particle size fractions was high between replicates. Figure 18 shows the OC and N content and the C/N ratio of the $<20\mu\text{m}$ fractions and the expected OC, N and C/N values for these fractions based on the particle size distribution and OC and N content of the original manure used in the incubations. The OC content of the $<20\mu\text{m}$ fraction clearly increased in the first 3 months of incubation compared with that expected from the manure properties, whereas the nitrogen content stayed approximately constant for the first 6 months, after which it increased in all artificial soils.

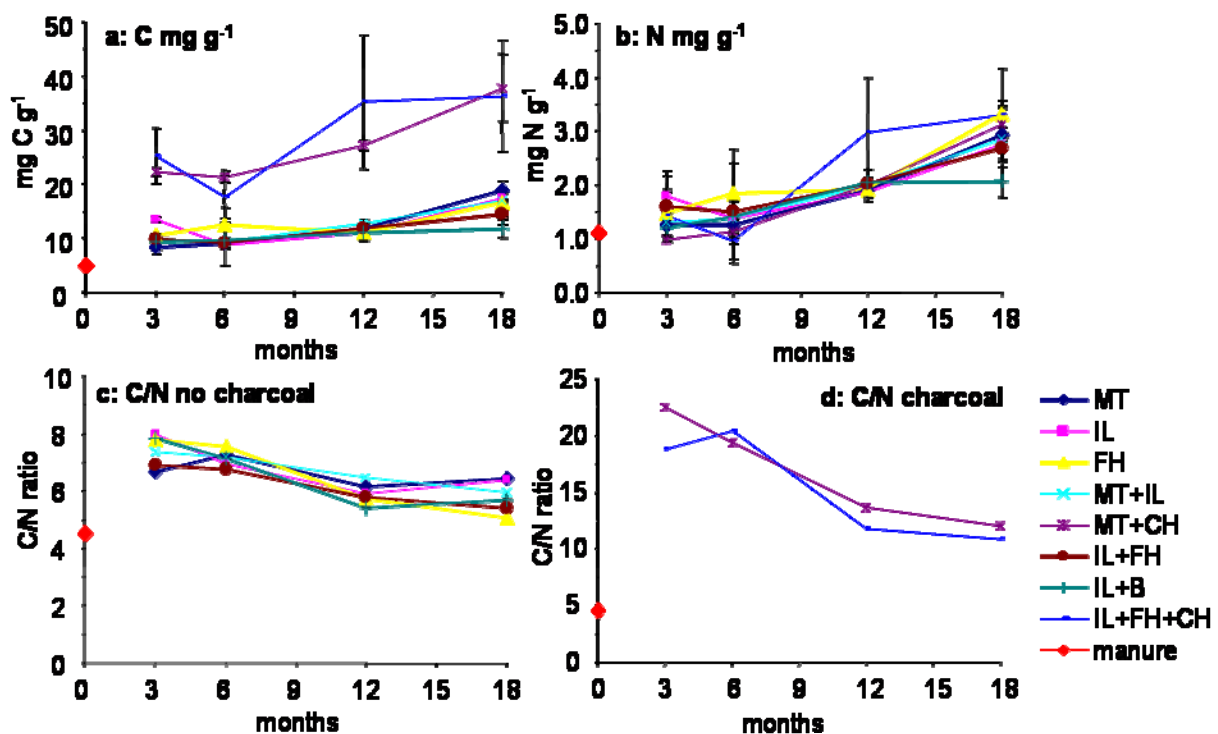


Figure 18. Carbon and nitrogen content in mg g^{-1} of the $<20\mu\text{m}$ particle size fractions. Soil composition is indicated by MT (montmorillonite), IL (illite), FH (ferrihydrite), CH (charcoal) and B (boehmite). The C and N content and C/N ratio of the $<20\mu\text{m}$ particle size fractions expected from the original manure is indicated by the red diamond. Error margins are based on the difference between 2 replicates per soil composition.

The organic matter (OM) composition of selected artificial soil samples and the model materials manure and charcoal was characterized by solid-state ^{13}C NMR. The bulk manure spectrum (figure 19) was dominated by a large double signal in the O/N-alkyl-C range. The spectrum of the $<20\mu\text{m}$ fraction of the manure had higher relative abundances of alkyl-C ($<50\text{ ppm}$) and the carboxyl-C (160-220) than the bulk soil material. The charcoal spectrum only showed one major signal in the aromatic region (figure 19). The solid-state ^{13}C NMR

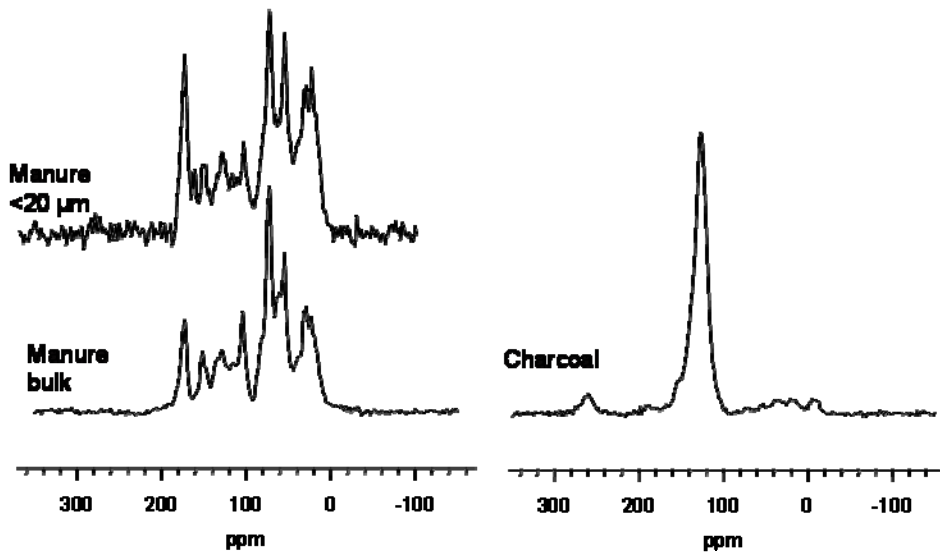


Figure 19. Solid-state ^{13}C NMR spectra of the charcoal and manure model materials used and $<20\ \mu\text{m}$ particle size fraction of the manure, chemical shift is indicated in ppm.

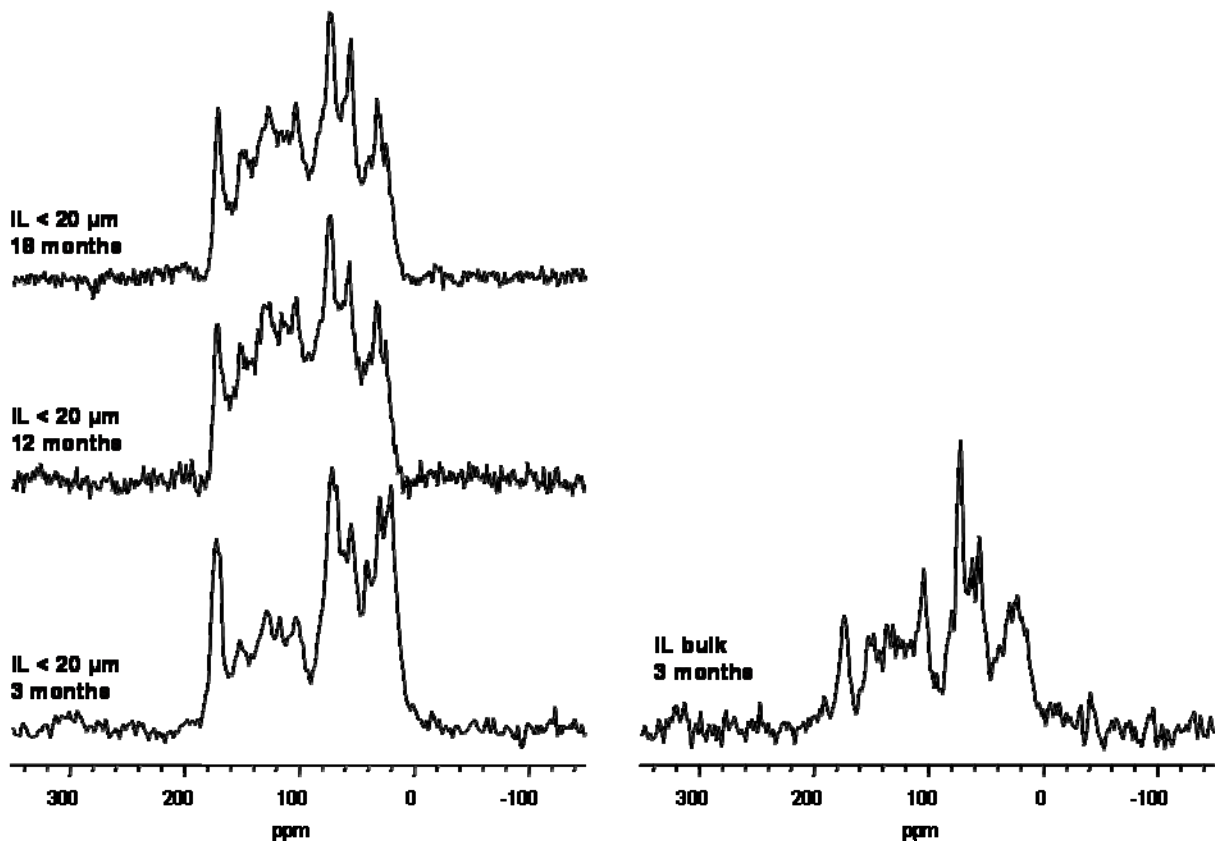


Figure 20. Solid-state ^{13}C NMR spectra of the $<20\ \mu\text{m}$ fraction, and the bulk sample after 3 months of incubation, of the artificial soil containing illite (IL) with incubation time, chemical shift is indicated in ppm.

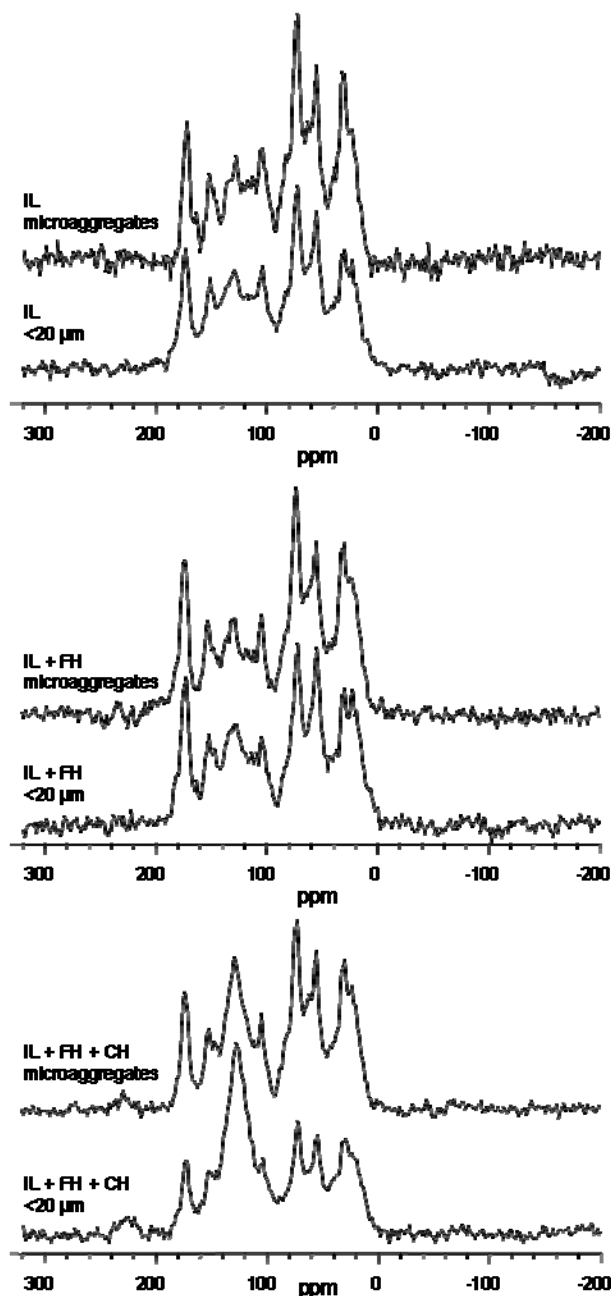


Figure 21. Solid-state ^{13}C NMR spectra of the $<20\ \mu\text{m}$ particle size fraction and the microaggregate (1.8-2.4 g cm^{-3}) density fraction for the artificial soil containing illite (IL), illite and ferrihydrite (IL+FH) and illite, ferrihydrite and charcoal (IL+FH+CH) after 12 months of incubation, chemical shift is indicated in ppm.

spectra of the bulk soil and $<20\ \mu\text{m}$ fraction of the illite containing artificial soil (IL) (figure 20) reflect the respective composition of the bulk and $<20\ \mu\text{m}$ fraction of the manure, with higher relative abundances of alkyl-C and the carboxyl-C in the $<20\ \mu\text{m}$ fraction compared to the bulk soil. The spectrum of the $<20\ \mu\text{m}$ fraction after 3 months of incubation was similar to that of the $<20\ \mu\text{m}$ fraction of the manure. With incubation time, the relative abundance of the alkyl-C and the carboxyl-C decreased, whereas O/N-alkyl-C groups increased. Furthermore,

there seems to be a relative increase of the 56 ppm peak, which can be an indicator for proteins, versus the 65 and 72 ppm peaks that may point to the presence of polysaccharides (Baldock, Oades et al. 1992; Kögel-Knabner 2002). The solid-state ^{13}C NMR spectra of the microaggregate fraction ($1.8\text{-}2.4\text{ g cm}^{-3}$) were compared to the $<20\mu\text{m}$ fraction of the respective soil. The spectra (figure 21) show that overall, OC composition was similar. However, there was a small increase in the relative abundance of O/N-alkyl-C, mainly the 72 ppm signal, and alkyl-C, mainly in the 29-33 ppm region indicative for longer chain structures like e.g. lipids (Baldock, Oades et al. 1992; Quideau, Chadwick et al. 2001; Kögel-Knabner 2002), in the microaggregate fractions compared to the respective $<20\mu\text{m}$ fractions. There was a clear aromatic signal in the microaggregate fraction of the sample containing charcoal (IL + FH + CH). However, the signal was lower than that of the corresponding $<20\mu\text{m}$ fraction.

6.1.2 Phenanthrene sorption

Phenanthrene sorption experiments were performed with the $<20\text{ }\mu\text{m}$ fraction of the artificial soils incubated for 3 ($t=1$) and 12 ($t=3$) months. The soil compositions considered for $t=1$ were IL (containing illite and quartz), FH (ferrihydrite and quartz) and IL + FH (illite + ferrihydrite + quartz) and those for $t=3$ were IL, IL + FH and IL + FH + CH (illite + ferrihydrite + charcoal + quartz). An overview of the properties of the samples used for the sorption experiments can be found in table 14.

Table 14. Properties of the samples used for phenanthrene sorption experiments; organic carbon content (OC), C/N ratio and the BET- N_2 specific surface area (SSA). Soil composition is indicated by IL (illite), FH (ferrihydrite) and CH (charcoal).

incubation time	composition	OC mg g^{-1}	C/N	SSA $\text{m}^2 \text{g}^{-1}$
3 months	IL	8.8 ± 0.8	6.7	9.0 ± 0.4
	FH	12.8 ± 0.1	6.7	6.8 ± 0.4
	IL+FH	7.8 ± 0.2	6.4	9.6 ± 0.4
12 months	IL	11.1 ± 0.2	6.2	5.8 ± 0.4
	IL+FH	12.9 ± 0.1	6.3	8.0 ± 0.4
	IL+FH+CH	22.9 ± 0.8	11.7	6.2 ± 0.4

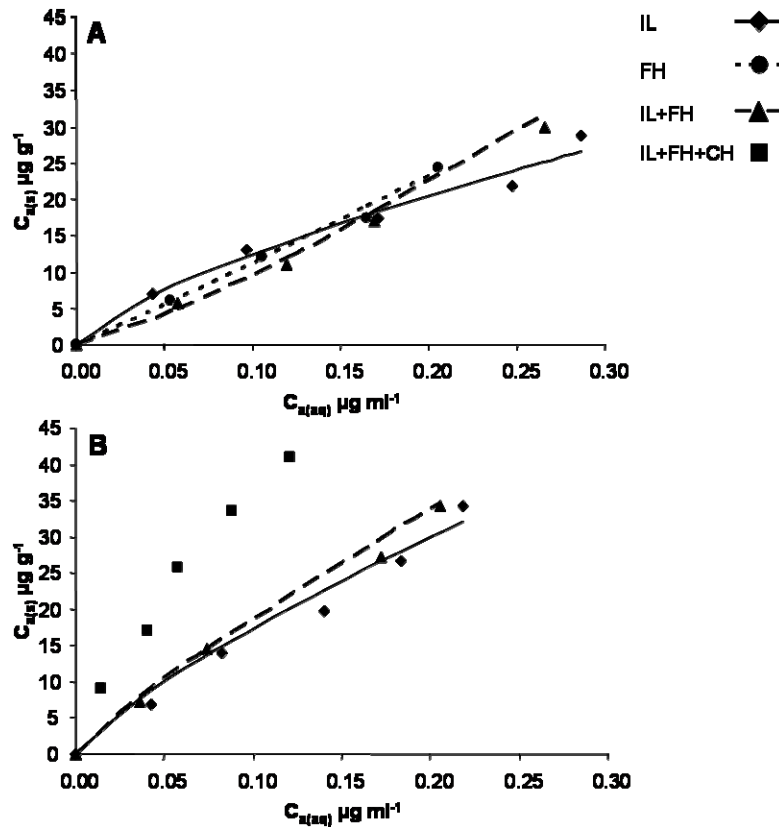


Figure 22. Phenanthrene sorption isotherms of the <math><20\ \mu\text{m}</math> particle size fractions of the artificial soils after 3 (A) and 12 (B) months of incubation. $C_{(s)aq}$ represents the phenanthrene concentration in solution after equilibration in $\mu\text{g phenanthrene ml}^{-1}$ and $C_{(s)s}$ represents the concentration of phenanthrene adsorbed on the sample in $\mu\text{g phenanthrene g}^{-1}$.

The data of all isotherms are well described by both the Freundlich and Langmuir isotherm model (table 15, figure 22). The more complex models like the multi-site Langmuir and BET models did not result in a better description of the sorption isotherms than the Freundlich and Langmuir isotherm model (data not shown) and were not further considered in this study. The Freundlich isotherm method gives slightly better R^2_{adj} results than the Langmuir model for all samples except IL at $t=3$ (table 15). The Freundlich isotherm was therefore used for the further evaluation of the data. Phenanthrene sorption was carried out at two additional high phenanthrene concentrations for the 12 month ($t=3$) incubated samples in order to study the behaviour of sorption closer to the maximum water solubility of phenanthrene. It was expected that this would allow for a better determination of the type and mechanisms of sorption taking place, and may lead to a better isotherm model describing phenanthrene sorption to the artificial soils. Sorption at high concentrations was still best described by the Freundlich isotherm model, and the isotherm shape was similar for all soil compositions considered (figure 23).

Table 15. Sorption isotherm coefficients calculated using the Freundlich and Langmuir isotherm models. Artificial soil composition is indicated by IL (illite), FH (ferrihydrite) and CH (charcoal) ‘high’ indicates the sorption isotherms with two additional points at high phenanthrene concentration. The best fit, as determined by the correlation coefficient adjusted to the number of parameters used (R^2_{adj}), is highlighted.

incubation time	composition	Freundlich				Langmuir		
		K_f	K_{fOC}	$1/n$	R^2_{adj}	K_l	A_{max}	R^2_{adj}
3 months	IL	66 ± 4.4	7.5	0.73 ± 0.04	0.975	1.95 ± 0.47	78 ± 17	0.962
	FH	125 ± 15	9.7	1.04 ± 0.06	0.990	0.51 ± 0.05	248 ± 23	0.984
	IL+FH	160 ± 56	20.5	1.22 ± 0.17	0.988	0.37 ± 0.04	313 ± 29	0.971
12 months	IL	108 ± 3.4	9.7	0.79 ± 0.03	0.989	0.81 ± 0.13	225 ± 28	0.994
	IL+FH	132 ± 4.3	10.2	0.84 ± 0.03	0.992	0.59 ± 0.14	343 ± 65	0.990
	IL+FH+CH	n.m						
	IL high	144 ± 10	12.9	0.97 ± 0.04	0.990	0.45 ± 0.13	383 ± 68	0.979
	IL+FH high	127 ± 10	9.8	0.85 ± 0.03	0.994	0.37 ± 0.18	178 ± 25	0.992
	IL+FH+CH high	n.m						

n.m: no modelling data available

The phenanthrene sorption isotherms of the 3 months incubated samples show a clear difference between the sorption isotherm of IL and that of the artificial soils containing ferrihydrite, FH and IL+FH (figure 22a). The K_f of the ferrihydrite containing samples is significantly higher than for IL (table 15). Furthermore, the sorption isotherm of IL is nonlinear and has a convex shape, which is reflected in its nonlinearity ($1/n$) lower than 1, whereas the isotherm for FH and IL+FH at $t=1$ are close to linear and have a slightly concave shape and a $1/n$ larger than 1. The sorption isotherms for the 12 months incubated artificial soils (figure 22b) show a slight increase in phenanthrene sorption compared to the respective soil compositions that were incubated for only 3 months. No difference was found between IL and IL+FH for this time step, whereas phenanthrene sorption to IL+FH+CH was higher than of IL and IL+FH. The sorption isotherms for all 12 month incubated samples were nonlinear and convex with an $1/n$ smaller than 1. The K_f of IL increased with incubation time whereas that of IL+FH decreased slightly (table 3). This decrease in K_f for IL+FH was due to the lower $1/n$ and the different shape of the isotherm, as the actually measured phenanthrene sorption of IL+FH increased slightly from the 3 months to the 12 months incubated sample.

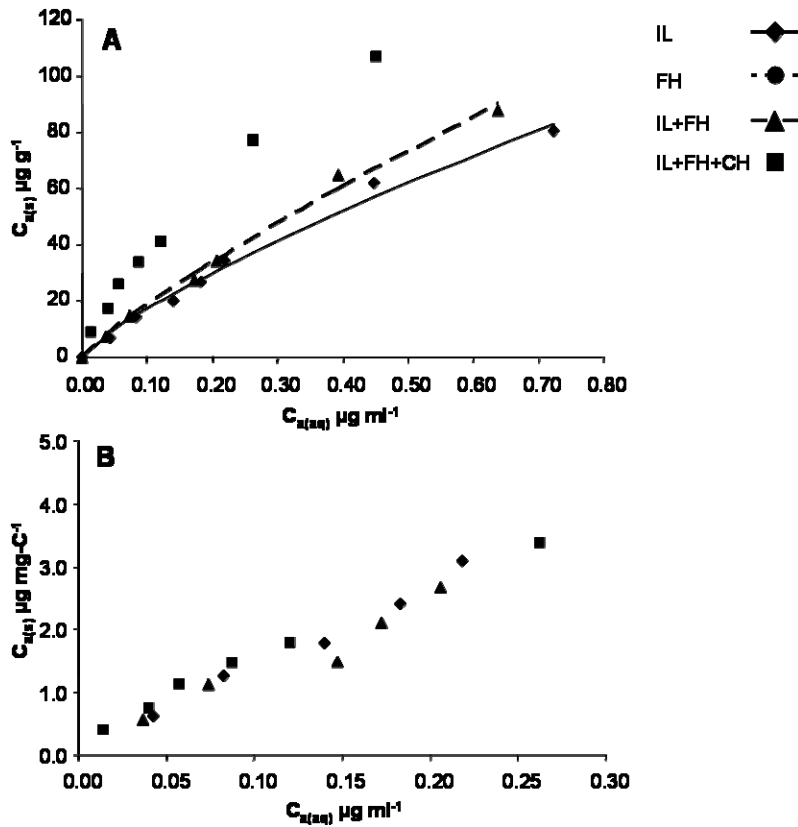


Figure 23. Phenanthrene sorption isotherms of the $<20 \mu\text{m}$ fraction of the artificial soils after 12 months of incubation were phenanthrene concentration adsorbed to the sample is expressed in $\mu\text{g (g sample)}^{-1}$ (A) and in $\mu\text{g (mg OC)}^{-1}$ (B). $C_{s(aq)}$ represents the concentration of phenanthrene in solution after equilibration in $\mu\text{g phenanthrene ml}^{-1}$.

The carbon normalized isotherms for the samples from $t=3$ (figure 23b) show that differences in phenanthrene sorption between samples after 12 months of incubation could be explained by the carbon concentration. The calculated K_{f_OC} values for these samples were also similar (table 15). The isotherms normalized to OC all lie directly on top of each other, and only at the highest concentration point for the charcoal containing soil, slight differences between the compositions could be seen. For the 3 months incubated samples there are differences after normalization to the OC content, as can be seen from the calculated K_{f_OC} values (table 15). This is mainly due to the differences in shape of the isotherms from this time-step, which did not change by normalizing to OC content.

6.2 Discussion

6.2.1 OM dynamics

The similar OC losses and cumulative CO₂ respiration rates determined for all artificial soils show that soil composition did not have an effect on respiration in this experiment. The amount of OM added to the artificial soils was relatively low with an initial carbon content of 15 mg g⁻¹, and no additional OC was added to the artificial soils during incubation. It is likely that microbial activity was limited by substrate availability after the first few weeks of incubation, and that soil composition was of secondary importance for respiration. There is no indication that degradation of charcoal occurred during incubation. The CO₂ respiration rates and changes in carbon content for the artificial soils containing charcoal are not higher than those of the other soils. Degradation of carbonaceous materials has been observed in other studies (e.g. Hilscher and Knicker, 2011) but may depend on the degree of charring of the material used. The charcoal added in this study was well-charred and consisted almost exclusively of aromatic compounds, as indicated by the solid-state ¹³C NMR spectroscopy (figure 19), and may therefore have been less degradable for microorganisms.

The transport of OC from the coarse to the finer fractions during incubation (figure 17) can be explained by microbial degradation and break up of larger particulate OM particles. The development of the OC distribution corresponds well with current knowledge (Christensen 2001; Kleber, Sollins et al. 2007). As there was no fresh input of OM in this experiment, it is natural that the OM present was gradually degraded and decreased in particle size. Approximately half of the OC of the coarse fraction was lost or transported to the smaller fractions after 18 months of incubation. The C/N ratio of the <20 μm fraction decreases to values between 5 and 6 after 18 months of incubation. This is low compared with data for natural soils studied. The C/N ratio of the total <20 μm particle size fraction of the natural soils from Ultuna, UL-Ca and UL-m, was calculated to be 9.4 and 9.2 respectively (calculated from table 2). This low C/N ratio could be caused by a large abundance of proteins and amino acids present in the fine fraction, but it is also likely that some inorganic nitrogen in the form of nitrate or ammonium was present. The only way for compounds to be lost from the artificial soils was to the atmosphere, whereas in a natural soil system, soluble nitrogen compounds can also be lost due to leaching to the groundwater. If no denitrification took place, this means that nitrogen was selectively preserved in the artificial soils relative to carbon, which was respired as CO₂.

The carbon content of the <20 μm fraction clearly increased in the first 3 months of incubation, whereas the nitrogen content stayed approximately constant for the first 6 months, after which it increased in all soils (figure 18). One possible explanation for this different behaviour of nitrogen could be that nitrogen was utilized by microorganisms for growth during the first 6 months of incubation, and incorporated in fungal hyphae and microbes living on coarse particulate OM. The artificial soils started as mixtures of clean materials not colonized by microorganisms. After inoculation, growth of bacteria and fungi occurred until a microbial community was established. Growth of fungi was even observed in some artificial soils after approximately 1 month of incubation (figure 16). It may be that during the first 6 months nitrogen was taken up by these microorganisms and used for growth and the production of biomass. After 6 months, microbial activity may have reached a level where it was limited by nutrient and substrate availability and nitrogen was no longer incorporated into biomass in the coarser fractions. As substrate availability declined during incubation due to CO_2 respiration and increasing formation of microaggregates and organo-mineral association, microbial activity probably gradually decreased. This would then have led to the degradation of the microbial biomass and increased transport of nitrogen to the fine fraction. The elucidation of microbial activity and community development during the artificial soil incubation should be a subject of further study that may be of use to test this hypothesis.

The ^{13}C NMR spectra of the bulk soil and <20 μm fraction of IL after 3 months of incubation are still similar to those of the bulk and <20 μm fraction of the manure. The difference in composition between the bulk artificial soils and <20 μm fraction can therefore be explained by the composition and particle size distribution of the manure. The increase of the 56 ppm signal relative to the 72 ppm signal of the ^{13}C NMR spectra with time (figure 20) points to a relative increase with time in the abundance of amino acids and proteins in the <20 μm fraction of the artificial soils. This fits well with the low C/N values found for this fraction. This decreasing C/N ratio and relative enrichment of proteinaceous material in the fine fraction is consistent with observations made in literature, as is extensively discussed in the review by Klebel et al. (2007). In recent studies, Sollins et al. (2009) also found that OM of microbial origin was preferentially associated with minerals using sequential density fractionation, and that OM composition was affected by surface characteristics of the minerals in the heaviest fraction. Miltner et al. (2009) studied the fate of microbial biomass in a soil incubation experiment and found that peptides and amino acids were relatively stable, which

was further confirmed by Spence et al. (2011) who also found that peptides can be stabilized by interactions with minerals. The accumulation of proteins in the <20 μm fraction of the artificial soils over time is in agreement with the conceptual model proposed by Kleber et al. (2007), who proposed that organo-mineral formations are build in a layered structure starting with a film of organic molecules that consists mainly of proteins that bind to the mineral surface followed by attachment of other types of organic molecules mainly by hydrophobic interactions. This effect may be enhanced by the relatively high pH of 7-7.6 of the artificial soils. At this pH the mineral surfaces are likely to have a negative surface charge. Proteins are well suited to interact with both positively and negatively charged surface due to their chemical characteristics (Kleber et al., 2007). More analyses are needed in order to determine whether the mineral composition of the artificial soils had an effect on OM composition during incubation.

The solid-state ^{13}C NMR spectra of the <20 μm were compared to that of the respective microaggregate fractions of the artificial soils containing illite, ferrihydrite and charcoal (IL, IL+FH and IL+FH+CH) (figure 21). From the high SSA of the microaggregate fraction (table 11), it was assumed that this material has small particle size, and the <20 μm fraction is probably most representative for comparison. The spectra of the <20 μm fraction and the microaggregate fraction are similar, although there seems to be a preferential uptake of aliphatic carbon in the microaggregates. This may indicate the preferential uptake of lipids into the microaggregates. There is a clear aromatic peak in the sample containing charcoal (IL + FH + CH), which shows that charcoal does interact with minerals and is included in microaggregates. However, the aromatic peak of the microaggregate fraction is clearly lower than that of the <20 μm fraction, indicating other types of organic carbon present are more likely to be incorporated into the microaggregates. This could be because charcoal consists of larger particles that are too light to be recovered in the microaggregate (1.8-2.4 g cm^{-3}) fraction, or because the charcoal used did not have many functional groups that can interact easily with mineral surfaces.

6.2.2 Development of the phenanthrene sorptive interface

The difference in isotherm shape between IL and FH and IL+FH in the 3 months incubated samples signifies that the presence of ferrihydrite provided different types of sorption sites or mechanisms for phenanthrene sorption, resulting in a different shape of the phenanthrene

sorption isotherm. It may be that ferrihydrite itself provided sorption sites for phenanthrene, or it could be that the presence of ferrihydrite led to a different development of the artificial soils, leading to different properties of the sorptive interface. It is generally considered that phenanthrene sorption to mineral surfaces is only relevant at low organic matter contents based on the work by Schwarzenbach and Westall (1981). However, several studies have shown that significant sorption of phenanthrene to mineral surfaces can also occur in model systems containing smectites, iron and aluminium oxides and goethite coated quartz (Mader, Uwe-Goss et al. 1997; Hundal, Thompson et al. 2001; Müller, Totsche et al. 2007). It has been suggested that π bonding systems between aromatic rings and oxides in particular may be of importance for sorption of aromatic molecules like phenanthrene to mineral surfaces (Keiluweit and Kleber 2009). Recent developments in research into PAH sorption to soil materials further show that mineral presence affects sorption due to interactions with organic matter and consequent changes in the organic matter structure and availability of sorption sites (Celis, Jonge et al. 2006; Bonin and Simpson 2007; Pan, Xing et al. 2007; Ahangar, Smernik et al. 2008). Both of these processes may have occurred in the artificial soils. The results in chapter 5 show that ferrihydrite probably was of less importance for the formation of organo-mineral associations in the artificial soils. Furthermore, the OC contents of the samples used for the phenanthrene sorption was low (table 14). It can therefore be concluded that the mineral surface of ferrihydrite itself provided a sorptive interface for phenanthrene in the 3 months incubated samples.

After 12 months of incubation, no difference in phenanthrene sorption between IL and IL+FH could be seen. This shows that the phenanthrene sorptive interface of the artificial soils developed over time. The mineral surfaces may have been increasingly covered by organic matter, and may therefore no longer have affected phenanthrene sorption. This is further supported by the increasing amount of microaggregation and mineral-associated OM with time, as was discussed in chapter 5, and the increasing OC content of the <20 μm fractions with time (table 14). The development of the phenanthrene sorptive interface with time may well be related to the accumulation of proteins and other compounds on mineral surfaces in the fine fraction. According to the model of Kleber et al. (2007), amphiphilic OM compounds form a film on the mineral surfaces that then serve as a 'hydrophobic zone', where sorption of hydrophobic moieties like phenanthrene can take place.

The phenanthrene sorption isotherms of the 12 months incubated samples normalized to OC all lie directly on top of each other, and only at the highest concentration point for the charcoal containing soil, slight differences between the compositions could be seen (figure 23b). This shows that differences in sorption between these samples could be explained by the OC content of the samples. This is unexpected, as charcoal has a very different structure and porosity from OM, which would be expected to lead to different sorption behaviour of phenanthrene. Several studies have shown that phenanthrene interacts especially strongly with aromatic carbon (Abelmann, Kleineidam et al. 2005; Chefetz and Xing 2009). It was therefore expected that phenanthrene would interact more strongly with charcoal, leading to a higher sorption isotherm, even when normalized to OC content. The differences in sorption isotherms between soil compositions after 12 months of incubation could be explained by the organic carbon content of the samples over the entire range of phenanthrene concentrations tested. The additional testing of phenanthrene sorption at concentrations closer to the phenanthrene water solubility concentration therefore did not give additional information on the sorption behaviour of these samples. It may be useful to study sorption at high concentration with the samples that were incubated only 3 months. Here, the isotherms of the samples containing ferrihydrite were linear or even concave in shape. It would be interesting to see how this trend proceeds at higher concentrations, and may lead to further insights into the mechanisms of sorption in a system where mineral composition is important for phenanthrene sorption.

6.3 The artificial soil system in comparison to natural soils

The ^{13}C NMR spectrum of the bulk manure is relatively similar to that of the Ultuna bulk soils and particle size fractions (chapter 4, data not shown). This confirms that the manure used was a suitable model material to simulate this natural soil, although larger differences between the bulk soil and fine fraction were found for the artificial soil than for the Ultuna soils. This may be because due to the lack of input of fresh organic matter from root and plant material, the OM in the $<20\ \mu\text{m}$ fraction of the artificial soils has become dominated by OM of microbial origin. The redistribution of organic matter from the coarse to the fine fraction, and the gradual accumulation of organic matter with a low C/N ratio in the fine fraction during the artificial soil incubation experiment is consistent with literatures as extensively discussed by e. g. Christensen (1992) and (2001) and Kleber et al. (2007). Rapid turnover of coarse OM and redistribution to the fine fraction within one year was also found in an

incubation experiment with well developed soil material and compost by Grosbellet et al. (2011). The accumulation rates of OM in the fine fraction is difficult to compare with initial soils in natural systems because there was no fresh organic matter input into the artificial soils after the start of incubation. Furthermore, there are much more clean mineral surfaces present in the artificial soils compared to natural initial soils of, for example, proglacial areas where weathering of minerals may not yet be well progressed. The development of soil OM and formation of organo-mineral formations in these systems is usually studied on a time-scale of years and decades rather than months (Egli, Mavris et al. 2010; Dümig, Smittenberg et al. 2011). The results from this artificial soil incubation experiment shows that these processes may occur on a much shorter time scale if mineral surfaces are available.

The calculated Freundlich isotherm coefficients (K_f) for phenanthrene sorption to the $< 20 \mu\text{m}$ fraction of the artificial soils were between 60 and 144, which is in the lower range of the K_f determined for the natural soil UL-Ca (Chapter 4, table 8) which had the same bulk OC content as the artificial soils. Phenanthrene sorption to the fine fraction ($0.2\text{-}6.3 \mu\text{m}$) of UL-Ca was higher with a K_f of 178, but this can probably be explained by its higher OC content and clay content of this fraction. The sorption isotherms determined for all natural soil samples were non-linear to close to linear and convex shaped. This fits better with the isotherm shape found in the artificial soils after 12 months of incubation. The concave isotherms found for the ferrihydrite containing samples after 3 months of incubation are probably not a good representation of a natural topsoil. Differences in phenanthrene sorption with mineral composition were seen after 3, but not after 12 months of incubation. This indicates that the interface matured with time, and the effect of mineral composition became less relevant than the OM content of the samples. Over incubation time, the shape of the sorption isotherms became more similar to those observed in the natural soils (Chapter 4). This demonstrates that the artificial soils are developing over time and are becoming more like a soil-like system. From this study, it can be concluded that mineral composition can be relevant for phenanthrene sorption in systems that are not yet far developed, and in systems with low organic matter content. However, in natural soils with well-developed biogeochemical interfaces, it would be expected that organic matter content and composition, and the interaction between OM and minerals is the main factor controlling phenanthrene sorption.

7 Development of the artificial soils over time; processes and open questions

The data presented in chapter 5 and 6 demonstrate the gradual development of the artificial soils over time. The development of the biogeochemical interfaces in the artificial soils, and the interaction between the different components is presented schematically in figure 24.

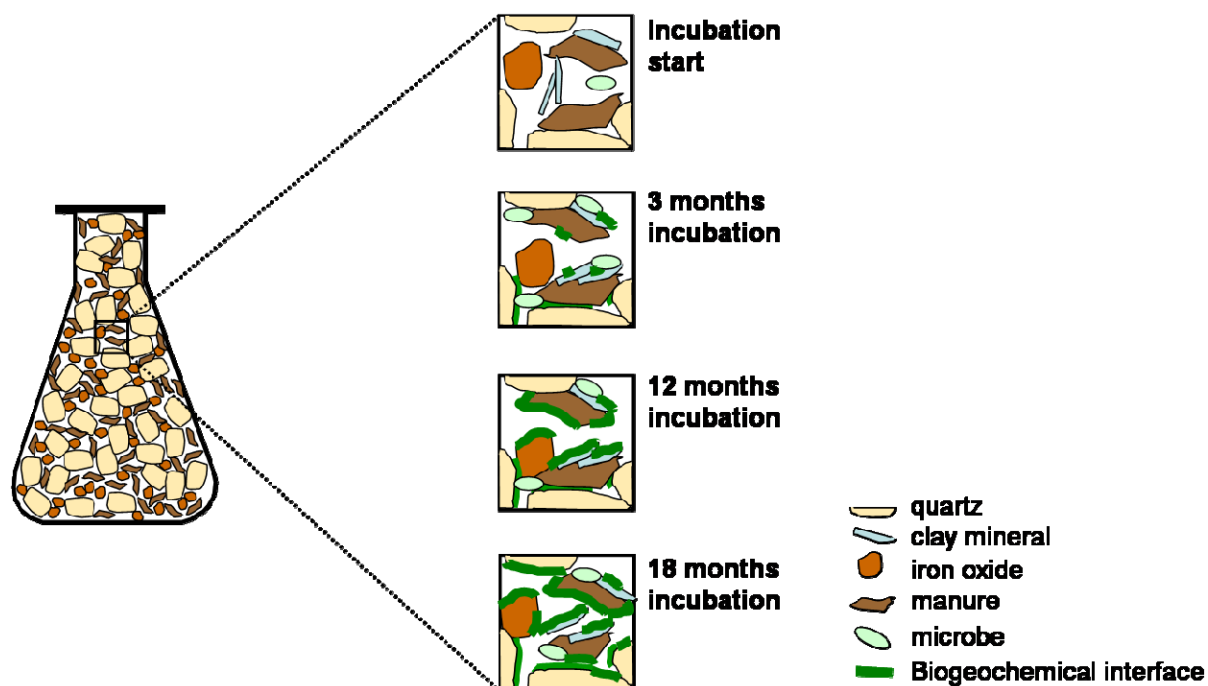


Figure 24. Schematic overview of the development of the artificial soils with incubation time.

During the 18 months of incubation the artificial soils were colonized by microorganisms, an active microbial community grew and started to decline after 3 to 6 months of incubation. At the same time macroaggregation developed and decreased again at the end of incubation and microaggregates were formed. This development took place faster than was expected, and after 18 months of incubation the artificial soils were already approaching the amount of interactions between OM and minerals, and phenanthrene sorption behaviour found in natural systems. The changing OM distribution and composition points to an increasing presence of organo-mineral associations in the small particle size fraction of the artificial soils. And at the same time, a change in phenanthrene sorption behaviour with incubation time occurred, indicating that not only the properties, but also the functionality of the soil interfaces developed and changed with incubation time. An overview of these processes and their relative timing can be found in figure 25.

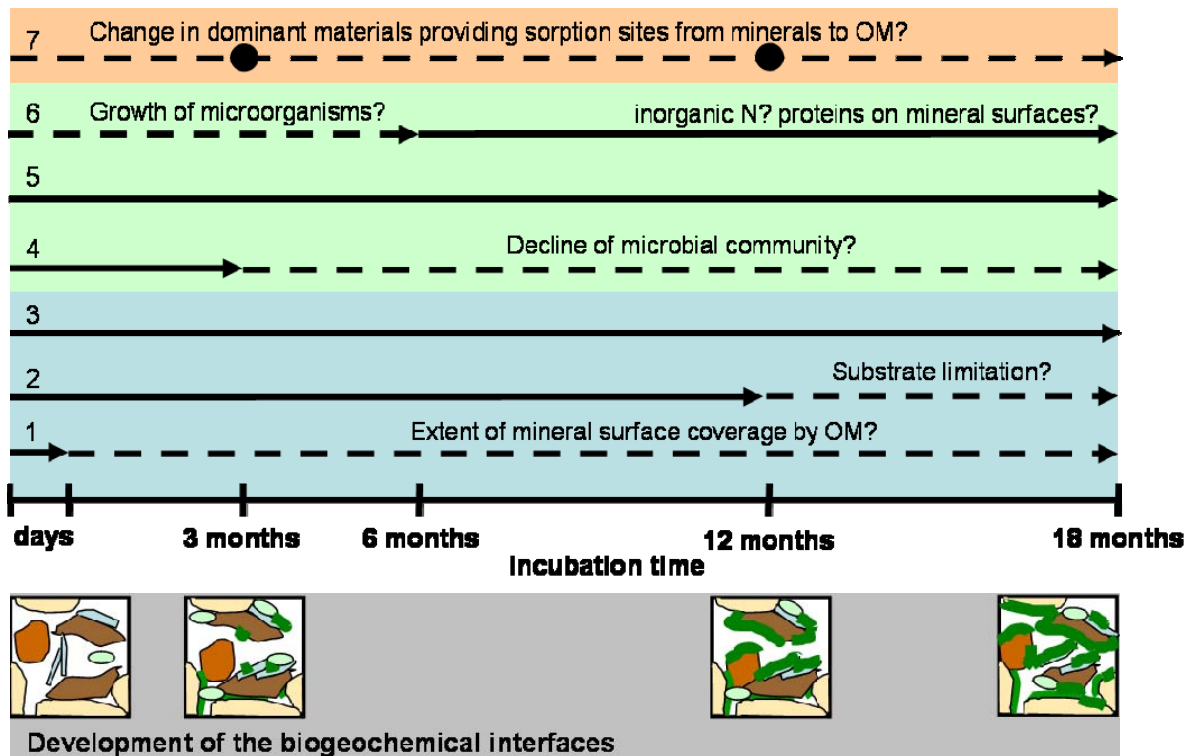


Figure 25. Schematic overview of the studied processes occurring in the artificial soils with incubation time, and related open questions and hypotheses.

There are still some open questions regarding the development of the artificial soils and the interaction of the different processes taking place. There are several hypothesis offered in figure 25, which need to be supported by additional data.

1. The occlusion of mineral surfaces was observed within the first days of incubation. However it is not yet clear if further coverage of mineral surfaces with OM took place with incubation time. This may especially be of interest for the further characterization of the sorptive interface, as phenanthrene sorption indicated a shift in phases providing sorption sites from mineral surfaces to OM.
2. The hypotheses considering the development, growth and possible decline of the microbial community and biomass in the artificial soils with time, as put forward this dissertation, could be further supported by characterization of the microbial

community by microbiological methods. This may also lead to a better understanding of the dynamics of aggregation and the development of the OM.

3. Further analysis of the distribution and form in which nitrogen is present, and especially inorganic N and proteins could give additional evidence for the hypothesis that proteins are preferentially associated with mineral surfaces
4. More analyses are needed in order to determine whether the mineral composition of the artificial soils had an effect on OM composition during incubation.

These questions may be addressed in cooperation with other groups within the Priority Program “Biogeochemical interfaces in soil”. Overall, the artificial soil incubation experiment offers a great opportunity to study all of these processes in the same simplified and well-defined system from known initial conditions. It shows how mineral components, organic matter and microorganisms interact and affect each other to form biogeochemical interfaces.

8 Conclusions and outlook

In order to elucidate the effect of different components on the development and properties of biogeochemical interfaces in soil, existing, matured interfaces were characterized by particle size fractionation, oxide extraction, specific surface area determination and phenanthrene sorption of three natural arable soils. The development of biogeochemical interfaces depending on different mineral components and charcoal was studied in a so-called artificial soil incubation experiment. The artificial soils were composed of well-characterized model materials in order to study the effect of mineral composition and the presence of charcoal on the formation of biogeochemical interfaces.

In the natural soils a very close association was found between mineral components, and especially iron oxides, and OM. These materials were so strongly bound that they could no longer be divided into primary particles by physical fractionation methods. Iron oxides provided a major part of the surface area of these soils, although the low SSA of weakly crystalline oxides indicated that they were associated with or covered by organic matter. In some cases, weakly crystalline oxides even occluded other mineral surfaces with a larger SSA. Overall, the results show that the available interfaces in the studied topsoils can be envisaged as close and complex associations between organic matter, iron oxides and other minerals functioning as stable entities. The BGI properties of a soil therefore depend not only on which components are present, but also on how these components are bound together, providing available surfaces. This was confirmed by the results of the phenanthrene sorption experiments. Phenanthrene sorption could not be explained by OM content and composition alone. The results of the sorption experiments to soil particle size fractions and materials with different SSA show that phenanthrene sorption is related to SSA, and the amount of OC per m^2 . The higher phenanthrene sorption after particle size fractionation showed that the aggregated structure does have an effect on the soils sorption capacity for phenanthrene. Overall it could be concluded that the affinity of hydrophobic molecules to the biogeochemical interfaces of this soil will depend on both the size of the interface and the amount of organic matter available on it

The artificial soil incubation experiment provided a system in which the interaction between different soil components, and following that the formation of BGI could be followed from clean and well-defined model components in a simplified system. The results

from this experiment show that interaction between OM and minerals was fast. Reduction of BET-N₂ SSA took place within days, indicating occlusion of mineral surfaces by organic matter or aggregation. Macro- and microaggregates developed within the first 3 months of incubation and developed during the incubation experiment in a way that is consistent with the aggregate hierarchy model presented by Tisdall and Oades (1982) and Oades (1984). OC was redistributed from the coarse to the fine fractions of the artificial soils, and C/N ratios and ¹³C NMR spectroscopy indicate that proteinacious material may have been selectively preserved in the fine fractions. This could point to interactions between proteins and mineral surfaces, which is in agreement with the conceptual model presented by Kleber et al. (2007).

The development of the artificial soils was limited by biological activity and substrate availability, whereas artificial soil composition was of secondary importance. It was found that the presence of clay minerals was important for the formation of macroaggregates, and that the decline in macroaggregation after 12 months of incubation was faster for the artificial soils containing charcoal. The presence of iron and aluminum oxide did not affect aggregation and formation of OM-mineral associations, contrarily to the natural soils studied, due to the relatively high pH of the artificial soils. Although more analyses are still needed to determine if mineral composition had an effect on OM properties. The phenanthrene sorption isotherms of the artificial soils changed from the 3 months incubated artificial soils to the 12 months incubated soils. After 3 months the presence of ferrihydrite had an effect on the shape of the sorption isotherm, and sorption of phenanthrene to the ferrihydrite may have taken place, whereas after 12 months, phenanthrene sorption was entirely controlled by OM content. This shows that the sorptive interface of the artificial soils matured during the incubation experiment, leading to an increased OM content and association of OM and minerals in the fine fraction, where OM presence was most important factor for phenanthrene sorption behaviour.

The artificial soil incubation experiment showed that interface development and the building of macro- and microaggregates and interactions between OM and minerals took place in these artificial soils within a relatively short time scale. During the 18 months of incubation, the artificial soils developed from a mixture of clean model materials to a soil-like system. Although care has to be taken in extrapolating the results of aggregation and OM dynamics found in the artificial soils to natural soils. The artificial soil incubation experiment represents a simplified system in which the effect of changing environmental conditions and

OM input from litter and roots is excluded. The materials offer a valuable model system where the formation and interactions of a wide range of soil properties and processes can be studied in a well-defined system.

Overall, the results presented in this dissertation demonstrate that the effect of different components on biogeochemical interfaces in soil depended on the properties and the maturity of the system studied. Iron oxides provided a large and reactive interface in the natural soils, but clay minerals were more important in the artificial soils due to the different pH. Furthermore, the phenanthrene sorption experiments showed that the phenanthrene sorptive interface is mainly determined by the interaction between organic and mineral particles, where mineral surfaces themselves become less relevant for sorption with maturation of the interface. Biogeochemical interfaces in soil are therefore not only determined by the different components present, but foremost by the interaction between these components. Further study of available interfaces in soils should therefore focus on the complexes of organic matter and minerals, and aggregates, as they are present in soil.

9 References

- Abelmann, K., Kleineidam, S., Knicker, H., Grathwohl, P. and Kögel-Knabner, I., 2005. Sorption of HOC in soils with carbonaceous contamination: Influence of organic-matter composition. *Journal of Plant Nutrition and Soil Science*, 168(3): 293-306.
- Abiven, S., Menasseri, S. and Chenu, C., 2009. The effects of organic inputs over time on soil aggregate stability - A literature analysis. *Soil Biology and Biochemistry*, 41(1): 1-12.
- Ahangar, A.G., Smernik, R.J., Kookana, R.S. and Chittleborough, D.J., 2008. Separating the effects of organic matter-mineral interactions and organic matter chemistry on the sorption of diuron and phenanthrene. *Chemosphere*, 72(6): 886-890.
- Amellal, S., Boivin, A., Ganier, C.P. and Schiavon, M., 2006. High sorption of phenanthrene in agricultural soils. *Agronomy for Sustainable Development*, 26(2): 99-106.
- Amelung, W. and Zech, W., 1999. Minimisation of organic matter disruption during particle-size fractionation of grassland epipedons. *Geoderma*, 92(1-2): 73-85.
- Angers, D.A. and Caron, J., 1998. Plant-induced changes in soil structure: Processes and feedbacks. *Biogeochemistry*, 42: 55-72.
- Bachmann, J., Woche, S.K., Goebel, M.-O., Kirkham, M.B. and Horton, R., 2003. Extended methodology for determining wetting properties of porous media. *Water Resources Research*, 39: 1353-1366.
- Baldock, J. et al., 1992. Aspects of the chemical structure of soil organic materials as revealed by solid-state ^{13}C NMR spectroscopy, *Biogeochemistry*. Springer Netherlands, pp. 1-42.
- Baldock, J.A. et al., 1997. Assessing the extent of decomposition of natural organic materials using solid-state ^{13}C NMR spectroscopy. *Australian Journal of Soil Research*, 35: 1061-1084.
- Barral, M.T., Arias, M. and Guérif, J., 1998. Effects of iron and organic matter on the porosity and structural stability of soil aggregates. *Soil and Tillage Research*, 46(3-4): 261-272.
- Bonin, J.L. and Simpson, M.J., 2007. Variation in phenanthrene sorption coefficients with soil organic matter fractionation: The result of structure or conformation? *Environmental Science & Technology*, 41(1): 153-159.
- Borggaard, O.K., 1982. The influence of iron oxides on the surface area of soil. *European Journal of Soil Science*, 33(3): 443-449.

- Bravo-Garza, M.R., Bryan, R.B. and Voroney, P., 2009. Influence of wetting and drying cycles and maize residue addition on the formation of water stable aggregates in Vertisols. *Geoderma*, 151: 150-156.
- Brodowski, S., Amelung, W., Haumaier, L., Abetz, C. and Zech, W., 2005. Morphological and chemical properties of black carbon in physical soil fractions as revealed by scanning electron microscopy and energy-dispersive X-ray spectroscopy. *Geoderma Mechanisms and regulation of organic matter stabilisation in soils*, 128(1-2): 116-129.
- Brodowski, S., John, B., Flessa, H. and Amelung, W., 2006. Aggregate-occluded black carbon in soil. *European Journal of Soil Science*, 57(4): 539-546.
- Brunauer, S., Emmett, P.H. and Teller, E., 1938. Adsorption of gases in multimolecular layers. *Journal of American Chemical Society*, 60(2): 309-319.
- Bullock, M.S., Kemper, W.D. and Nelson, S.D., 1988. Soil cohesion as affected by freezing, water content, time and tillage. *Soil Science Society of America Journal*, 52: 770-776.
- Carmo, A.M., Hundal, L.S. and Thompson, M.L., 2000. Sorption of hydrophobic organic compounds by soil materials: Application of unit equivalent Freundlich coefficients. *Environmental Science & Technology*, 34(20): 4363-4369.
- Celis, R. et al., 2006. The role of mineral and organic components in phenanthrene and dibenzofuran sorption by soil. *European Journal of Soil Science*, 57(3): 308-319.
- Chaplain, V., Brault, A., Tessier, D. and Défossez, P., 2008. Soil hydrophobicity: a contribution of diuron sorption experiments. *European Journal of Soil Science*, 59: 1202-1208.
- Chefetz, B. and Xing, B., 2009. Relative role of aliphatic and aromatic moieties as sorption domains for organic compounds: A review. *Environmental Science & Technology*, 43(6): 1680-1688.
- Chenu, C. and Plante, A.F., 2006. Clay-sized organo-mineral complexes in a cultivation chronosequence: revisiting the concept of the 'primary organo-mineral complex'. *European Journal of Soil Science*, 57(4): 596-607.
- Childs, C.W., 1992. Ferrihydrite: A review of structure, properties and occurrence in relation to soils. *Zeitschrift für Pflanzenernährung und Bodenkunde*, 155(5): 441-448.
- Chiou, C.T., Lee, J.F. and Boyd, S.A., 1990. The surface area of soil organic matter. *Environmental Science & Technology*, 24(8): 1164-1166.
- Chorover, J. and Amistadi, M.K., 2001. Reaction of forest floor organic matter at goethite, birnessite and smectite surfaces. *Geochimica et Cosmochimica Acta*, 65(1): 95-109.

- Christensen, B.T., 1992. Physical fractionation of soil and organic matter in primary particle size and density separates. *Advances in Soil Science*, 20: 1-90.
- Christensen, B.T., 2001. Physical fractionation of soil and structural and functional complexity in organic matter turnover. *European Journal of Soil Science*, 52(3): 345-353.
- Cornell, R.M. and Schwertmann, U., 1996. *The Iron Oxides*. VCH, Weinheim.
- De Jonge, H. and Mittelmeijer-Hazeleger, M.C., 1996. Adsorption of CO₂ and N₂ on Soil Organic Matter: Nature of Porosity, Surface Area, and Diffusion Mechanisms. *Environmental Science and Technology*, 30(2): 408-413.
- Delle Site, A., 2001. Factors affecting sorption of organic compounds in natural sorbent/water systems and sorption coefficients for selected pollutants. A review. *Journal of Physical and Chemical Reference Data*, 30(1): 187-439.
- Denef, K. and Six, J., 2005. Clay mineralogy determines the importance of biological versus abiotic processes for macroaggregate formation and stabilization. *European Journal of Soil Science*, 56(4): 469-479.
- Denef, K. et al., 2001a. Influence of dry-wet cycles on the interrelationship between aggregate, particulate organic matter, and microbial community dynamics. *Soil Biology and Biochemistry*, 33(12-13): 1599-1611.
- Denef, K., Six, J., Merckx, R. and Paustian, K., 2002. Short-term effects of biological and physical forces on aggregate formation in soils with different clay mineralogy. *Plant and Soil*. Springer Netherlands, pp. 185-200.
- Denef, K., Six, J., Paustian, K. and Merckx, R., 2001b. Importance of macroaggregate dynamics in controlling soil carbon stabilization: short-term effects of physical disturbance induced by dry-wet cycles. *Soil Biology and Biochemistry*, 33: 2145-2153.
- Duiker, S.W., Rhoton, F.E., Torrent, J., Smeck, N.E. and Lal, R., 2003. Iron (hydr)oxide crystallinity effects on soil aggregation. *Soil Science Society of America Journal*, 67(2): 606-611.
- Dümig, A., Smittenberg, R. and Kögel-Knabner, I., 2011. Concurrent evolution of organic and mineral components during initial soil development after retreat of the Damma glacier, Switzerland. *Geoderma*, 163(1-2): 83-94.
- Echeverria, J.C., Morera, M.T., Mazkaran, C. and Garrido, J.J., 1999. Characterization of the porous structure of soils: adsorption of nitrogen (77°K) and carbon dioxide (273°K), and mercury porosimetry. *European Journal of Soil Science*, 50(3): 497-503.

- Egli, M., Mavris, C., Mirabella, A. and Giaccai, D., 2010. Soil organic matter formation along a chronosequence in the Morteratsch proglacial area (Upper Engadine, Switzerland). *Catena*, 82(2): 61-69.
- Ellerbrock, R.H., Gerke, H.H., Bachmann, J. and Goebel, M.-O., 2005. Composition of Organic Matter Fractions for Explaining Wettability of Three Forest Soils. *Soil Science Society of America Journal*, 69(1): 57-66.
- Eusterhues, K., Rumpel, C., Kleber, M. and Kögel-Knabner, I., 2003. Stabilisation of soil organic matter by interactions with minerals as revealed by mineral dissolution and oxidative degradation. *Organic Geochemistry*, 34(12): 1591-1600.
- Eusterhues, K., Rumpel, C. and Kögel-Knabner, I., 2005a. Stabilization of soil organic matter isolated via oxidative degradation. *Organic Geochemistry*, 36(11): 1567-1575.
- Eusterhues, K., Rumpel, C. and Kögel-Knabner, I., 2005b. Organo-mineral associations in sandy acid forest soils: importance of specific surface area, iron oxides and micropores. *European Journal of Soil Science*, 56(6): 753-763.
- Eusterhues, K. et al., 2008. Characterization of Ferrihydrite-Soil Organic Matter Coprecipitates by X-ray Diffraction and Mössbauer Spectroscopy. *Environmental Science & Technology*, 42(21): 7891-7897.
- Fall, C., Chaouki, J., Chavarie, C. and Elena-Ortega, R., 2003. Multivariate Study on Phenanthrene Sorption in Soils. *Journal of Environmental Engineering*, 129(11): 1030-1040.
- Falsone, G., Celi, L. and Bonifacio, E., 2007. Aggregate formation in chloritic and serpentinitic alpine soils. *Soil Science*, 172(12): 1019-1030.
- Gerzabek, M.H. et al., 2006. How are soil use and management reflected by soil organic matter characteristics: a spectroscopic approach. *European Journal of Soil Science*, 57(4): 485-494.
- Gonçalves, C.N. et al., 2003. The effect of 10% HF treatment on the resolution of CPMAS ¹³C NMR spectra and on the quality of organic matter in Ferralsols. *Geoderma*, 116(3-4): 373-392.
- Grosbellet, C., Vidal-Beaudet, L., Caubel, V. and Charpentier, S., 2011. Improvement of soil structure formation by degradation of coarse organic matter. *Geoderma*, 162(1-2): 27-38.
- Heister, K., Höschen, C., Pronk, G., Mueller, C. and Kögel-Knabner, I., 2011. NanoSIMS as a tool for characterizing soil model compounds and organomineral associations in artificial soils, 10.1007/5 11368-011-0386-8. *Journal of Soils and Sediments*: 1-13.

- Helios Rybicka, E. and Calmano, W., 1988. Changes in physico-chemical properties of some clay minerals by reducing extraction reagents. *Applied Clay Science*, 3(1): 75-84.
- Hiemstra, T., Antelo, J., Rahnemaie, R. and Riemsdijk, W.H.v., 2010a. Nanoparticles in natural systems I: The effective reactive surface area of the natural oxide fraction in field samples. *Geochimica et Cosmochimica Acta*, 74(1): 41-58.
- Hiemstra, T., Antelo, J., van Rotterdam, A.M.D.D. and van Riemsdijk, W.H., 2010b. Nanoparticles in natural systems II: The natural oxide fraction at interaction with natural organic matter and phosphate. *Geochimica et Cosmochimica Acta*, 74(1): 59-69.
- Hilscher, A. and Knicker, H., 2011a. Carbon and nitrogen degradation on molecular scale of grass-derived pyrogenic organic material during 28 months of incubation in soil. *Soil Biology and Biochemistry*, 43(2): 261-270.
- Hilscher, A. and Knicker, H., 2011b. Degradation of grass-derived pyrogenic organic material, transport of the residues within a soil column and distribution in soil organic matter fractions during a 28 month microcosm experiment. *Organic Geochemistry*, 42(1): 42-54.
- Hochella, M.F. et al., 2008. Nanominerals, mineral nanoparticles, and earth systems, 10.1126/science.1141134. *Science*, 319(5870): 1631-1635.
- Huang, P.-M., Wang, M.-K. and Chiu, C.-Y., 2005. Soil mineral-organic matter-microbe interactions: Impacts on biogeochemical processes and biodiversity in soils. *Pedobiologia*, 49(6): 609-635.
- Huang, W., Peng, P., Yu, Z. and Fu, J., 2003. Effects of organic matter heterogeneity on sorption and desorption of organic contaminants by soils and sediments. *Applied Geochemistry*, 18(7): 955-972.
- Hundal, L.S. and Thompson, M.L., 2006. Soil aggregation as a source of variation in sorption isotherms of hydrophobic organic compounds. *Soil Science*, 171(5): 355-363.
- Hundal, L.S., Thompson, M.L., Laird, D.A. and Carmo, A.M., 2001. Sorption of phenanthrene by reference smectites. *Environmental Science & Technology*, 35(17): 3456-3461.
- Isermeyer, H., 1951. Eine einfache Methode zur Bestimmung der Bodenatmung und der Karbonate im Boden. *Zeitschrift für Pflanzenernaehrung und Bodenkunde*, 56: 26-38.
- Juo, A.S.R. and Kamprath, E.J., 1979. Copper chloride as an extractant for estimating the potentially reactive aluminium pool in acid soils. *Soil Science Society of America Journal*, 43: 35-38.

- Kaiser, K. and Guggenberger, G., 2000. The role of DOM sorption to mineral surfaces in the preservation of organic matter in soils. *Organic Geochemistry*, 31(7-8): 711-725.
- Kaiser, K. and Guggenberger, G., 2003. Mineral surfaces and soil organic matter. *European Journal of Soil Science*, 54(2): 219-236.
- Kaiser, K. and Guggenberger, G., 2007. Sorptive stabilization of organic matter by microporous goethite: sorption into small pores vs. surface complexation. *European Journal of Soil Science*, 58(1): 45-59.
- Kaiser, K. and Zech, W., 1996. Defects in estimation of aluminum in humus complexes of podzolic soils by pyrophosphate extraction. *Soil Science*, 161(7): 452-458.
- Kang, S. and Xing, B., 2005. Phenanthrene sorption to sequentially extracted soil humic acids and humins. *Environmental Science & Technology*, 39(1): 134-140.
- Karickhoff, S.W., Brown, D.S. and Scott, T.A., 1979. Sorption of hydrophobic pollutants on natural sediments. *Water Research*, 13(3): 241-248.
- Keiluweit, M. and Kleber, M., 2009. Molecular-Level Interactions in Soils and Sediments: The Role of Aromatic pi-Systems. *Environmental Science & Technology*, 43(10): 3421-3429.
- Kiem, R. and Kögel-Knabner, I., 2002. Refractory organic carbon in particle-size fractions of arable soils II: organic carbon in relation to mineral surface area and iron oxides in fractions <6 μm . *Organic Geochemistry*, 33: 1699-1713.
- Kleber, M., Mikutta, R., Torn, M.S. and Jahn, R., 2005. Poorly crystalline mineral phases protect organic matter in acid subsoil horizons. *European Journal of Soil Science*, 56(6): 717-725.
- Kleber, M., Sollins, P. and Sutton, R., 2007. A conceptual model of organo-mineral interactions in soils: self-assembly of organic molecular fragments into zonal structures on mineral surfaces. *Biogeochemistry*, 85(1): 9-24.
- Knicker, H. and Lüdemann, H.-D., 1995. N-15 and C-13 CPMAS and solution NMR studies of N-15 enriched plant material during 600 days of microbial degradation. *Organic Geochemistry*, 23(4): 329-341.
- Kögel-Knabner, I., 2002. The macromolecular organic composition of plant and microbial residues as inputs to soil organic matter. *Soil Biology and Biochemistry*, 34(2): 139-162.
- Kögel-Knabner, I. et al., 2008. Organo-mineral associations in temperate soils: Integrating biology, mineralogy, and organic matter chemistry. *Journal of Plant Nutrition and Soil Science*, 171(1): 61-82.

- Kuzyakov, Y., Subbotina, I., Chen, H., Bogomolova, I. and Xu, X., 2009. Black carbon decomposition and incorporation into soil microbial biomass estimated by ¹⁴C labeling. *Soil Biology and Biochemistry*, 41(2): 210-219.
- Lehmann, J. et al., 2008. Spatial complexity of soil organic matter forms at nanometre scales. *Nature Geoscience*, 1: 238-242.
- Leifeld, J. and Kögel-Knabner, I., 2003. Microaggregates in agricultural soils and their size distribution determined by X-ray attenuation. *European Journal of Soil Science*, 54(1): 167-174.
- Leinweber, P. and Reuter, G., 1992. The influence of different fertilization practices on concentrations of organic carbon and total nitrogen in particle-size fractions during 34 years of a soil formation experiment in loamy marl. *Biology and Fertility of Soils*, 13(2): 119-124.
- Limousin, G. et al., 2007. Sorption isotherms: A review on physical bases, modeling and measurement. *Applied Geochemistry*, 22(2): 249-275.
- Luo, L., Zhang, S. and Ma, Y., 2008. Evaluation of impacts of soil fractions on phenanthrene sorption. *Chemosphere*, 72(6): 891-896.
- Macht, F., Eusterhues, K., Pronk, G.J. and Totsche, K.U., in press. Specific surface area of clay minerals: Comparison between atomic force microscopy measurements and bulk-gas (N₂) and -liquid (EGME) adsorption methods. *Applied Clay Science*, In Press, Corrected Proof.
- Mader, B.T., Uwe-Goss, K. and Eisenreich, S.J., 1997. Sorption of nonionic, hydrophobic organic chemicals to mineral surfaces. *Environmental Science & Technology*, 31(4): 1079-1086.
- Materechera, S.A., Dexter, A.R. and Alston, A.M., 1992. Formation of aggregates by plant roots in homogenised soils. *Plant and Soil*, 142: 69-79.
- Mayer, L.M., 1999. Extent of coverage of mineral surfaces by organic matter in marine sediments. *Geochimica et Cosmochimica Acta*, 63(2): 207-215.
- Mehra, O.P. and Jackson, M.L., 1960. Iron oxide removal from soils and clays by a dithionite-citrate system buffered with sodium bicarbonate. *Clays and Clay Minerals*, 7: 317-327.
- Mikutta, R., Kleber, M., Kaiser, K. and Jahn, R., 2005. Review: Organic matter removal from soils using hydrogen peroxide, sodium hypochlorite, and disodium peroxodisulfate. *Soil Science Society of America Journal*, 69(1): 120-135.

- Miltner, A., Kindler, R., Knicker, H., Richnow, H.-H. and Kästner, M., 2009. Fate of microbial biomass-derived amino acids in soil and their contribution to soil organic matter. *Organic Geochemistry*, 40(9): 978-985.
- Mittal, M. and Rockne, K.J., 2008. Naphthalene and phenanthrene sorption to very low organic content diatomaceous earth: Modeling implications for microbial bioavailability. *Chemosphere*, 74(8): 1134-1144.
- Müller, S., Totsche, K.U. and Kögel-Knabner, I., 2007. Sorption of polycyclic aromatic hydrocarbons to mineral surfaces. *European Journal of Soil Science*, 58(4): 918-931.
- Oades, J., 1984. Soil organic matter and structural stability: mechanisms and implications for management. *Plant and Soil*, 76(1): 319-337.
- Oades, J.M., 1993. The role of biology in the formation, stabilization and degradation of soil structure. *Geoderma, International Workshop on Methods of Research on Soil Structure/Soil Biota Interrelationships*, 56(1-4): 377-400.
- OECD, 2000. Adsorption/desorption using a batch equilibrium method, test guideline 106. *Guidelines for testing chemicals*, OECD publications, Paris.
- Omoike, A. and Chorover, J., 2006. Adsorption to goethite of extracellular polymeric substances from *Bacillus subtilis*. *Geochimica et Cosmochimica Acta*, 70(4): 827-838.
- Pan, B. et al., 2007. Effect of physical forms of soil organic matter on phenanthrene sorption. *Chemosphere*, 68(7): 1262-1269.
- Pinheiro-Dick, D. and Schwertmann, U., 1996. Microaggregates from Oxisols and Inceptisols: dispersion through selective dissolutions and physicochemical treatments. *Geoderma*, 74(1-2): 49-63.
- Qafoku, N.P., 2010. Terrestrial nanoparticles and their controls on soil-/geo-processes and reactions. *Advances in Agronomy*, 107: 33-91.
- Quideau, S.A., Anderson, M.A., Graham, R.C., Chadwick, O.A. and Trumbore, S.E., 2000. Soil organic matter processes: characterization by ^{13}C NMR and ^{14}C measurements. *Forest Ecology and Management*, 138(1-3): 19-27.
- Quideau, S.A., Chadwick, O.A., Benesi, A., Graham, R.C. and Anderson, M.A., 2001. A direct link between forest vegetation type and soil organic matter composition. *Geoderma*, 104(1-2): 41-60.
- Ruiz-Vera, V.M. and Wu, L., 2006. Influence of sodicity, clay mineralogy, prewetting rate, and their interaction on aggregate stability, 10.2136/sssaj2005.0285. *Soil Science Society of America Journal*, 70(6): 1825-1833.

- Schaaf, W. et al., 2011. Patterns and processes of initial terrestrial-ecosystem development. *Journal of Plant Nutrition and Soil Science*, 174(2): 229-239.
- Schmidt, M.W.I., Rumpel, C. and Kögel-Knabner, I., 1999a. Evaluation of an ultrasonic dispersion procedure to isolate primary organomineral complexes from soils. *European Journal of Soil Science*, 50(1): 87-94.
- Schmidt, M.W.I., Rumpel, C. and Kögel-Knabner, I., 1999b. Particle size fractionation of soil containing coal and combusted particles. *European Journal of Soil Science*, 50(3): 515-522.
- Schwarzenbach, R.P. and Westall, J., 1981. Transport of nonpolar organic compounds from surface water to groundwater. Laboratory sorption studies. *Environmental Science & Technology*, 15(11): 1360-1367.
- Schwertmann, U., 1964. Differenzierung der Eisenoxide des Bodens durch Extraktion mit Ammoniumoxalat-Lösung. *Zeitschrift für Pflanzenernährung, Düngung, Bodenkunde*, 105(3): 194-202.
- Schwertmann, U. and Cornell, R.M., 1991. *Iron Oxides in the Laboratory, Preparation and Characterisation*. VCH Verlag GmbH.
- Schwertmann, U. and Fechter, H., 1982. The point of zero charge of natural and synthetic ferrihydrites and its relation to adsorbed silicate. *Clay Minerals*, 17: 471-476.
- Schwertmann, U. and Taylor, R.M., 1989. Iron oxides. In: J.B. Dixon and S.B. Weed (Editors), *Minerals in Soil Environments*. Soil Science of America, Wisconsin, pp. 379-438.
- Siebold, A., Walliser, A., Nardin, M., Oppliger, M. and Schultz, J., 1997. Capillary Rise for Thermodynamic Characterization of Solid Particle Surface. *Journal of Colloid and Interface Science*, 186(1): 60-70.
- Six, J., Bossuyt, H., Degryze, S. and Deneff, K., 2004. A history of research on the link between (micro)aggregates, soil biota, and soil organic matter dynamics. *Soil and Tillage Research, Advances in Soil Structure Research*, 79(1): 7-31.
- Six, J., Elliott, E.T. and Paustian, K., 2000. Soil macroaggregate turnover and microaggregate formation: a mechanism for C sequestration under no-tillage agriculture. *Soil Biology and Biochemistry*, 32(14): 2099-2103.
- Smucker, A.J.M., Park, E.-J., Dorner, J. and Horn, R., 2007. Soil micropore development and contributions to soluble carbon transport within macroaggregates. *Vadose Zone Journal*, 6(2): 282-286.

- Sohi, S.P., Krull, E., Lopez-Capel, E. and Bol, R., 2010. A Review of Biochar and Its Use and Function in Soil, *Advances in Agronomy*. 105: 47-82.
- Sollins, P. et al., 2009. Sequential density fractionation across soils of contrasting mineralogy: evidence for both microbial- and mineral-controlled soil organic matter stabilization. *Biogeochemistry*, 96(1-3): 209-231.
- Sollins, P., Swanston, C. and Kramer, M., 2007. Stabilization and destabilization of soil organic matter - a new focus, *Biogeochemistry*. Springer Netherlands, pp. 1-7.
- Spence, A. et al., 2011. The degradation characteristics of microbial biomass in soil. *Geochimica et Cosmochimica Acta*, 75(10): 2571-2581.
- Tipping, E., 1981. The adsorption of aquatic humic substances by iron oxides. *Geochimica et Cosmochimica Acta*, 45(2): 191-199.
- Tisdall, J.M. and Oades, J.M., 1982. Organic matter and water-stable aggregates in soils. *Journal of Soil Science*, 33(2): 141-163.
- Tisdall, J.M., Smith, S.E. and Rengasamy, P., 1997. Aggregation of soil by fungal hyphae. *Australian Journal of Soil Research*, 35: 55-60.
- Totsche, K.U. et al., 2010. Biogeochemical interfaces in soil: The interdisciplinary challenge for soil science. *Journal of Plant Nutrition and Soil Science*, 173(1): 88-99.
- van Reeuwijk, L., 2002. Procedures for soil analysis. 6th ed. ISRIC, Wageningen, The Netherlands.
- Virto, I., Barré, P. and Chenu, C., 2008. Microaggregation and organic matter storage at the silt-size scale. *Geoderma*, 146: 326-335.
- von Lützow, M. et al., 2007. SOM fractionation methods: Relevance to functional pools and to stabilization mechanisms. *Soil Biology and Biochemistry*, 39: 2183-2207.
- von Lützow, M. et al., 2006. Stabilization of organic matter in temperate soils: mechanisms and their relevance under different soil conditions - a review. *European Journal of Soil Science*, 57(4): 426-445.
- von Lützow, M. et al., 2008. Stabilization mechanisms of organic matter in four temperate soils: Development and application of a conceptual model. *Journal of Plant Nutrition and Soil Science*, 171(1): 111-124.
- Vowles, P.D. and Mantoura, R.F.C., 1987. Sediment-water partition coefficients and HPLC retention factors of aromatic hydrocarbons. *Chemosphere*, 16(1): 109-116.
- Wagai, R. and Mayer, L.M., 2007. Sorptive stabilisation of organic matter in soils by hydrous iron oxides. *Geochimica et Cosmochimica Acta*, 71: 25-35.

- Wagai, R., Mayer, L.M. and Kitayama, K., 2009. Extent and nature of organic coverage of soil mineral surfaces assessed by a gas sorption approach. *Geoderma*, 149: 152-160.
- Watts, C.W., Whalley, W.R., Brookes, P.C., Devonshire, B.J. and Whitmore, A.P., 2005. Biological and physical processes that mediate micro-aggregation of clays. *Soil Science*, 170(8): 573-583.
- Webmineral.com, 2010. <http://www.webmineral.com/>. David Barthelmy.
- Xing, B. and Pignatello, J., 2005. Sorption | Organic Chemicals, In: *Encyclopaedia of Soils in the Environment*. D. Hillel (Editor). Elsevier, Oxford, pp. 537-548.
- Young, I.M. and Crawford, J.W., 2004. Interactions and self-organization in the soil-microbe complex, 10.1126/science.1097394. *Science*, 304(5677): 1634-1637.
- Yukselen, Y. and Kaya, A., 2006. Comparison of methods for determining specific surface area of soils. *Journal of Geotechnical and Geoenvironmental Engineering*, 132(7): 931-936.

10 Acknowledgements

To begin with, I would like to thank Prof. Dr. Ingrid Kögel-Knabner for allowing me to work on this project. Thank you for the support, the helpful and interesting discussions and feedback in carrying out and publishing this work. I thank Prof. Dr. Kai Uwe Totsche for the many inspiring and helpful discussions in the framework of the Priority program “biogeochemical interfaces in soil” and the help and support in modeling and interpreting the phenanthrene sorption data. I thank Prof. Dr. Jürgen Geist for the chairmanship of the examination commission. The German Research Foundation (DFG) and the TUM Gender Centre are gratefully acknowledged for financial support.

My foremost thanks go to Dr. Katja Heister, my excellent supervisor and mentor. Thank you for always being ready to answer my many questions, discuss my ideas and patiently read my first attempts at scientific writing. You were always able to keep me motivated and inspire me with your suggestions, ideas and support. And thank you for speaking my language and helping me deal with the difficulties of living in a foreign country.

All participants of the priority program “biogeochemical interfaces in soil” are gratefully acknowledged for providing a network with many inspiring discussions and opportunities for cooperation. I thank PD Dr. Thilo Rennert for the coordination of the project and the exchange of data and ideas, Prof. Dr. Holger Kirchman and Stephan Schulz for providing soil samples and Esther Cyrus and Dr. Anja Miltner for the preparation of the manure used in the artificial soils. I thank Guo-Chun Ding and Prof. Dr. Kornelia Smalla for their help in preparing the microbial inoculum, the great cooperation and for teaching me many things about microbiology. Dr. Susanne Woche, Felix Macht and Dr. Karin Eusterhues are thanked for the good cooperation and exchange of data.

My colleagues at the Lehrstuhl for Bodenkunde were helpful in many ways, but most of all I thank you for providing a good working atmosphere, and for introducing me to the interesting peculiarities of German, and Bavarian culture.

I thank Bärbel Angres for her great work in the laboratory performing and analyzing the phenanthrene sorption experiments and for patiently introducing me to the complexities of the analytical methods. Urike Maul and Maria Greiner are thanked for their assistance in the

preparation and analysis of the artificial soils. I would like to thank in particular Dr. Angelika Kölb and Dr. Markus Steffens for their constructive comments on my manuscripts, and Florian Schmalzl and Elfriede Schuhbauer for their help in keeping my computer running and the preparation of posters and presentations.

To all my present and former colleagues at the Lehrstuhl Für Bodenkunde, I thank you for the help and support you have given me at various times and occasions, and for the many interesting discussions we had.

This work would not have been possible without the great help of the student assistants and interns Daniela Muller, Sachin KC and the master students Katharina Günthner, Anupama Baroo, and especially Zohre Javaheri, Zahra Kazemi, Samira Ravash for their commitment and enthusiasm in working on this project, and for always remaining cheerful and motivated. It was a pleasure to work with you. Thank you!

I thank the TUM graduate school and the DoctoraTUM program and in particular Dr. Markus Schaller for providing a framework of courses to develop my academic skills. The international PhD program of the TUM was of particular help in building contacts and friendships with other foreign students in Munich.

And last but not least, I thank my parents for their continuous trust and support...for everything. And my friends, Annemiek and Elvira for keeping on reminding me to have fun and relax now and then.

Curriculum Vitae

Persönliche Daten

Name Geertje Pronk
 Geboren am 05.07.1983 in Haarlem, die Niederlande
 Nationalität Niederländisch

Derzeitige Tätigkeit:

seid 08.2011 Wissenschaftlicher Mitarbeiter am Lehrstuhl für Bodenkunde, TU München, Freising-Weihenstephan

Promotion

seid 10.2007

10.2007-10.2010 Wissenschaftlicher Mitarbeiter am Lehrstuhl für Bodenkunde, TU München, Freising-Weihenstephan

10.2010-07.2011 Stipendium im Rahmen des Programms „Chancengleichheit für Frauen in Forschung und Lehre

Projekt: Einfluss verschiedener Bodenbestandteile auf die Bildung biogeochemischer Grenzflächen

Studium

09.2005 – 09.2007 **Masterstudium Geochemie**, Universität Utrecht, Niederlande (Abschluss am 28. September 2007, Cum Laude)

Thema der Masterarbeit: Modeling nitrogen cycling and retention in a South Western Australian estuary (Modellierung des Stickstoffzyklus und -retention in einem südwest-australischen Ästuar)

01.2007-07.2007 6-monatiges Praktikum am Geoscience Australia, Canberra, Australien

09.2002 – 07.2005 **Bachelorstudium Geowissenschaften**, Universität Utrecht, Niederlande (Abschluss im September 2005)

Thema der Bachelorarbeit: The chemical evolution of the Poás crater lake, Costa Rica, with respect to the major cationic species (Die chemische Entwicklung des Poás Kratersees, Costa Rica, im Hinblick auf die bedeutendsten Kationspezies)

Schulabschluss

09.1996 – 07.2002 VWO (Gymnasium), De Leeuwenhorst, Noordwijkerhout, Niederlande

Publications and presentations

Peer-reviewed journals

- Ding G.-C, Heuer H, Zuhlke S, Spiteller M, Pronk G J, Heister K, Kögel-Knabner I, Smalla K (2010) Soil Type-Dependent Responses to Phenanthrene as Revealed by Determining the Diversity and Abundance of Polycyclic Aromatic Hydrocarbon Ring-Hydroxylating Dioxygenase Genes by Using a Novel PCR Detection System. 10.1128/AEM.00047-10. *Applied Environmental Microbiology* 76, 4765-4771.
- Haese R, Pronk G J (2011) Intra-annual Variability in Primary Producer Groups and Nitrogen Dynamics in an Intermittently Closed Estuary Exposed to Mediterranean Climate. 10.1007/s12237-010-9363-5. *Estuaries and Coasts* 34 557-568.
- Heister K, Höschel C, Pronk G J, Müller C W, Kögel-Knabner I, NanoSIMS as a tool for characterizing soil model compounds and organo-mineral associations in artificial soils. 10.1007/s11368-011-0386-8. *Journal of Soils and Sediments*, In press.
- Macht F, Eusterhues K, Pronk G J, Totsche K U, Specific surface area of clay minerals: Comparison between atomic force microscopy measurements and bulk-gas (N₂) and - liquid (EGME) adsorption methods. 10.1016/j.clay.2011.04.006. *Applied Clay Science*, In Press, Corrected Proof.
- Pronk, G. J, Heister, K, Kögel-Knabner, I (2011) Iron oxides as major available interface component in loamy arable topsoils, *Soil Science Society of America Journal*, In press.
- Pronk, G. J, Heister, K, Kögel-Knabner, I (2011) Development of biogeochemical interfaces in an artificial soil incubation experiment; aggregation and formation of organo-mineral associations, *Geoderma*, submitted.
- Pronk, G. J, Heister, K, Woche, S. K, Totsche, K. U, Kögel-Knabner, I (2011) Combining Specific Surface Area and Organic Matter Content to Determine the Phenanthrene Sorptive Interface of an Arable Topsoil, *European Journal of Soil Science*, submitted.

Conference abstracts

- Pronk, G.J., Heister, K., Kögel-Knabner, I. Characterisation of particle size fractions in relation to specific surface area in a Eutric Cambisol. (oral presentation) European Geosciences Union, General Assembly, Vienna, Austria, 2009

-
- Pronk, G. J., Heister, K., Kögel-Knabner, I., Investigating the effect of different minerals on biogeochemical interface formation in soil using artificial soil incubations. (poster presentation) European Geosciences Union, General Assembly, Vienna, Austria, 2009
- Pronk, G.J., Heister, K. and Kögel-Knabner, I. Phenanthrene sorption to particle size fractions of a Eutric Cambisol from Ultuna, Sweden related to specific surface area and organic matter properties. (oral presentation) Goldschmidt conference, Davos, Switzerland, 2009
- Pronk, G. J., Heister, K., Kögel-Knabner, I., The effect of mineral composition on biogeochemical interface formation in an artificial soil incubation experiment. (poster presentation) Deutsche Bodenkundliche Gesellschaft, Jahrestagung, Bonn, Germany, 2009
- Pronk G.J., Heister K, Kögel-Knabner I, Ferrihydrite enhances phenanthrene sorption to artificial soils. (poster presentation) World Congress of Soil Science, Brisbane, Australia, 2010